

Abstract

Strongly Correlated States in Low Dimensions

Dmitry Green

2001

This thesis is a theoretical analysis of sample two- and one-dimensional systems. The two-dimensional examples are the quantum Hall liquid and anomalous paired states. The most widely accepted effective theory of the quantum Hall liquid is based on the so-called Chern Simons Lagrangian, but it is not entirely satisfactory. We obtain the first derivation of an alternative effective theory from microscopic principles. Our formulation allows for a first principles derivation of physical quantities such as the effective mass and compressibility and contains the first analytical observation of the magnetoroton. The formalism developed along the way is also applied to paired states in anomalous superconductors, a topic of much recent interest. The one-dimensional system is the carbon nanotube. Gas uptake in nanotube bundles is currently attracting a wealth of research with both applied and fundamental implications. We propose adsorption of gases on the surface of a single tube, finding strong correlations and symmetries that have not been observed yet. The properties of these states are directly relevant to other one-dimensional structures such as spin ladders and stripes and raise interesting and open questions.

Strongly Correlated States in Low Dimensions

A Dissertation
Presented to the Faculty of the Graduate School
of
Yale University
in Candidacy for the Degree of
Doctor of Philosophy

by
Dmitry Green

Dissertation Director: Prof. Nicholas Read

December, 2001

Contents

Acknowledgements	6
1 Introduction	8
1.1 Composite Particles in the Fractional Quantum Hall Effect	8
1.2 Pairing in Two Dimensions	14
1.3 Adsorption on Carbon Nanotubes	16
2 Lowest Landau Level I: Composite Fermions	18
2.1 Formalism	19
2.1.a Single Particle in a Magnetic Field	19
2.1.b Two Particles in a Magnetic Field	22
2.1.c Fock Space, Operators, and Constraints	24
2.2 Hartree-Fock Approximation	27
2.3 Conserving Approximation and the Ward Identity	29
2.4 Response Functions	32
2.5 Effective Theory	38
3 Lowest Landau Level II: Composite Bosons	42
3.1 Formalism	42
3.1.a Fock Space	43
3.1.b Physical Operators and Constraints	43
3.1.c Remarks on Many-Particle Wavefunctions	47
3.2 Energy Functional	48

3.2.a	Mass Term	50
3.2.b	Spin Term	53
3.3	Constraints	55
3.4	Density Response and the Magnetoroton	57
3.4.a	The case $p = 2$	58
3.4.b	The case $p = 3$	60
4	Paired States of Bosons in Two Dimensions	62
4.1	The Permanent: p-wave Pairing	63
4.1.a	Analytic Structure of the Ground State	63
4.1.b	Magnetic Translations on the Plane	65
4.1.c	Spin-Waves and Instability; Exact Results	66
4.1.d	Spin Order of the Permanent	71
4.1.e	Effective Field Theory Near the Transition	76
4.1.f	Lattice Model	78
4.2	The Haffnian: d-wave Pairing	79
4.2.a	Analytic Structure of the Haffnian	80
4.2.b	The Haffnian Hamiltonian on the Sphere	81
4.2.c	Zero Energy Eigenstates	83
4.2.d	d-wave Pairing of Spinless Bosons	85
5	Fermion Pairing: Quantum Hall Effect for Spin	92
5.1	BCS Hamiltonian	92
5.2	Spin Response in a Conserving Approximation	94
5.3	Discussion and Generalizations	99
6	Adsorption on Carbon Nanotubes	102
6.1	Nanotube geometry	102
6.2	The Hamiltonian and Classical Limit	105
6.3	Macroscopic Degeneracy and Quantum Fluctuations	109
6.3.a	Continuum Limit	110

6.3.b	Numerics	114
6.3.c	Higher Order Corrections	115
6.4	Special Case: $N = 2$	117
6.5	Discussion and Conclusion	118
7	Summary	120
	Appendix: Non-Commutative Fourier Transform	123
	Bibliography	127

List of Figures

2.1	The vertex $\rho_{\mathbf{q}}(\mu_1 \mu_2)\rho_{\mathbf{q}}^L(\lambda_1 \lambda_2)$. The dotted line represents the interaction $\tilde{V}(\mathbf{q})$.	28
2.2	Diagrammatics of the conserving approximation. (a) The exchange self energy; (b) the ladder series renormalization of the vertices, Λ ; and (c) the response functions in terms of Λ	32
2.3	(a) Ladder series for the scattering matrix Γ and (b) response functions in terms of Γ .	34
2.4	Bubble summation for the gauge field propagator. (a) The shaded circle includes the diamagnetic coupling and the $\langle g\bar{g} \rangle_0$ bubble; (b) The thick wavy line represents $\langle a\bar{a} \rangle$	40
2.5	χ^{LL} as a bubble sum. The wavy line is the gauge field propagator from equation (2.93). See also fig. 2.4.	40
3.1	The composite with three vortices attached. The underlying particle is at z with charge $+1$, and the vortices are at η_i with charge $-1/3$. The (unnormalized) Jacobi vectors are dotted lines. z and the center of mass of the vortices, ξ_{cm} , are connected by $\wedge \mathbf{k}$, which we will later interpret as a dipole moment. Since the composite is neutral, it drifts with momentum \mathbf{k}	45
3.2	Lowest mode at $\nu = 1/2$ obtained from the action expanded to $\mathcal{O}(k^3)$. \mathbf{k} is in units of inverse magnetic length. The parameters are $m = 3$ and $J = 1$	59
3.3	Lowest two modes at $\nu = 1/3$ obtained by expanding the action to $\mathcal{O}(k^2)$. The higher mode is doubly degenerate. \mathbf{k} is in units of inverse magnetic length. The parameters are $m = 3$ and $J = 1$	61

4.1	Spin-Wave Dispersion: Points are numerical data for $N = 10, N_\phi = 9$ (computed by E. Rezayi). Solid line is the spectrum in (4.15), with C determined by matching to the data at the highest k . For comparison, the dotted line is the spectrum for a two body interaction (4.16) with $V_2 = 0$	68
4.2	$\langle S_z S_z \rangle$ of the Permanent and, for comparison, of the Laughlin state with one fewer flux. λ is the magnetic length. (Computed by E. Rezayi)	69
4.3	Phases of bosons in two dimensions.	91
6.1	An example of wrapping of the graphite sheet to make a $(2, 1)$ tube. \mathbf{a}_\pm are the primitive lattice vectors of the honeycomb lattice. The solid rectangle is the primitive cell of the tube. The tube can also be built up by stacking the dotted region along the axis with the solid dotted lines identified. Also shown is the tripartite lattice labeling A, B, C.	103
6.2	Adsorption sites on a $(7, 0)$ zig-zag nanotube	104
6.3	Phase diagram of the (N, M) tube	105
6.4	Magnetization and entropy per site at $k_B T = 0.05V$	107
6.5	Fillings and zipper of the $(5, 0)$ zig-zag tube. n_\pm corresponds to m_\mp	108
6.6	LEFT: Typical configuration in n_+ (or m_-) of the $(5, 0)$ tube. Alternating numbering within layers allows a symmetric description from bottom-to-top or top-to-bottom. RIGHT: Allowed states as paths on a wrapped square lattice. The vertex labels may be dropped.	110
6.7	The left ring shows the \mathbf{Z}_N impurity on the anchor bond (wavy line). The right ring shows the equivalent alternative, where the impurity is replaced by a flux tube through the torus.	113
6.8	The gap scales as $1/N^2 L$	114
6.9	The fillings for $N = 2$. $n_+ = 1/2$ (a) and $n_- = 1/4$ (b). Each adatom can live at either site in its layer because each site is connected to every site in the neighboring layers. (c) shows the triangular lattice in the plane; the horizontal double bond is due to the periodicity around a cylinder. (c) is exactly the geometry of the spin ladder studied by other authors (albeit with different coupling).	117

Acknowledgements

I learned a great deal from the faculty at Yale. My advisor, Nick Read, has been my main guide and teacher, and I have benefitted from courses and discussions with (in alphabetical order) Sean Barrett, Subir Sachdev, R. Shankar, Samson Shatashvili, and Doug Stone.

Jo-Ann Bonnett (Graduate Registrar, Physics) and her predecessor, Jean Belfonti, have made my life at Yale immeasurably easier. And, I appreciate the various fellowships from the NSF and Yale that have helped me along the way.

I also want to go back in time a little to thank my undergraduate thesis advisor at the University of Chicago, Prof. Ugo Fano, who passed away recently. His combination of humor, warmth, and intellectual vitality and integrity are unique, and it was truly exciting to have worked with him.

Last, but best, thanks to my fiancée, Katie.

For my grandmother,

Rakhil Babinskaya

Chapter 1

Introduction

1.1 Composite Particles in the Fractional Quantum Hall Effect

The technological innovation that made discovery of the quantum Hall effect (QHE) possible is called a MOSFET, or metal oxide semiconductor field effect transistor. Under suitable conditions, electrons are effectively confined to two dimensions by an inversion layer [1]. Inversion layers are formed at an interface of a semiconductor and an insulator or between two semiconductors with one of them acting as an insulator. The original system in which the QHE was discovered was between Si (semiconductor) and SiO₂ (insulator). More recently the semiconductor-semiconductor system GaAs-Al_xGa_{1-x}As (with GaAs acting as the semiconductor) has been used. The parameter is approximately $x \sim 0.2$. Typically the layers of GaAs and AlGaAs are grown with atomic precision using molecular beam epitaxy. The necessary donors that are required for the inversion layer to form are implanted away from the interface allowing very high electron mobility within the inversion layer. For some samples, an external voltage may be used to control the density of electrons.

The original discovery by von Klitzing, Dorda, and Pepper in 1980 has come to be known as the integer quantum Hall effect (IQHE). In brief, they found that when a magnetic field is applied perpendicular to the electron layer, the electron current response is purely transverse and quantized. More precisely, the current density responds to an electric field

by $j_i = \sum_j \sigma_{ij} E_j$, where the conductivity tensor is

$$\sigma = \begin{bmatrix} 0 & -\nu e^2/h \\ \nu e^2/h & 0 \end{bmatrix}.$$

h is Planck's constant, e is the electron charge, and ν is a small integer. Thus the conductivity is quantized in fundamental units, independently of specific material parameters. The diagonal conductivity vanishes, so the state is dissipationless. The actual measured quantities are the conductance and/or resistance. Theoretical understanding of this effect is based on models of independent electrons in the presence of disorder, and is quite developed by now.

In this thesis we will be concerned with an effect that was discovered shortly after the IQHE, which is known as the fractional quantum Hall effect (FQHE). In 1982, Tsui, Störmer, and Gossard found that, in extremely pure samples at very low temperature, the integer ν above can be replaced by a hierarchy of rational numbers, $\nu = p/q$. In the quantum limit $\omega_c \tau \gg 1$, where $\omega_c = eB/m$ and τ is the electronic scattering time, ν shows plateaus at these fractions as the chemical potential is varied. The leading fractions were found to have $q = \text{odd}$, forming an incompressible quantum liquid. Since then, $q = \text{even}$ states are understood to have their own complementary set of phenomena [2]. In contrast to the odd denominator fillings, they are compressible Fermi liquid-like states and are not characterized by plateaus in the conductivity (at least for $p \leq 3$; $\nu = 5/2$ may be an exception [3]). Theoretical understanding of the FQHE has progressed rapidly, but is not yet complete. For instance, problems which depend in detail on the interaction and disorder, such as transitions between the plateaus, are not well understood. Questions have also arisen recently on the nature of the effective theory for $\nu < 1$ even in pure samples. This is the issue we will tackle in this part of the thesis.

Let us briefly summarize the salient ingredients of the theory. The fundamental length scale for electrons in a magnetic field B is

$$\ell_B = \left(\frac{\hbar c}{eB} \right)^{1/2}.$$

It is independent of material parameters and is in the range of $50 - 100 \text{ \AA}$. The independent particle states are parameterized by Landau levels (LL) of energy $E_n = \hbar \omega_c (n + 1/2)$. Each

LL is highly degenerate; the number of states per unit area of one full LL is given by

$$\rho_0 = 1/2\pi\ell_B^2 = eB/hc$$

The last equality can be rewritten as $\rho_0 = B/\Phi_0$, where Φ_0 is the unit flux quantum, so that the degeneracy of one full LL is counted by the number of flux quanta in the external field. In this simplified model, electrons successively occupy the Landau levels, and the proportion of occupied states is denoted by the filling fraction, ν . If the electron density is ρ then

$$\nu = \rho/\rho_0 . \tag{1.1}$$

The IQHE occurs at integral ν , when an integral number of levels are full.

However, the FQHE occurs when certain rational fractions of LL's are filled. The theoretical understanding of this phenomenon starts with Laughlin's approach in 1983 [4]. He proposed a variational wavefunction for the ground state at $\nu = 1/p$, $p = \text{odd}$, which is a fractionally filled lowest Landau level (LLL). Assuming that ω_c is large compared to the electron-electron interaction, only the LLL should describe the physics at low energies. For N electrons with coordinates $z_i = x_i + iy_i$, the Laughlin wavefunction is,

$$\psi(z_1, \dots, z_N) = \prod_{i < j}^N (z_i - z_j)^p \prod_i^N e^{-|z_i|^2/4\ell_B^2} .$$

This function is composed of single particle states in the LLL and is properly antisymmetric in keeping with fermionic statistics. The two main features of Ψ are (i) there is a zero on each electron, and (ii) each electron sees other electrons as magnetic flux due to the accumulated phase in dragging one coordinate around another. The basic excitations are quasiholes and quasielectrons with fractional charge $\pm e/p$. Clearly this kind of effect is due to strong correlations in the fluid. The quasiparticles also obey fractional statistics, as articulated by Halperin [5] and by Arovas et al. [6]. Experimental data is consistent with fractional charge at $\nu = 1/3$ and that the basic excitations at $\nu = 1/2$ are neutral [7, 8, 9]. Already we see a collective behavior that is very different from Fermi liquids. In fact, the Laughlin state describes a strongly correlated quantum liquid that cannot be reached perturbatively from the Fermi liquid. As originally noted by Laughlin, it is accepted that the FQHE liquid is isotropic and incompressible.

Much of the current understanding of quantum liquids relies on effective field theories. In the case of the FQHE the most successful has been the Chern-Simons (CS) theory [10]. Fortuitously, CS actions were being formally developed concurrently in a purely field theoretic context [11]. One starts with a transformation that represents each electron as a boson plus an odd number of $\tilde{\phi}$ of δ -flux tubes. Fractional statistics emerges as a Berry phase when particles or vortices are dragged around flux tubes. After the transformation, the action contains a U(1) Chern-Simons term that couples to the fermion density. At the fractions $\nu = 1/q$ (q =odd), the statistical gauge potential \mathbf{a} is determined by the relation

$$\rho = -\frac{\nu}{2\pi}\nabla \times \mathbf{a} \quad (1.2)$$

(where $\hbar = c = 1$). The full Lagrangian includes \mathbf{a} by minimal coupling and the statistical gauge transformation allows us to replace the fermions by a bosonic field, ϕ . The complete gauge invariant Lagrangian is

$$\begin{aligned} \mathcal{L}_{CS} = & \phi^\dagger (i\partial_t - A_0 - a_0)\phi - \frac{1}{2m} |(i\nabla + \mathbf{A} + \mathbf{a})\phi|^2 + \frac{\nu}{4\pi}\epsilon^{\mu\nu\lambda}a_\mu\partial_\nu a_\lambda \\ & - \frac{1}{2}\int d^2y \rho(x)V(x-y)\rho(y) , \end{aligned} \quad (1.3)$$

where A_0, \mathbf{A} is the external potential. The third term is the U(1) CS term (ϵ is the Levi-Civita symbol) and the last term is the interaction. The defining equation (1.2) for \mathbf{a} can be viewed as an equation of motion. To completely determine \mathbf{a} , one can use conservation of charge, $\partial_t \rho + \partial_i J_i = 0$, to obtain the dynamics equation, $J_i = -\frac{\nu}{2\pi}\epsilon^{ij}\partial_t a_j$. Together with eqn. (1.2) this completely determines the statistical gauge field \mathbf{a} .

The net field is the sum of the external field and the δ -flux tubes. On the average, for a uniform density of particles, the two fields cancel when $\nu = 1/\tilde{\phi}$ (that is, $\langle \mathbf{A} + \mathbf{a} \rangle = 0$) and we are left with bosons in zero net field. The Laughlin state can thus be interpreted as a bose condensate of the electron-flux tube composite. In principle, one can substitute bosonic particles for electrons and use an even $\tilde{\phi}$. Some understanding of the states with even denominator, e.g. $\nu = 1/2$, has been achieved in this framework [2]. In this case, the composite fermions form a Fermi sea and the resultant phase is Fermi-liquid like. Paired states of fermions or bosons are envisioned as pairing of particle-flux tube composites in zero field, since the external field vanishes at mean field, as discussed in the introductory

Section 1.2 and in Chapters 4 and 5. Any analysis beyond mean field must proceed with caution in any case; standard techniques are exact only in the limit $\tilde{\phi} \rightarrow 0$, but the FQHE states require $\tilde{\phi} \geq 2$.

Other, perhaps more fundamental, difficulties with the CS approach have been appreciated by several workers since the beginning (see e.g. [12]). At zero temperature, the usual assumption is that the inter-electron interactions $\sim \nu^{1/2}e^2/\varepsilon\ell_B$ are weak compared to the cyclotron frequency ω_c so the physics should be dominated by LLL states when $\nu < 1$. The kinetic energy is just a constant in any given LL so we are faced with a macroscopically degenerate perturbation theory with a purely dynamical Hamiltonian. In particular, consider the Fermi liquid-like state at $\nu = 1/2$. In the mean field approximation, the effective mass of excitations close to the Fermi surface is the bare mass m , however the low-energy excitations should have an effective mass m^* determined solely by the interactions. The problem is partially resolved by Fermi liquid fluctuations, which introduce a Landau interaction parameter F_1 that renormalizes the bare mass by $m^{-1} = m^{*-1}(1 + F_1)$. The most serious problem is that interactions do not play a role in the compressibility; whether or not interactions are included in the fluctuations, the result is a finite compressibility for the Fermi liquid due to the mass m . On the other hand, a partially filled Landau level of non-interacting particles should have an infinite compressibility. The same difficulty is present in the odd denominator filling fractions; regardless of the interaction, the compressibility vanishes [10]. There has been a renewed interest in these puzzles recently, stemming from new developments in composite fermion theory.

It has become clear that a more physical way of looking at the composite particles is as bound states of one particle and $\tilde{\phi}$ vortices. The composites are literally dipoles. Since the quantum Hall liquid cannot be reached perturbatively from a normal electron fluid, Landau's Fermi liquid theory cannot be applied, and the new quasiparticle must be built up from scratch. This notion developed steadily starting from Laughlin's observation that particles see other particles as flux [4]. Jain used it to obtain the basic sequence of fractional quantum Hall plateaus [13], and Haldane [14] and Halperin [5] constructed a complete hierarchy of states. Their approach relied solely on the analytic properties of ground state wavefunctions. The corresponding field theoretic implementation is the class

of CS models outlined above. In spite of the successes of these descriptions, neither does justice to the particle-vortex composites as bound states (dipoles) in their own right.

This thesis will clarify that perhaps this is the essential ingredient required for a self-consistent understanding of the effective mass and compressibility issues. Several authors have applied the dipole scenario with some success [12, 15, 16, 17, 18, 19, 20]. The works of Lee [20] and of Shankar and Murthy [15, 16, 17] reconsider the Chern-Simons action and recover some of the dipole physics. Here, we will approach the problem from the opposite direction by working in the LLL at the outset without any singular flux attachment. The language no longer includes δ -flux tubes or $\tilde{\phi}$, rather particle-vortex dipoles are the basic building blocks. Our guide is a formalism introduced by Haldane and Pasquier [19] and applied by Read [18]. These authors considered *bosons* at $\nu = 1$, which is presumably qualitatively identical to fermions at even denominator filling fractions. Both the effective mass and compressibility puzzles inherent in the original Chern-Simons approach are resolved in this way (at least for bosons at $\nu = 1$).

Our first task, in the following chapter, is to extend the Haldane-Pasquier formalism to arbitrary ν for either fermions or bosons. In the case of bosons, Chapter 2, we will obtain an effective theory microscopically by following Read's analysis at $\nu = 1$. The effective action does lead to a consistent picture of the mass and compressibility, but differs fundamentally from the CS action; there is no *a priori* reason the two actions ought to look similar since we project to the LLL from the beginning. However, it is gratifying that some of our results overlap with those of Shankar and Murthy, who do start with CS.

In Chapter 3, we construct a phenomenological Landau-Ginzburg field theory for $\nu = 1/p$, i.e. the underlying particles must be fermions for $p = \text{odd}$ and bosons for $p = \text{even}$. The spectrum in this case contains a magnetoroton dip, which is the first analytical observation of this phenomenon.

A central theme running through both of these chapters is the internal structure of the composite particles. To compensate for the extra degrees of freedom of the vortices, a set of constraints is introduced and appears throughout our models.

1.2 Pairing in Two Dimensions

The standard theory for superconductivity was introduced by Bardeen, Cooper, and Schrieffer (BCS) almost fifty years ago [21]. The original ground state was a paired state of fermions in the s-wave channel, or relative angular momentum $l = 0$. Since then, there have been numerous generalizations to non-zero angular momentum and to other more complicated order parameters. For a review, of the rich phase diagrams in He^3 , see the book by Vollhardt and Wölfle [22]. We refer to the non-zero angular momentum states as anomalous in the sense that they violate both parity and time reversal symmetry. Typically, BCS theory is applied to fermionic particles, which can be thought of as pairing into bosons which then condense. A less widely appreciated body of work treats pairing of bosons [23]. We explore instances of both statistics in Chapters 4 and 5. There is growing evidence of anisotropic superconductivity in the perovskite oxides. In Sr_2RuO_4 , both experiment [24] and theory [25] support p-wave ($l = -1$) pairing. Similarly, d-wave pairing ($l = -2$) is by now well established in the high temperature superconductors [26]. p-wave pairing has also been observed in superfluid He^3 in the so-called “A-phase” [22].

In the context of the fractional quantum Hall effect, Halperin [27] proposed that under certain conditions, electrons can form pairs that condense into a Laughlin state of charge-2 bosons. Since then, various alternatives for p- and d-wave pairing have been explored by several groups [28, 30, 31, 32, 33, 34, 35]. An intriguing possibility is that the observed plateau at $\nu = 5/2$ is the Pfaffian state of Moore and Read [28, 33, 36].

Recently it has been proposed that the spin conductivity of the class of p- and d-wave states is transverse and quantized [37]. A remarkable series of earlier papers by Volovik [38] contained some of these predictions, as well. However, the precise proof of this proposal has not been shown. Section 5 contains our derivation of this effect with a conserving approximation. In the context of the original BCS theory, a conserving approximation is required for a correct description of the collective mode [21, 39] since it respects charge conservation. Analogously, in our case, the conserving approximation will respect the conservation of spin current, leading to the correct result.

A less familiar application of BCS theory is to paired states of bosons (see for example [23]). Typically, there is a competition between the usual single-particle condensate and a

pure paired state, or a phase of coexistence is possible.

Pure p-wave pairing of spin-1/2 bosons is characterized by a BCS wavefunction in the form of a permanent. We will show that p-wave pairing can be interpreted as a condensate of spin waves. As parameters in the Hamiltonian are tuned, one reaches another single particle condensate with helical spin order. The permanent sits right on the transition and contains a single anti-Skyrmion, which is yet another single particle condensate.

In the context of the fractional quantum Hall effect (FQHE), the permanent describes singlet pairs of spin-1/2 composite bosons with filling factor $\nu = 1/p$, p odd [28, 30]. It is the unique ground state wavefunction of a Hamiltonian which penalizes the closest approach of three spin-1/2 fermions for a fixed number of flux quanta piercing the bulk. The exact number of flux threading the bulk depends upon the geometry, e.g. on whether the system is on the torus, on the sphere, or on the plane. Although the permanent itself is difficult to treat analytically, its Hamiltonian contains an infinite set of degenerate zero-energy eigenstates when flux is added, among which is the polarized Laughlin state, and the rest are interpreted in one of two equivalent ways as either quasiholes or as spin wave excitations. The $p = 1$ Laughlin state is most amenable to analysis as it is a Slater determinant of single particle wavefunctions (Section 3.1.c). Accordingly, it will serve as the prototype for our exact statements.

We also consider d-wave pairing of spinless bosons, which is known as the Haffnian in FQHE literature [32]. A rich phase diagram of competing single particle and paired condensates emerges, with the Haffnian sitting on a phase boundary.

In the case of pairing in the FQHE, the bosons (fermions) are to be thought of as composite bosons (fermions), as described in Chapter 2. We can use CS mean field theory such that the CS gauge field cancels the external field on the average, and we are left with composite particles in zero net field. Then we can treat the composite particles within a BCS approximation. The case of composite fermions, which was addressed recently [35], serves as a point of reference for composite boson pairing. The central theme in ref. [35] was the existence of two regimes, weak- and strong-pairing. The weak-pairing phase can be characterized by a nontrivial topological winding of the BCS order parameter in momentum space; we will see an example in the discussion of the quantum Hall effect for spin in Chapter

5. On the other hand, the strong-pairing phase is topologically trivial, and, in the simplest case, the two phases are separated by a transition at zero chemical potential. For example, the Pfaffian state [28] is a weak-pairing phase, while the Haldane-Rezayi state [29], which is an $l = -2$ state, was found to lie at the weak-strong transition point. It is useful to keep these results in mind as we consider composite boson pairing in this chapter.

1.3 Adsorption on Carbon Nanotubes

Monolayer adsorption of noble gases onto graphite sheets has proven to be an interesting problem both theoretically and experimentally [40, 41, 42]. Many of the observed features can be understood within a lattice gas model, where the underlying hexagonal substrate layer forms a triangular lattice of preferred adsorption sites. An equivalent formulation is in the language of spin models on a triangular lattice, where the repulsion between adsorbed atoms in neighboring sites translates into an antiferromagnetic Ising coupling. The frustration of the couplings by the triangular lattice leads to the rich phase diagram of the monolayer adsorption problem [41]. Introducing hopping adds quantum fluctuations, further enriching the phase diagram [42, 43].

In this Chapter we address what happens if, in addition to the triangular lattice frustration, one has an extra geometric frustration due to periodic boundary conditions. In fact, such a system is physically realized by a single walled carbon nanotube [44], which may be viewed as a rolled graphite sheet. In this context, adsorption has been the subject of growing experimental and theoretical interest [45, 46] spurred by potential applications. Stan and Cole [45] have considered the limit of non-interacting adatoms at low density, finding that they are localized radially near a nanotube's surface at a distance comparable to that in flat graphite ($\sim 3\text{\AA}$). In that work, it was sufficient to omit the hexagonal structure of the substrate. However, the corrugation potential selects the hexagon centers as additional commensurate localization points [40]. In view of the similarity to flat graphite, we include both the substrate lattice and adatom interactions and consider a wider range of densities. In fact, very recently, it has been shown [47] that the adsorbate stays within a cylindrical shell for fillings less than $\approx 0.1/\text{\AA}^2$ (or ≈ 0.5 adatom/hexagon), justifying the densities

studied here.

Our adsorption model is equivalent to a new sort of XXZ Heisenberg quantum spin tube, which is type of spin ladder with periodic boundary conditions. A simple example with highly anisotropic couplings was considered recently in references [48]. We find density plateau structures for armchair, zig-zag and chiral nanotubes. In the language of spin systems, the density plateaus correspond to magnetization plateaus. The zig-zag tubes turn out to be special, and have extensive zero temperature entropy plateaus in the classical limit. Quantum effects lift the degeneracy, leaving gapless excitations described by a $c = 1$ conformal field theory with compactification radius quantized by the tube circumference. This is an interesting conformal symmetry because the only other systems in nature with a quantized compactification radius, that we are aware of, are the chiral edge states in the FQHE [49].

Chapter 2

Lowest Landau Level I: Composite Fermions

We begin this chapter by developing the Haldane-Pasquier formalism in Section 2.1.

In the rest of the chapter we apply the composite fermion formalism to bosons in the lowest Landau level. In particular, we obtain an effective theory for an incompressible quantum Hall liquid of bosons with one attached vortex at general filling. As discussed in the introduction, theories based on the flux attachment, or Chern-Simons approach [10], have not been entirely satisfactory. More recently there have been several attempts to obtain an effective theory microscopically [15, 19, 20], which too have had difficulties. In this work we avoid the Chern-Simons approach and follow an alternative that was developed for the Fermi liquid-like state of bosons at $\nu = 1$ [18].

The effective filling factor in our composite fermion model can be obtained as follows. As we will see below, the composite feels an effective magnetic field $B = B_L + B_R$, where B_L is the physical field felt by the underlying particle and B_R is an arbitrary field felt by the vortex. The total charge of the composite is $q^* = 1 + B_R/B_L$. In the introduction we showed that the filling factor can be written as $\nu = \rho\Phi_0/B_L$, where ρ is the density of the underlying particles and Φ_0 is the magnetic flux quantum. Since the composite particles must have the same density as the underlying particles, the effective filling is $\nu_{\text{eff}} = \rho\Phi_0/B$,

which can be rewritten as

$$\nu_{\text{eff}} = \frac{\nu}{q^*}, \quad (2.1)$$

The original Jain construction [13] begins with particles of charge $+1$ at $\nu = 1/p$ and attaches $\tilde{\phi}$ flux tubes. On the average, the flux tubes renormalize the real magnetic field by $B_L \rightarrow q^* B_L$ with $q^* = 1 - \tilde{\phi}\nu$. In our framework, q^* can be any real number, so there is a family of theories, i.e. anyons [50], for *any* given ν parameterized by q^* and an integer ν_{eff} .

Strictly speaking, Jain's model does not require fermionic statistics for the underlying particles, so the bosonic case is a valid quantum Hall state. In fact, there have been recent theoretical proposals that quantum Hall liquids of bosons are realizable in rotating Bose-Einstein condensates [51]. In this case, the magnetic field is due to the angular velocity ω ; roughly, the velocity is modified in the rotating frame by $\mathbf{v} \rightarrow \mathbf{v} + \omega \times \mathbf{r}$, which is like minimal coupling of a magnetic field ($\nabla \times (\omega \times \mathbf{r})$ is a constant in the same direction as ω).

In section 2.2 we obtain an effective mass by extracting a kinetic term from the interaction Hamiltonian. This problem has been central to the recent work in references [15, 19]. The simplest starting point is a Hartree-Fock approximation. Next, we use a conserving approximation, which restores the constraints, in order to calculate the correct density-density response function. The self-consistent diagrammatics consist of summing ring and ladder diagrams; it is essentially the same framework that we use for paired states of fermions in Chapter 5 of this thesis.

2.1 Formalism

2.1.a Single Particle in a Magnetic Field

A convenient framework for a quantum particle in two dimensions is an operator description. We begin with the simplest case of a single charged particle in two dimensions and a perpendicular magnetic field.

The Hamiltonian is

$$H = \frac{1}{2m}(\mathbf{p} - q\mathbf{A})^2, \quad (2.2)$$

where \mathbf{p} is the canonical momentum, \mathbf{A} is the vector potential for a magnetic field B , in the $\hat{\mathbf{z}}$ direction, and q and m are the charge and mass. The units are set to $\hbar = c = 1$.

The kinetic momentum is defined by

$$\pi = \mathbf{p} - q\mathbf{A} \quad (2.3)$$

with the corresponding commutator

$$[\pi_\mu, \pi_\nu] = i\epsilon_{\mu\nu}qB \quad (2.4)$$

where μ and ν are space indices, x and y , and $\epsilon_{\mu\nu}$ is the Levi-Civita symbol. The dynamics of π follow simply,

$$\dot{\pi}_\mu = i[H, \pi_\mu] = \omega_c \epsilon_{\mu\nu} \pi_\nu, \quad (2.5)$$

where $\omega_c = qB/m$ is the cyclotron frequency. Therefore π precesses.

As the particle executes cyclotron motion it is located by the guiding center operator

$$\mathbf{R} = \mathbf{r} + \hat{\mathbf{z}} \times \pi \frac{1}{qB} \quad (2.6)$$

which obeys

$$[R_\mu, R_\nu] = -i\epsilon_{\mu\nu} \frac{1}{qB}. \quad (2.7)$$

The operators π and \mathbf{R} commute. Projection to the lowest Landau level is accomplished by replacing the particle's coordinates by the guiding center. Note that the coordinates no longer commute, a consequence of frozen degrees of freedom. The appropriate generator of translations, or “pseudomomentum”, is defined by

$$\mathbf{K} = qB\hat{\mathbf{z}} \times \mathbf{R}, \quad (2.8)$$

and obeys $[K_\mu, K_\nu] = i\epsilon_{\mu\nu} \frac{1}{qB}$. The planar coordinates of a quantum particle in a magnetic field are a well-known example of non-commutative space [91].

Noting the commutation relations of π and R , we can define two independent harmonic oscillator operators:

$$a = \sqrt{\frac{1}{2qB}} \bar{K}, \quad a^\dagger = \sqrt{\frac{1}{2qB}} K \quad (2.9)$$

$$b = \sqrt{\frac{1}{2qB}} \pi, \quad b^\dagger = \sqrt{\frac{1}{2qB}} \bar{\pi} \quad (2.10)$$

where $\pi = \pi_x + i\pi_y$ and $\bar{\pi} = \pi_x - i\pi_y$, and similarly for K . The Hamiltonian then becomes the familiar harmonic oscillator Hamiltonian:

$$H = \omega_c \left(b^\dagger b + \frac{1}{2} \right) . \quad (2.11)$$

Its eigenstates are known as Landau levels (LL). Each level is macroscopically degenerate since a commutes with b and drops out of the Hamiltonian. The complete set of eigenstates is labeled by two integers, m and n :

$$|n, m\rangle = \frac{a^{\dagger m}}{\sqrt{m!}} \frac{b^{\dagger n}}{\sqrt{n!}} |0, 0\rangle \quad (2.12)$$

In this convention, π (or b) is a purely inter-Landau level operator, and \mathbf{K} (or a) is intra-Landau level.

To obtain the wavefunctions, we will use complex coordinates, $\mathbf{r} = z = x + iy$, and the symmetric gauge, $\mathbf{A} = -\frac{1}{2}\mathbf{r} \times \mathbf{B} = \frac{1}{2}B(-y, x)$. The single particle operators become

$$\pi = -2i\partial_{\bar{z}} - \frac{qB}{2}iz \quad (2.13)$$

$$K = -2i\partial_{\bar{z}} + \frac{qB}{2}iz \quad (2.14)$$

If we restrict ourselves to the lowest Landau level (LLL), then the wavefunctions, $\psi_{0,m}(\mathbf{r})$, are annihilated by b . The general solution to this first order partial differential equation (up to gauge transformations) is

$$\psi_{0,m}(\mathbf{r}) = f_m(z) e^{-|z|^2/4\ell_B^2} , \quad (2.15)$$

where $\ell_B^2 = 1/|qB|$ is the magnetic length. The great simplification is that $f_m(z)$ must be an analytic function in z . Further requiring that $a\psi_{0,0} = 0$ yields f_0 and the rest of the f_m 's are generated by applying a^\dagger . The result is the set of states spanning the LLL:

$$u_m(z) = \frac{1}{\sqrt{2\pi 2^m m! \ell_B^{m+2}}} z^m e^{-|z|^2/4\ell_B^2} . \quad (2.16)$$

It should be remarked that the intra-LL ladder operator has a very simple action on the u_m : $a^\dagger = z/\sqrt{2}\ell_B$ and $a = (\ell_B/\sqrt{2})\partial_z$.

2.1.b Two Particles in a Magnetic Field

In this section, we introduce a bound state of two oppositely charged particles in a perpendicular magnetic field. This formalism will be useful in interpreting the Haldane-Pasquier approach.

Each component is characterized by its charge q_i and the magnetic field that it feels, B_i . For convenience, we define

$$B_i = q_i B \quad (2.17)$$

We will assume that $B_1 > 0$ and $B_2 < 0$, guaranteeing the existence of a bound state. In these units the charge is dimensionless. If we fix $q_1 = 1$ then the total charge is

$$q^* = \frac{B}{B_1} \quad (2.18)$$

There are two sets of guiding centers, $R_{\mu i}$, and pseudomomenta, $K_{\mu i}$, which are defined in the same way as in section 2.1.a. The algebra consists of two copies of the single particle, for example

$$[R_{\mu i}, R_{\nu j}] = -i\epsilon_{\mu\nu}\delta_{ij}\frac{1}{B_i}, \quad (2.19)$$

and so on.

It turns out that this algebra can be mapped exactly into a single particle in an effective magnetic field B [52],

$$B = B_1 + B_2 .$$

If we construct the effective translation and momentum operators by

$$K = K_1 + K_2 \quad (2.20)$$

$$\pi = \sqrt{-B_1 B_2} \left(\frac{1}{B_2} K_2 - \frac{1}{B_1} K_1 \right) \quad (2.21)$$

then the commutators of this algebra are exactly that of a single particle, equations (2.4, 2.7, 2.8). For example $[\pi_\mu, \pi_\nu] = i\epsilon_{\mu\nu}B$. The physical picture becomes clearer once we define an effective position \mathbf{r} by eqn. (2.6). Solving for \mathbf{r} , we find

$$\begin{aligned} \mathbf{r} &= -\hat{z} \times (K + \pi)\ell_B^2 \\ &= \frac{B_1 \mathbf{R}_1 + B_2 \mathbf{R}_2}{B} - (\mathbf{R}_1 - \mathbf{R}_2) \frac{\sqrt{-B_1 B_2}}{B} . \end{aligned} \quad (2.22)$$

In the limit $B \rightarrow 0$, \mathbf{r} becomes $(\mathbf{R}_1 + \mathbf{R}_2)/2$. This is not surprising from a classical point of view; two opposite but equal charges travel in a straight line due to $\mathbf{E} \times \mathbf{B}$ drift, the “guiding center” moves off to infinity, and their position is given by a point exactly midway between them.

To proceed with the wavefunctions of the composite, label the real-space coordinates of each particle by z and η . The differential operators are given by

$$K_1 = -2i\partial_{\bar{z}} + \frac{i}{2\ell_{B_1}^2}z \quad (2.23)$$

$$K_2 = -2i\partial_{\bar{\eta}} - \frac{i}{2\ell_{B_2}^2}\eta \quad (2.24)$$

Note the relative minus sign, which comes from assuming $B_1 > 0$ and $B_2 < 0$. The ladder operators are given in terms of π and K by equation (2.10). The lowest eigenfunction is determined from $a\psi_{0,0} = b\psi_{0,0} = 0$:

$$\begin{aligned} \frac{i}{\sqrt{2B}} \left[\left(-2\partial_z - \frac{1}{2\ell_{B_1}^2}\bar{z} \right) + \left(-2\partial_{\eta} + \frac{1}{2\ell_{B_2}^2}\bar{\eta} \right) \right] \psi_{0,0} &= 0 \\ \frac{i}{\sqrt{2B}} \left[\frac{1}{B_1} \left(-2\partial_{\bar{z}} + \frac{1}{2\ell_{B_1}^2}z \right) - \frac{1}{B_2} \left(-2\partial_{\bar{\eta}} - \frac{1}{2\ell_{B_2}^2}\eta \right) \right] \psi_{0,0} &= 0 \end{aligned} \quad (2.25)$$

By analogy with a single particle, we expect that the solution is an analytic function in z and η times two Gaussian factors. Indeed, if we choose

$$\psi_{0,0}(z, \eta) = \phi(z, \bar{\eta}) e^{-|z|^2/4\ell_{B_1}^2} e^{-|\eta|^2/4\ell_{B_2}^2}$$

then equations (2.25) are solved by

$$\phi(z, \eta) = \frac{1}{2\pi\ell_{B_1}\ell_{B_2}} e^{z\bar{\eta}/2\ell_{B_2}^2} . \quad (2.26)$$

Note the asymmetry between $B_1 \leftrightarrow B_2$, stemming from the sign of B . We have implicitly assumed that $B > 0$, but if $B < 0$ then the Gaussian factor in eqn. (2.26) would be $\ell_{B_1}^2$.

The complete set of states is generated by a^\dagger and b^\dagger just as it was for one particle in eqn. (2.12),

$$\psi_{\lambda\mu}(z, \bar{\eta}) = \langle z, \bar{\eta} | \lambda\mu \rangle = \frac{b^{\dagger\lambda}}{\sqrt{\lambda!}} \frac{a^{\dagger\mu}}{\sqrt{\mu!}} \psi_{0,0}(z, \bar{\eta}) . \quad (2.27)$$

The $\psi_{\lambda\mu}$ are linear combinations of the independent particle basis

$$\langle z, \bar{\eta} | mn \rangle = u_m(z) \overline{v_n(\eta)} , \quad (2.28)$$

where u and v are LLL single particle states corresponding to the two magnetic lengths ℓ_{B_1} and ℓ_{B_2} , as in eqn. (2.16).

2.1.c Fock Space, Operators, and Constraints

Having constructed the basis functions for a particle-vortex pair in the previous section, we move on to the Fock space for a many-particle system.

We begin with canonical fermionic or bosonic operators which are matrices with two indices, c_{mn} , with (anti-)commutation relations

$$[c_{mn}, c_{n'm'}^\dagger]_\pm = \delta_{mm'} \delta_{nn'} \quad (2.29)$$

The left index, m , runs from 1 to N_ϕ , the number of available states in the LLL. The right index, n , runs 1 through N , which we will interpret later as the number of vortices. In the thermodynamic limit, the filling factor is $\nu = N/N_\phi$. Strictly speaking, this construction must be carried out on a finite geometry (e.g. m runs from 1 to $N_\phi + 1$ on the sphere), but we will ignore this subtlety here since we will only be interested in the thermodynamic limit.

The anticommutation relations are invariant under independent transformations on the left and right indices:

$$c \mapsto U_L c U_R, \quad (2.30)$$

where U_L and U_R are $N_\phi \times N_\phi$ and $N \times N$ unitary matrices. These transformations are generated by the left and right “density” operators

$$\begin{aligned} \rho_{nn'}^R &= \sum_{m=1}^{N_\phi} c_{nm}^\dagger c_{mn'} \\ \rho_{mm'}^L &= \sum_{n=1}^N c_{nm}^\dagger c_{m'n} \end{aligned} \quad (2.31)$$

The left density ρ^L will represent the physical density, as we will see below. The right density ρ^R specifies a set of N^2 constraints, which we use to define a set of physical states,

$$\left(\rho_{nn'}^R - \delta_{nn'} \right) |\Psi_{\text{phys}}\rangle = 0. \quad (2.32)$$

It will be shown shortly that the set of $|\Psi_{\text{phys}}\rangle$ do indeed give the correct Fock space.

Because the ρ^R generate the unitary group $U(N)_R$ and there is a phase factor, $U(1)$, common to both ρ^R and ρ^L , the physical states must be singlets under $SU(N)_R$. The physical states solving this constraint are linear combinations of

$$|\Psi_{\text{phys}}^{m_1 \dots m_N}\rangle = \sum_{n_1 \dots n_N} \epsilon^{n_1 \dots n_N} c_{n_1 m_1}^\dagger c_{n_2 m_2}^\dagger \dots c_{n_N m_N}^\dagger |0\rangle, \quad (2.33)$$

where $|0\rangle$ is the vacuum with no fermions. The Levi-Civita symbol ϵ ensures that these states are singlets under $SU(N)_R$. If the c 's are fermions their anticommutation relations ensure that $|\Psi_{\text{phys}}^{m_1 \dots m_N}\rangle$ is symmetric under the interchange of any pair $m_i \leftrightarrow m_j$. Therefore, the physical space is equivalent to N bosons each of which can occupy any one of N_ϕ states, i.e. the Fock space of bosons at filling $\nu = N/N_\phi$. Had the c 's been bosonic operators rather than fermionic, the result would have been a Fock space of fermions at the same filling.

We now construct the many body operators. By mapping into a single particle, we showed that the effective magnetic length is

$$\frac{1}{\ell_B^2} = \frac{1}{\ell_{B_L}^2} - \frac{1}{\ell_{B_R}^2} \quad (2.34)$$

As a reminder of the physical picture, we have made the notation change from $1, 2$ to L, R . Our convention guarantees that ℓ_B is positive since $\ell_{B_L} < \ell_{B_R}$ (equivalently, $|B_L| > |B_R|$ and $B = B_L + B_R > 0$).

In real space the matter field is defined by

$$c(z, \bar{\eta}) = \sum_{mn} u_m^L(z) \overline{u_n^R(\eta)} c_{mn} \quad (2.35)$$

where $u_m^L(z) = z^m \exp\{-|z|^2/4\ell_{B_L}^2\}$ and $u_n^R(\eta) = z^m \exp\{-|\eta|^2/4\ell_{B_R}^2\}$ (apart from normalizations). A unitary transformation connects the $|mn\rangle$ independent particle basis to the $|\mu\lambda\rangle$ bound state basis in section 2.1.b. Accordingly, the fermions c_{mn} transform into

$$c_{\mu\lambda} = \sum_{mn} c_{mn} \langle mn | \mu\lambda \rangle, \quad (2.36)$$

where

$$|\mu\lambda\rangle = \frac{a^{\dagger\mu}}{\sqrt{\mu!}} \frac{b^{\dagger\lambda}}{\sqrt{\lambda!}} |0, 0\rangle. \quad (2.37)$$

The overlap $\langle mn|\mu\lambda\rangle$ is obtained from the definitions in eqns. (2.27) and (2.28). To write the density operators, we observe that they take a plane wave form in the operator language: $\hat{\rho}_{\mathbf{q}}^R = \sum_i e^{i\mathbf{q}\cdot\mathbf{R}_{i,R}}$ and $\hat{\rho}_{\mathbf{q}}^L = \sum_i e^{i\mathbf{q}\cdot\mathbf{R}_{i,L}}$, where $\mathbf{R}_{i,R}$ and $\mathbf{R}_{i,L}$ are the two guiding center coordinates of the i 'th particle.* In second quantization, the left density becomes

$$\hat{\rho}_{\mathbf{q}}^L = \sum_{\mu\lambda, \mu'\lambda'} c_{\lambda\mu}^\dagger c_{\mu'\lambda'} \langle \mu\lambda | e^{i\mathbf{q}\cdot\mathbf{R}_L} | \mu'\lambda' \rangle \quad (2.38)$$

and similarly for $\hat{\rho}_{\mathbf{q}}^R$. The matrix element can be calculated by solving for $\mathbf{R}_{R,L}$ in terms of \mathbf{K} , π , giving

$$\begin{aligned} \mathbf{R}_L &= \wedge(\mathbf{K} + \frac{\ell_{B_L}}{\ell_{B_R}} \pi) \ell_B^2 \\ \mathbf{R}_R &= \wedge(\mathbf{K} + \frac{\ell_{B_R}}{\ell_{B_L}} \pi) \ell_B^2 . \end{aligned} \quad (2.39)$$

We have introduced the shorthand notation, $\wedge \mathbf{a} = -\hat{z} \times \mathbf{a}$ (for the vector \mathbf{a}). Because $[\mathbf{K}, \pi] = 0$, the plane wave factors into an intra- and an inter-Landau level piece. We write

$$\begin{aligned} \hat{\rho}_{\mathbf{q}}^L &= \sum_{\mu\lambda, \mu'\lambda'} \rho_{\mathbf{q}}(\mu|\mu') \rho_{\mathbf{q}}^L(\lambda|\lambda') c_{\lambda\mu}^\dagger c_{\mu'\lambda'} \\ \hat{\rho}_{\mathbf{q}}^R &= \sum_{\mu\lambda, \mu'\lambda'} \rho_{\mathbf{q}}(\mu|\mu') \rho_{\mathbf{q}}^R(\lambda|\lambda') c_{\lambda\mu}^\dagger c_{\mu'\lambda'} , \end{aligned} \quad (2.40)$$

where the ρ -coefficients are defined by

$$\begin{aligned} \rho_{\mathbf{q}}(\mu|\mu') &= \langle \mu | \exp \left\{ i \ell_B^2 \mathbf{q} \wedge \mathbf{K} \right\} | \mu' \rangle \\ \rho_{\mathbf{q}}^L(\lambda|\lambda') &= \langle \lambda | \exp \left\{ i \ell_B^2 \frac{\ell_{B_L}}{\ell_{B_R}} \mathbf{q} \wedge \pi \right\} | \lambda' \rangle \\ \rho_{\mathbf{q}}^R(\lambda|\lambda') &= \langle \lambda | \exp \left\{ i \ell_B^2 \frac{\ell_{B_R}}{\ell_{B_L}} \mathbf{q} \wedge \pi \right\} | \lambda' \rangle . \end{aligned} \quad (2.41)$$

The operation $\mathbf{a} \wedge \mathbf{b}$ stands for $\mathbf{a} \cdot \wedge \mathbf{b}$. Note that $\hat{\rho}_{\mathbf{q}}$ is identical to $\hat{\tau}_{\mathbf{q}}$ for a particle in field B and therefore follow the same orthonormality properties and commutation relations. $\rho_{\mathbf{q}}^L$ and $\rho_{\mathbf{q}}^R$ are similar but with an additional factor of ℓ_{B_L}/ℓ_{B_R} or ℓ_{B_R}/ℓ_{B_L} in the phase of the commutator.

Since K and π are nothing other than harmonic oscillator operators, the $\hat{\rho}$'s can be calculated explicitly. The one that we need later is $\hat{\rho}_{\mathbf{q}}^L$, so we use it as an example. First,

*I was reminded by R. Shankar that he had guessed the same density expressions based on a small \mathbf{q} limit of the Chern-Simons formulation [16].

rewrite $i\mathbf{q} \wedge \pi$ in complex coordinates as $\frac{1}{2}(\bar{q}\pi - q\bar{\pi})$. Secondly, recall that $b \sim \pi$ and $|\lambda\rangle \sim b^\dagger|\lambda\rangle|0\rangle$, which reduces the calculation to a harmonic oscillator matrix element. The rest is straightforward and we quote the final result:

$$\rho_{\frac{\sqrt{2}}{\ell_B} \frac{\ell_{B_R}}{\ell_{B_L}} \mathbf{q}}^L(\lambda|\lambda') = \frac{1}{\sqrt{\lambda!}} \frac{1}{\sqrt{\lambda'!}} e^{q\bar{q}/2} (-\partial_{\bar{q}})^\lambda (\partial_q)^{\lambda'} e^{-q\bar{q}}. \quad (2.42)$$

A bunch of factors were absorbed into \mathbf{q} on the left-hand side to avoid repetitiously writing them on the right.

The final step in the construction is the Hamiltonian. In coordinate space it involves only the diagonal components of $\hat{\rho}^L$ [18],

$$H = \frac{1}{2} \int d^2 z_1 d^2 z_2 V(\mathbf{r}_1 - \mathbf{r}_2) : \rho^L(z_1, \bar{z}_1) \rho^L(z_2, \bar{z}_2) : \quad (2.43)$$

Or in Fourier space (Appendix),

$$H = \frac{1}{2} \int \frac{d^2 \mathbf{q}}{(2\pi)^2} V(\mathbf{q}) e^{-|\mathbf{q}|^2/2\ell_{B_L}^2} : \hat{\rho}_{\mathbf{q}}^L \hat{\rho}_{-\mathbf{q}}^L : \quad (2.44)$$

where $V(\mathbf{q})$ is the ordinary Fourier transform of $V(\mathbf{r})$. As required, this Hamiltonian is both translationally and rotationally invariant. By construction, the right density $\hat{\rho}^R$ is a constant of the motion because the Hamiltonian acts only on the left indices, i.e.

$$[H, \hat{\rho}_{\mathbf{q}}^R] = 0. \quad (2.45)$$

The system of Hamiltonian plus constraints is the starting point for Read's analysis of composite bosons at $\nu = 1$ [18].

2.2 Hartree-Fock Approximation

For convenience, we restate here the Hamiltonian that we derived in the last section.

$$H = \frac{1}{2} \sum_{\mu_i, \lambda_i} \int \frac{d^2 \mathbf{q}}{(2\pi)^2} \tilde{V}(\mathbf{q}) F_{\mathbf{q}}(\mu_1 \lambda_1, \mu_3 \lambda_3 | \mu_2 \lambda_2, \mu_4 \lambda_4) c_{\lambda_1 \mu_1}^\dagger c_{\lambda_3 \mu_3}^\dagger c_{\mu_4 \lambda_4} c_{\mu_2 \lambda_2}, \quad (2.46)$$

where the matrix element is given by

$$F_{\mathbf{q}}(\mu_1 \lambda_1, \mu_3 \lambda_3 | \mu_2 \lambda_2, \mu_4 \lambda_4) = \rho_{\mathbf{q}}(\mu_1 | \mu_2) \rho_{-\mathbf{q}}(\mu_3 | \mu_4) \rho_{\mathbf{q}}^L(\lambda_1 | \lambda_2) \rho_{-\mathbf{q}}^L(\lambda_3 | \lambda_4) \quad (2.47)$$

and $\tilde{V}(\mathbf{q}) = V(\mathbf{q}) e^{-|\mathbf{q}|^2/2\ell_{B_L}^2}$ is the apodized potential. The vertex is shown in Fig. 2.1

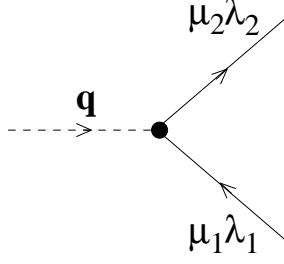


Figure 2.1: The vertex $\rho_{\mathbf{q}}(\mu_1|\mu_2)\rho_{\mathbf{q}}^L(\lambda_1|\lambda_2)$. The dotted line represents the interaction $\tilde{V}(\mathbf{q})$

The Hartree-Fock (HF) approximation consists of replacing pairs of fermion operators by their expectation value at zero temperature:

$$\langle c_{\mu\lambda}^\dagger c_{\mu'\lambda'} \rangle_0 = \delta_{\mu\mu'} \delta_{\lambda\lambda'} \Theta(\lambda_{max} - \lambda) , \quad (2.48)$$

which fills $\lambda_{max} + 1$ Landau levels of composite bosons. In Jain's mapping [13], this corresponds to an effective filling fraction $\nu_{\text{eff}} = \lambda_{max} + 1$. At finite temperature, the Θ -function is replaced by the Fermi distribution $f(\varepsilon_\lambda - \mu_c)$, where μ_c is the chemical potential. Since the chemical potential is restricted to $\varepsilon_{\lambda_{max}} < \mu_c < \varepsilon_{\lambda_{max}+1}$ but is otherwise arbitrary, we will drop it in the following.

Expanding the Hamiltonian around this ground state allows us to sum over the intra-level indices μ_i . In the following, we ignore the direct term, which only shifts the chemical potential. In the exchange term, completeness of the $|\mu\rangle$ basis within a Landau level, $\sum_\mu |\mu\rangle\langle\mu| = 1$, gives $\delta_{\mu_1\mu_4}$ or $\delta_{\mu_2\mu_3}$. Completeness of the intra-LL basis is tantamount to translation invariance. Rotation invariance, on the other hand, shows up in $\tilde{V}(\mathbf{q})$, which is required to be a function of only $|\mathbf{q}|$ for an isotropic system. This gives terms diagonal in λ , $\delta_{\lambda_1\lambda_4}$ or $\delta_{\lambda_2\lambda_3}$, since the others vanish when we consider the explicit expression for \hat{f}^L in equation (2.42). The HF Hamiltonian is now

$$H_0 = \sum_{\mu\lambda} \varepsilon_\lambda c_{\lambda\mu}^\dagger c_{\mu\lambda} \quad (2.49)$$

with the exchange energy

$$\varepsilon_\lambda = - \int \frac{d^2\mathbf{q}}{(2\pi)^2} \tilde{V}(\mathbf{q}) \sum_{\lambda'=0}^{\lambda_{max}} |\rho_{\mathbf{q}}^L(\lambda|\lambda')|^2 . \quad (2.50)$$

For concreteness, we choose the simplest non-trivial case: we fill only the LLL, $\lambda_{max} = 0$, and take a hard-core repulsive interaction, $V(\mathbf{q}) = V(0)$. Using the explicit form of $\hat{f}_{\mathbf{q}}^L$ from equation (2.42) the energy becomes

$$\begin{aligned}\varepsilon_\lambda &= - \left(2 \frac{\ell_{B_L}^2}{\ell_{B_R}^2} \ell_B^2 \right)^\lambda \frac{1}{\lambda!} \int \frac{d^2 \mathbf{q}}{(2\pi)^2} V(\mathbf{q}) e^{-\frac{1}{2} \ell_B^2 |\mathbf{q}|^2} |\mathbf{q}|^{2\lambda} \\ &= - \left(\frac{\ell_{B_L}}{\ell_{B_R}} \right)^{2\lambda} V(0) \bar{\rho} ,\end{aligned}\tag{2.51}$$

where $\bar{\rho} = 1/2\pi\ell_B^2$ is the density of the composite fermions. Note how the apodized potential now has ℓ_B^2 , not $\ell_{B_L}^2$, in the Gaussian, which is a consequence of the relation $1/\ell_B^2 = 1/\ell_{B_L}^2 - 1/\ell_{B_R}^2$. Because $\ell_{B_L}^2 < \ell_{B_R}^2$, the energy vanishes asymptotically as $\lambda \rightarrow \infty$. Furthermore, the exponential form implies a linear dependence on λ at small λ , exactly the kind of behavior that one would expect for non-interacting particles in a magnetic field. The cyclotron frequency, from equation (2.11), is given by $\omega_c = 1/m\ell_B^2$ so we can identify an effective mass with the gap Δ by $1/m^* = (\varepsilon_1 - \varepsilon_0)\ell_B^2$. More generally when $\lambda_{max} > 0$, the low energy physics is dominated by transitions between the highest occupied LL and the lowest unoccupied one, which gives

$$\begin{aligned}\frac{1}{m^*} &= (\varepsilon_{\lambda_{max}+1} - \varepsilon_{\lambda_{max}}) \ell_B^2 \\ &= \ell_B^2 \Delta .\end{aligned}\tag{2.52}$$

Further justification for this interpretation will emerge as we consider fluctuations around the ground state. At any rate, our calculation provides a framework to calculate m^* in the LLL. Note that equation (2.50) shows that m^* has contributions from the lowest LL's (of composite particles) and identifies it with a particular integral over the interaction.

As a stand-alone approximation, HF does not preserve the constraints because the commutator $[H_0, \hat{\rho}_{\mathbf{q}}^R] \neq 0$ for all $\mathbf{q} \neq 0$. In the next section we augment HF in a fully self-consistent manner to restore this symmetry.

2.3 Conserving Approximation and the Ward Identity

Our goal is to find a perturbative series such that all correlation function that involve the constraint $\hat{\rho}_{\mathbf{q}}^R - \bar{\rho}\delta_{\mathbf{q},0}$ vanish. In other words, the constraints would vanish to any

order of approximation. This is guaranteed by an exact (non-perturbative) Ward identity, which is derived below. We illustrate the method by calculating the response functions, or generalized susceptibilities, of $\hat{\rho}^R - \hat{\rho}^L$, $\hat{\rho}^R - \hat{\rho}^L$, and $\hat{\rho}^L - \hat{\rho}^L$. The latter is related to the physical quantity of interest, the compressibility.

It is well known in the theory of metals [21, 53] that if a Hartree-Fock approximation is used for the two-particle Green's function, then a fully self-consistent approximation that conserves charge includes ladder and bubble diagrams in the response functions. In fact this method preserves the constraints in the composite boson problem at $\nu = 1$ as well [18], and we will show that it works here, too.

In imaginary time, the response functions take the form

$$\chi^{AB}(\mathbf{q}, i\omega_n) = \langle \hat{\rho}_{\mathbf{q}}^A(i\omega_n) \hat{\rho}_{-\mathbf{q}}^B(-i\omega_n) \rangle, \quad (2.53)$$

where A, B stand for R or L and $\omega_n = 2n\pi/\beta$ are Matsubara frequencies. We implicitly keep only the connected part, thus dropping a term containing $\langle \hat{\rho}^A \rangle$'s. The fundamental diagrams are those that are irreducible, i.e. those that cannot be separated by cutting an interaction line. For a short range interaction, these are the qualitatively relevant pieces [21, 53], so we will not perform the bubble sums explicitly here. In any case, they are easily obtained as geometric series of the irreducible parts [18, 53].

The form of the conserving approximation in our case states that the irreducible response functions, χ_{irr}^{AB} , are to be calculated by including the ladder series with the HF Green's function lines. We sum the series by solving Dyson's equation; the next few equations will describe the structure of the theory.

First, let us recall the HF Green's function [53],

$$\mathcal{G}_0(\lambda, i\omega_\nu) = \frac{1}{i\omega_\nu - (\varepsilon_\lambda - \mu)}, \quad (2.54)$$

$$\begin{aligned} \varepsilon_\lambda &= -\frac{1}{\beta} \sum_\nu \sum_{\lambda'} \int \frac{d^2\mathbf{q}}{(2\pi)^2} \tilde{V}(\mathbf{q}) \rho_{\mathbf{q}}^L(\lambda|\lambda') \rho_{-\mathbf{q}}^L(\lambda'|\lambda) \mathcal{G}(\lambda', i\omega_\nu) \\ &= -\sum_{\lambda'} \int \frac{d^2\mathbf{q}}{(2\pi)^2} \tilde{V}(\mathbf{q}) |\rho_{\mathbf{q}}^L(\lambda|\lambda')|^2 f(\varepsilon_{\lambda'} - \mu_c), \end{aligned} \quad (2.55)$$

where $\omega_\nu = (2\nu + 1)\pi/\beta$ is a fermionic Matsubara frequency, and $f(\varepsilon_{\lambda'} - \mu_c)$ is the Fermi distribution with respect to the LL index (μ_c and ν should not be confused with the intra-LL index and the filling fraction).

Second, the renormalization of the vertices, Λ^A , by the ladder series can be written as a matrix Dyson equation:

$$\Lambda_{\mu\lambda, \mu'\lambda'}^A(\mathbf{q}, i\omega_n) = \rho_{\mathbf{q}}^A(\mu\lambda|\mu'\lambda') - \sum_{\mu_i, \lambda_i} \int \frac{d^2\mathbf{k}}{(2\pi)^2} \tilde{V}(\mathbf{k}) F_{\mathbf{k}}(\mu\lambda, \mu_2\lambda_2|\mu_1\lambda_1, \mu'\lambda') \mathcal{D}_{\lambda_1\lambda_2}(i\omega_n) \Lambda_{\mu_1\lambda_1, \mu_2\lambda_2}^A(\mathbf{q}, i\omega_n) \quad (2.56)$$

where $F_{\mathbf{k}}$ has been defined in equation (2.47) and \mathcal{D} is the frequency sum over the internal Green's functions,

$$\mathcal{D}_{\lambda_1\lambda_2}(i\omega_n) = \frac{1}{\beta} \sum_{\nu} \mathcal{G}_0(\lambda_2, i\omega_{\nu} + i\omega_n) \mathcal{G}_0(\lambda_1, i\omega_{\nu}) \quad (2.57)$$

$$= \frac{f(\varepsilon_{\lambda_2} - \mu_c) - f(\varepsilon_{\lambda_1} - \mu_c)}{\varepsilon_{\lambda_2} - \varepsilon_{\lambda_1} - i\omega_n} . \quad (2.58)$$

Because the Green's function is independent of the intra-LL index μ , it is convenient to define a purely inter-LL vertex, $\tilde{\Lambda}$ by

$$\Lambda_{\mu\lambda, \mu'\lambda'}^A(\mathbf{q}, i\omega_n) = \rho_{\mathbf{q}}(\mu|\mu') \tilde{\Lambda}_{\lambda\lambda'}^A(\mathbf{q}, i\omega_n) \quad (2.59)$$

so that Dyson's equation becomes

$$\tilde{\Lambda}_{\lambda\lambda'}^A(\mathbf{q}, i\omega_n) = \rho_{\mathbf{q}}^A(\lambda|\lambda') - \int \frac{d^2\mathbf{k}}{(2\pi)^2} \tilde{V}(\mathbf{k}) \rho_{\mathbf{k}}^L(\lambda|\lambda_1) \rho_{-\mathbf{k}}^L(\lambda_2|\lambda') \mathcal{D}_{\lambda_1\lambda_2}(i\omega_n) e^{i\mathbf{q} \wedge \mathbf{k} \ell_B^2} \tilde{\Lambda}_{\lambda_1\lambda_2}^A(\mathbf{q}, i\omega_n). \quad (2.60)$$

The phase factor is due to the magnetic translation commutator algebra—see the discussion immediately following equation (2.42).

The response functions are given in terms of the renormalized vertices by

$$\chi_{\text{irr}}^{AB}(\mathbf{q}, i\omega_n) = -\rho_0 \sum_{\lambda_i} \tilde{\Lambda}_{\lambda_1\lambda_2}^A(\mathbf{q}, i\omega_n) \mathcal{D}_{\lambda_1\lambda_2}(i\omega_n) \rho_{-\mathbf{q}}^B(\lambda_2|\lambda_1) , \quad (2.61)$$

where $\rho_0 = 1/2\pi\ell_B^2$ is the density of particles per LL, coming from the trace over μ 's. The diagrammatic structure is shown schematically in fig. 2.2

The key to showing that all response function containing Λ^R vanish, i.e $\chi_{\text{irr}}^{RR} = \chi_{\text{irr}}^{LR} = \chi_{\text{irr}}^{RL} = 0$, is the Ward identity for Λ^R , which we now derive. The first principles derivation follows standard field theoretic techniques [21]. Consider the exact vertex in real time:

$$\Lambda_{\mu_1\lambda_1, \mu_2\lambda_2}^R(\mathbf{q}, t, t_1, t_2) = \langle \mathcal{T} \left\{ \hat{\rho}_{\mathbf{q}}^R(t) c_{\mu_1\lambda_1}(t_1) c_{\lambda_2\mu_2}^{\dagger}(t_2) \right\} \rangle , \quad (2.62)$$

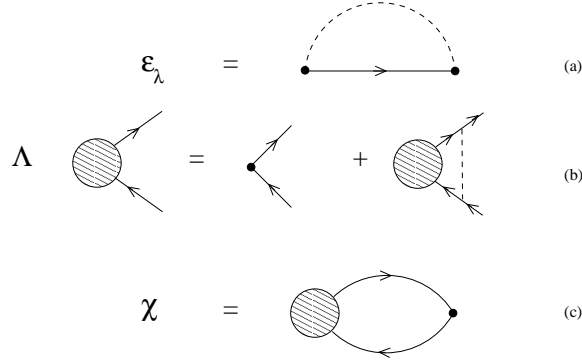


Figure 2.2: Diagrammatics of the conserving approximation. (a) The exchange self energy; (b) the ladder series renormalization of the vertices, Λ ; and (c) the response functions in terms of Λ .

where \mathcal{T} is the time ordering symbol. By taking the time derivative ∂_t of both sides, using $\partial_t \hat{\rho}_{\mathbf{q}}^R = 0$, and then Fourier transforming back to frequency space, we find the exact Ward identity

$$i\omega_n \tilde{\Lambda}_{\lambda_1 \lambda_2}^R(\mathbf{q}, i\omega_n) = \mathcal{G}^{-1}(\lambda_1, i\omega_n + i\omega_\nu) \rho_{\mathbf{q}}^R(\lambda_1 | \lambda_2) - \rho_{\mathbf{q}}^R(\lambda_1 | \lambda_2) \mathcal{G}^{-1}(\lambda_2, i\omega_\nu) . \quad (2.63)$$

Here, \mathcal{G} is the exact Green's function, and $i\omega_\nu$ on the right-hand side cancels identically, but is introduced for convenience. The two terms are due to differentiating the time ordering; physically, they are due to $c^\dagger(t_1)$ and $c(t_2)$ acting as sources in equation (2.62). For the particular HF and ladder series that we use here, we can verify the Ward identity by substituting \mathcal{G}_0 for the exact \mathcal{G} and plugging the whole expression into the right-hand side of the Dyson equation (2.60). Upon using the definition of \mathcal{G}_0 from equation (2.55), we find that the ladder series satisfies the Ward identity.

Therefore our diagrammatic scheme preserves the constraints, and we can be sure that the physical quantities that we calculate in this approximation will be consistent.

2.4 Response Functions

It is now straightforward to use the Ward identity in the response functions, equation (2.61), to verify that

$$\chi_{\text{irr}}^{RR}(\mathbf{q}, i\omega_n) = \chi_{\text{irr}}^{RL}(\mathbf{q}, i\omega_n) = \chi_{\text{irr}}^{LR}(\mathbf{q}, i\omega_n) = 0 \quad (2.64)$$

and in fact for any correlator containing Λ^R . There is one proviso in this procedure, that is discussed in detail in reference [18], having to do with the constraints at $i\omega_n = 0$. Our procedure is only valid at non-zero frequencies because we divided the Ward identity by $i\omega_n$ to isolate Λ^R . A complete proof requires more care, but we will not pursue this here. In any case, there is no problem with taking the limit $\omega \rightarrow 0$, which requires only small but non-zero frequencies.

It remains to calculate the physical density-density response, χ^{LL} . To this end, we first rewrite the vertex in a more symmetric fashion by introducing the scattering matrix, Γ , for the ladder series. Although the internal Green's functions do not carry momentum, which comes in only through the vertices, we can nonetheless absorb some of the momentum dependence into Γ by taking advantage of translation invariance again. We define

$$\tilde{\Gamma}_{\lambda_1\lambda'_1; \lambda_2\lambda'_2}(\mathbf{q}, i\omega_n) = \sum_{\mu_i, \mu'_i} \rho_{\mathbf{q}}(\mu'_1|\mu_1) \Gamma_{\mu_1\lambda_1, \mu'_1\lambda'_1; \mu_2\lambda_2, \mu'_2\lambda'_2}(i\omega_n) \rho_{-\mathbf{q}}(\mu_2|\mu'_2) \quad (2.65)$$

The Dyson equation for scattering, also known as the Bethe-Salpeter equation, takes the form

$$\begin{aligned} \tilde{\Gamma}_{\lambda_1\lambda'_1; \lambda_2\lambda'_2}(\mathbf{q}, i\omega_n) &= \int \frac{d^2\mathbf{k}}{(2\pi)^2} \tilde{V}(\mathbf{k}) \rho_{\mathbf{k}}^L(\lambda_1|\lambda_2) \rho_{-\mathbf{k}}^L(\lambda'_2|\lambda'_1) e^{i\mathbf{q} \wedge \mathbf{k} \ell_B^2} - \\ &\quad - \sum_{\lambda\lambda'} \int \frac{d^2\mathbf{k}}{(2\pi)^2} \tilde{V}(\mathbf{k}) \rho_{\mathbf{k}}^L(\lambda|\lambda_2) \rho_{-\mathbf{k}}^L(\lambda'_2|\lambda') e^{i\mathbf{q} \wedge \mathbf{k} \ell_B^2} \mathcal{D}_{\lambda\lambda'}(i\omega_n) \tilde{\Gamma}_{\lambda_1\lambda'_1; \lambda\lambda'}(\mathbf{q}, i\omega_n). \end{aligned} \quad (2.66)$$

It is convenient to view $\tilde{\Gamma}_{\lambda_1\lambda'_1; \lambda\lambda'}$ as a vector with components labeled by $\lambda\lambda'$, while $\lambda_1\lambda'_1$ and $(\mathbf{q}, i\omega_n)$ are parameters. Then the problem reduces to inverting a matrix in the indices $(\lambda_2\lambda'_2; \lambda\lambda')$.

The formal structure of this matrix equation is elucidated by reducing it to the eigenvalue equation,

$$\sum_{\lambda\lambda'} \mathbf{M}_{\lambda_2\lambda'_2; \lambda\lambda'}(\mathbf{q}, i\omega_n) \tilde{A}_{\lambda_1\lambda'_1; \lambda\lambda'}(\mathbf{q}, i\omega_n) = u_{\lambda_1\lambda'_1}(\mathbf{q}, i\omega_n) \tilde{A}_{\lambda_1\lambda'_1; \lambda_2\lambda'_2}(\mathbf{q}, i\omega_n), \quad (2.67)$$

where the kernel is

$$\mathbf{M}_{\lambda_2\lambda'_2; \lambda\lambda'}(\mathbf{q}, i\omega_n) = \delta_{\lambda\lambda_2} \delta_{\lambda'\lambda'_2} + \int \frac{d^2\mathbf{k}}{(2\pi)^2} \tilde{V}(\mathbf{k}) \rho_{\mathbf{k}}^L(\lambda|\lambda_2) \rho_{-\mathbf{k}}^L(\lambda'_2|\lambda') e^{i\mathbf{q} \wedge \mathbf{k} \ell_B^2} \mathcal{D}_{\lambda\lambda'}(i\omega_n) \quad (2.68)$$

and u , \tilde{A} are the eigenvalues, eigenvectors. We have obtained an exact zero eigenvalue solution of this equation at $i\omega_n = 0$. Using the properties of the commutator $[\rho_{\mathbf{k}}^L, \rho_{\mathbf{q}}^R]$ (c.f.

equation (2.42) and the immediately following discussion) and the definitions of ε_λ (2.55) and of $\mathcal{D}_{\lambda\lambda'}$ (2.58), we find that

$$\tilde{A}_{\lambda_1\lambda'_1;\lambda\lambda'}(\mathbf{q}, 0) = \varepsilon_\lambda \rho_{\mathbf{q}}^R(\lambda|\lambda') - \rho_{\mathbf{q}}^R(\lambda|\lambda') \varepsilon_{\lambda'} , \quad (2.69)$$

$$u_{\lambda_1\lambda'_1}(\mathbf{q}, 0) = 0 . \quad (2.70)$$

The similarity of this solution to the Ward identity (2.63) suggests that the existence of the scattering zero mode is related to the vanishing of correlators containing $\hat{\rho}^R$.

Another advantage of the Bethe-Salpeter equation is that we can rewrite the response functions symmetrically,

$$\begin{aligned} \chi_{\text{irr}}^{AB}(\mathbf{q}, i\omega_n) &= \chi_0^{AB}(\mathbf{q}, i\omega_n) + \\ &+ \rho_0 \sum_{\lambda_i\lambda'_i} \rho_{\mathbf{q}}^A(\lambda'_1|\lambda_1) \mathcal{D}_{\lambda_1\lambda'_1}(i\omega_n) \tilde{\Gamma}_{\lambda_1\lambda'_1;\lambda_2\lambda'_2}(\mathbf{q}, i\omega_n) \mathcal{D}_{\lambda_2\lambda'_2}(i\omega_n) \rho_{-\mathbf{q}}^B(\lambda_2|\lambda'_2) , \end{aligned} \quad (2.71)$$

where χ_0^{AB} is the bare bubble

$$\chi_0^{AB}(\mathbf{q}, i\omega_n) = -\rho_0 \sum_{\lambda\lambda'} \rho_{\mathbf{q}}^A(\lambda|\lambda') \mathcal{D}_{\lambda\lambda'}(i\omega_n) \rho_{-\mathbf{q}}^B(\lambda'|\lambda) \quad (2.72)$$

Fig. 2.3 illustrates the summation.

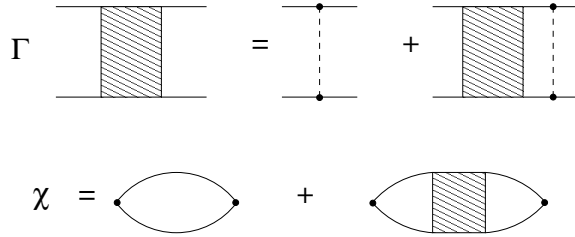


Figure 2.3: (a) Ladder series for the scattering matrix Γ and (b) response functions in terms of Γ .

To obtain the momentum expansion of χ^{LL} , consider the expansion of $\hat{\rho}^L$ from its definition in eqn. (2.42),

$$\rho_{\mathbf{q}}^L(\lambda|\lambda') = \delta_{\lambda\lambda'} + \ell_B^2 \frac{\ell_{BL}}{\ell_{BR}} \langle \lambda | i\mathbf{q} \wedge \pi | \rangle + \mathcal{O}(\mathbf{q}^2) . \quad (2.73)$$

The first term, diagonal in $\lambda\lambda'$, cannot contribute to the response because the transition amplitude $\mathcal{D}_{\lambda\lambda'}$ is purely an inter-LL operator. The expanded response becomes

$$\begin{aligned}
\chi_{\text{irr}}^{LL}(\mathbf{q}, i\omega_n) = & -\alpha \sum_{\lambda\lambda'} \langle \lambda' | \mathbf{q} \wedge \pi | \lambda \rangle \mathcal{D}_{\lambda\lambda'}(i\omega_n) \langle \lambda | \mathbf{q} \wedge \pi | \lambda' \rangle + \\
& + \alpha \sum_{\lambda_i \lambda'_i} \langle \lambda'_1 | \mathbf{q} \wedge \pi | \lambda_1 \rangle \mathcal{D}_{\lambda_1 \lambda'_1}(i\omega_n) \tilde{\Gamma}_{\lambda_1 \lambda'_1; \lambda_2 \lambda'_2}(\mathbf{q}, i\omega_n) \mathcal{D}_{\lambda_2 \lambda'_2}(i\omega_n) \langle \lambda_2 | \mathbf{q} \wedge \pi | \lambda'_2 \rangle + \dots,
\end{aligned} \tag{2.74}$$

where α is an overall constant.

To obtain χ_{irr}^{LL} through $\mathcal{O}(\mathbf{q}^2)$, we need only $\tilde{\Gamma}(0, i\omega_n)$. At $\mathbf{q} = 0$, the Bethe-Salpeter equation is

$$\tilde{\Gamma}_{\lambda_1 \lambda'_1; \lambda_2 \lambda'_2}(0, i\omega_n) = \tilde{V}_{\lambda_2 \lambda'_2; \lambda_1 \lambda'_1} - \sum_{\lambda\lambda'} \tilde{V}_{\lambda_2 \lambda'_2; \lambda\lambda'} \mathcal{D}_{\lambda\lambda'}(i\omega_n) \tilde{\Gamma}_{\lambda_1 \lambda'_1; \lambda\lambda'}(0, i\omega_n), \tag{2.75}$$

where the interaction matrix element is

$$\tilde{V}_{\lambda_2 \lambda'_2; \lambda_1 \lambda'_1} = \int \frac{d^2 \mathbf{k}}{(2\pi)^2} \tilde{V}(\mathbf{k}) \rho_{\mathbf{k}}^L(\lambda_1 | \lambda_2) \rho_{-\mathbf{k}}^L(\lambda'_2 | \lambda'_1). \tag{2.76}$$

Rotation invariance at $\mathbf{q} = 0$ requires that the matrix elements vanish unless

$$\lambda_1 + \lambda'_2 = \lambda'_1 + \lambda_2.$$

Now let us make two further restrictions that afford an exact solution for $\tilde{\Gamma}$. First, we choose $\lambda_{\text{max}} = 0$ as we did above to illustrate the exchange energy. Secondly, we work at zero temperature where the Fermi function is $f(\varepsilon_\lambda - \mu) = \Theta(\lambda_{\text{max}} - \lambda)$, restricting the \mathcal{D} -amplitude to

$$\begin{aligned}
\mathcal{D}_{0\lambda}(i\omega_n) &= -\frac{1}{\Delta_\lambda - i\omega_n} \\
\mathcal{D}_{\lambda 0}(i\omega_n) &= -\frac{1}{\Delta_\lambda + i\omega_n} \\
\Delta_\lambda &\equiv \varepsilon_\lambda - \varepsilon_0
\end{aligned} \tag{2.77}$$

Along with rotation invariance, these restrictions allow us to solve equation (2.75) for the scattering matrix (at $\mathbf{q} = 0$)

$$\begin{aligned}
\tilde{\Gamma}_{0\lambda; 0\lambda} &= \frac{\tilde{V}_{0\lambda; 0\lambda}}{1 + \tilde{V}_{0\lambda; 0\lambda} \mathcal{D}_{0\lambda}} \\
\tilde{\Gamma}_{\lambda 0; \lambda 0} &= \frac{\tilde{V}_{\lambda 0; \lambda 0}}{1 + \tilde{V}_{\lambda 0; \lambda 0} \mathcal{D}_{\lambda 0}}.
\end{aligned} \tag{2.78}$$

The two channels above represent a particle in the 0'th LL propagating on one leg of the ladder diagram and a particle in the λ 'th LL on the other, and *vice versa*. These channels

do not mix in our example. In fact, we will only need $\lambda = 1$ for the lowest order term in χ^{LL} because of the vertices $\langle \lambda | \mathbf{q} \wedge \pi | \lambda' \rangle$. At this point we find a crucial identity for $\lambda = 1$:

$$\tilde{V}_{01;01} = \tilde{V}_{10;10} = \Delta_1 , \quad (2.79)$$

which is easily proven by comparing equations (2.76) and (2.50). Plugging equations (2.78)-(2.79) into equation (2.75) for the response function, we find

$$\begin{aligned} \chi_{\text{irr}}^{LL}(\mathbf{q}, i\omega_n) &= -|\langle 0 | \pi | 1 \rangle|^2 \left\{ \mathcal{D}_{01} + \mathcal{D}_{01} - \frac{\mathcal{D}_{01} \Delta_1 \mathcal{D}_{01}}{1 + \Delta_1 \mathcal{D}_{01}} - \frac{\mathcal{D}_{10} \Delta_1 \mathcal{D}_{10}}{1 + \Delta_1 \mathcal{D}_{10}} \right\} |\mathbf{q}|^2 + \mathcal{O}(|\mathbf{q}|^4) \\ &= 0 + \mathcal{O}(|\mathbf{q}|^4) \end{aligned} \quad (2.80)$$

(an overall factor has been left out). Thus, the lowest order term in the density-density response is of order $|\mathbf{q}|^4$.

This is the main physical result that we wanted to reproduce within our composite fermion framework. Its main content is that the system is incompressible, i.e. the compressibility, κ , vanishes. The connection of compressibility to the density-density response is contained in the definition [54]

$$\kappa = \lim_{\mathbf{q} \rightarrow 0} \chi^{LL}(\mathbf{q}, 0) . \quad (2.81)$$

For the irreducible diagrams that we have considered so far, $\chi^{LL} = \chi_{\text{irr}}^{LL}$, so that $\kappa = 0$. We expect that the order of limits is consistent with our calculation of the ladder series, which is a Taylor expansion around $\mathbf{q} = 0$ at finite frequency.

The full response function χ^{LL} can be obtained from the irreducible part by a bubble summation [21, 53, 54]

$$\chi^{LL} = \frac{\chi_{\text{irr}}^{LL}}{1 + \tilde{V}(\mathbf{q}) \chi_{\text{irr}}^{LL}} . \quad (2.82)$$

For a short range interaction, such as ours, this geometric sum has no qualitative effect, so that κ remains at zero. A well-known early work by Girvin, MacDonald, and Platzman [55] contains general arguments for the momentum dependence of the density response function for incompressible liquids in the LLL, and is consistent with our result.

Before we close this section and move on to the effective field theory, the interaction-gap identity of equation (2.79) is worth a couple more words. A slightly more general case is

when $\lambda_{max} > 0$,

$$\tilde{V}_{\lambda, \lambda+1; \lambda, \lambda+1} = \tilde{V}_{\lambda+1, \lambda; \lambda+1, \lambda} = \varepsilon_{\lambda+1} - \varepsilon_{\lambda} , \quad (2.83)$$

where $\lambda \equiv \lambda_{max}$. We expect that the compressibility will vanish again, although we have not performed this calculation explicitly. This identity seems to have an analog in the Fermi liquid-like state of bosons at $\nu = 1$ [18]. There, the system has a divergent compressibility due to a fixed Landau parameter, $F_1 = -1$, and m^* is also coming from an integral of the interaction below the Fermi surface. In both cases, the identities lead to the correct compressibility because there is no bare kinetic term due to the LLL projection.

The form of the left and right density response functions, suggest a physical interpretation of the vertices. To lowest order in \mathbf{q} , all response functions vanish, and we can take any linear combination $\rho_{\mathbf{q}}^L - x\rho_{\mathbf{q}}^R$ for the physical response without changing the result. Suppose we choose the weighted combination

$$\rho_{\mathbf{q}}^L \rightarrow \rho_{\mathbf{q}}^L + \frac{B_R}{B_L} \rho_{\mathbf{q}}^R . \quad (2.84)$$

In operator language the densities are $\rho_{\mathbf{q}}^A = e^{i\mathbf{q}\cdot\mathbf{R}^A}$. Using the operator mapping in equations (2.21) and (2.22), the momentum expansion of the new vertex leaves

$$\begin{aligned} \rho_{\mathbf{q}}^L &\rightarrow \frac{B}{B_L} + \frac{1}{B_L} i\mathbf{q} \wedge \mathbf{K} + \mathcal{O}(\mathbf{q}^2) \\ &= \frac{B}{B_L} (1 + \mathbf{q} \cdot \mathbf{r}) - \frac{1}{B_L} i\mathbf{q} \wedge \pi + \mathcal{O}(\mathbf{q}^2) . \end{aligned} \quad (2.85)$$

The first term is the first order term of a plane wave for the composite particle with charge $q^* = B/B_L$ at position \mathbf{r} , which is consistent with the two-particle mapping of section 2.1.b. The second term is interpreted as the dipole moment. The charge of the composite does not show up in the response functions, but presumably would come out if backflow corrections are included as in the work of Lopez and Fradkin [57].

If the expansion is exponentiated, we obtain

$$\rho_{\mathbf{q}}^L \rightarrow e^{i\mathbf{q}\cdot\mathbf{r}} \left(\frac{B}{B_L} - \ell_{B_L}^2 i\mathbf{q} \wedge \pi \right) . \quad (2.86)$$

This form agrees with the work of Shankar [15], which starts from a different approach using the Chern-Simons theory at the outset. As the first line of eqn. (2.85) shows, this

particular choice of x makes the physical density a purely intra-LL operator. As such, it is obvious that the density-density response vanishes to $\mathcal{O}(\mathbf{q}^2)$ in the ladder approximation, since the vertices contain only inter-LL transitions. Further, our weighted combination agrees with Read's [18] density for $\nu = 1$ where $B_R/B_L = -1$. Nonetheless, we stress that our derivation does not specify x by itself.

2.5 Effective Theory

In this section we will show that the ladder series can be replaced with a dynamic gauge field, yielding an effective theory much like that for bosons at $\nu = 1$. It is not a Chern-Simons field theory, but the familiar relation of density to the curl of a gauge field will appear.

In accordance with the previous section, the low energy physics of bosons at $\nu \neq 1$ is that of composite fermions filling an integral number, $\nu_{\text{eff}} = \nu/q^*$, of Landau levels. Let us take an ordinary fermion field $c(\mathbf{x}, t)$ in a static magnetic field $B = \nabla \wedge \mathbf{A}$ such that exactly ν_{eff} levels are filled, and couple it to a nondynamic gauge field \mathbf{a} :

$$H_{\text{eff}} = \int dt d^2\mathbf{x} \frac{1}{2m^*} |(-i\nabla - \mathbf{A} - \mathbf{a})c|^2 - \mu c^\dagger c. \quad (2.87)$$

The fermion density is $\bar{\rho} = \nu_{\text{eff}}/2\pi\ell_B^2$, or equivalently $\bar{\rho} = \nu/2\pi\ell_{B_L}^2$. The chemical potential μ is tuned to lie between the uppermost filled LL and the lowest empty one. m^* is the only parameter in the theory and is obtained from the smallest energy gap of the original problem as defined in equation (2.52). The action of the theory is an action for \mathbf{a} as well as for c, c^\dagger , but in contrast to Chern-Simons theory, there is no kinetic term for \mathbf{a} ; it is a “strongly coupled” gauge field in the language of field theory. There is also the term $a_0 c^\dagger c$, however we will choose the temporal gauge in which $a_0 = 0$ at finite frequency, so that its fluctuations do not affect the response.

The gauge symmetry of H_{eff} is ordinary $U(1)$, which can be viewed as the long distance limit of the global $U(N)_R$ symmetry of the right coordinates. The gauge invariant density of this model, $c^\dagger c$, is identified with the constraint ρ^R , which fixes

$$\rho^R = c^\dagger c = \bar{\rho}. \quad (2.88)$$

This condition is the long distance limit of the full constraint that was constructed in Section 2.1.c. To obtain an expression for the physical density, consider the gauge invariant momentum density before \mathbf{a} is included,

$$\mathbf{g}(\mathbf{r}) = \frac{1}{2i} \left\{ c^\dagger (\nabla - i\mathbf{A}) c - \left[(\nabla + i\mathbf{A}) c^\dagger \right] c \right\} . \quad (2.89)$$

The single-particle version is the π operator of Section 2.1.a. This allows us to rewrite the density suggestively. The first term in equation (2.86), $q^* e^{i\mathbf{q}\cdot\mathbf{r}}$, is a plane wave for a charge of magnitude q^* ; at tree level its expectation value can be replaced by $\bar{\rho}$, which leaves

$$\rho = \bar{\rho} - q^* \ell_B^2 \nabla \wedge \mathbf{g} , \quad (2.90)$$

where $q^* = B/B_L$. Similarly, at tree level the gauge potential is related to the momentum density by $\mathbf{a} = \mathbf{g}/\bar{\rho}$. Therefore the physical density becomes

$$\rho = \bar{\rho} - \frac{\nu}{2\pi} \nabla \wedge \mathbf{a} , \quad (2.91)$$

where we used $\nu_{\text{eff}} = \nu/q^*$. Equation (2.91) is precisely the fluctuation piece of the Chern-Simons equation (1.2), despite the absence of a kinetic term for \mathbf{a} ! It should be borne in mind, however, that we have imposed the particular linear combination $\rho^L - x\rho^R$ with $x = B/B_L$, which is responsible for this appealing result; in principle, any coefficient of $\nabla \wedge \mathbf{a}$ is obtainable in this way.

Let us now consider the correlation functions. The basic conductivities are $\sigma_{ij} = \langle g_i g_j \rangle / m^{*2}$. Because of the Onsager relation $\sigma_{xy} = -\sigma_{yx}$ and isotropy $\sigma_{xx} = \sigma_{yy}$, it is convenient to use complex coordinates $g = g_x + i g_y$ and $\bar{g} = g_x - i g_y$ so that the expectation values $\langle gg \rangle$ and $\langle \bar{g} \bar{g} \rangle$ vanish. Our aim is to compare the susceptibility

$$\begin{aligned} \chi^{LL}(q) = \langle \delta\rho(q) \delta\rho(-q) \rangle &= \ell_{BL}^4 \langle \mathbf{q} \wedge \mathbf{g}(q) \cdot \mathbf{q} \wedge \mathbf{g}(-q) \rangle \\ &= \ell_{BL}^4 \frac{|\mathbf{q}|^2}{4} \langle g(q) \bar{g}(-q) + \bar{g}(q) g(-q) \rangle \end{aligned} \quad (2.92)$$

to the ladder series in the previous section. We will show that within a random phase approximation (RPA), the responses are identical (at least to $\mathcal{O}(q^2)$).

The RPA has been applied in the context of the quantum Hall effect by several authors [18, 57]. It is a bubble sum for the gauge field fluctuations. The basic terms, shown in fig. 2.4, consist of a diamagnetic and a bubble piece. The gauge field correlator is

(a)

(b)

Figure 2.4: Bubble summation for the gauge field propagator. (a) The shaded circle includes the diamagnetic coupling and the $\langle g\bar{g} \rangle_0$ bubble; (b) The thick wavy line represents $\langle a\bar{a} \rangle$

$$\langle a(q)\bar{a}(-q) \rangle = \left[-\frac{\bar{\rho}}{m^*} + \frac{1}{2m^{*2}} \langle g(q)\bar{g}(-q) \rangle_0 \right]^{-1}, \quad (2.93)$$

where $\langle g(q)\bar{g}(-q) \rangle_0$ is the bare bubble, which we can evaluate in the single particle basis:

$$\langle g(q)\bar{g}(-q) \rangle_0 = - \sum_{\mu\lambda, \mu'\lambda'} \langle \mu\lambda | \pi | \mu'\lambda' \rangle \mathcal{D}_{\lambda\lambda'}(i\omega_n) \langle \mu'\lambda' | \bar{\pi} | \mu\lambda \rangle. \quad (2.94)$$

The calculation of $\langle \bar{a}(q)a(-q) \rangle_0$ is analogous, but with $\langle \bar{g}(q)g(-q) \rangle_0$. The matrix elements of π produce a factor $2\nu_{\text{eff}}\ell_B^2$ since $\pi = \sqrt{2}\ell_B b$ is the inter-LL ladder operator and $\mathcal{D}_{\lambda\lambda'}$ connects only states on opposite sides of the Fermi surface, which restricts λ, λ' to $\lambda_{\text{max}}, \lambda_{\text{max}} + 1$. The sum over μ 's gives the density per LL, $1/2\pi\ell_B^2$, with the end result

$$\begin{aligned} \frac{1}{2m^{*2}} \langle g(q)\bar{g}(-q) \rangle_0 &= -\frac{\bar{\rho}}{m^*} \mathcal{D}_{\lambda_{\text{max}}, \lambda_{\text{max}}+1}(i\omega_n) \Delta \\ &\equiv \frac{\bar{\rho}}{m^*} \frac{\Delta}{\Delta + i\omega_n}, \end{aligned} \quad (2.95)$$

where one factor of m^* has been replaced by $1/\ell_B^2\Delta$.

Now, the RPA $g - \bar{g}$ response consists of the bubble sum shown in fig. 2.5.

Figure 2.5: χ^{LL} as a bubble sum. The wavy line is the gauge field propagator from equation (2.93). See also fig. 2.4.

$$\begin{aligned} \langle g(q)\bar{g}(-q) \rangle &= \langle g(q)\bar{g}(-q) \rangle_0 - \\ &\quad - 2 \langle g(q)\bar{g}(-q) \rangle_0 \frac{1}{2m^*} \langle a(q)\bar{a}(-q) \rangle \frac{1}{2m^*} \langle g(q)\bar{g}(-q) \rangle_0 \end{aligned} \quad (2.96)$$

Using $\langle g\bar{g} \rangle = \overline{\langle g\bar{g} \rangle}$ and the identities (2.93), (2.95) in equation (2.96) and plugging the result into the expression for χ^{LL} , equation (2.92), we find that

$$\chi^{LL}(q) = 0 + \mathcal{O}(q^4) . \quad (2.97)$$

This is the same result as in the conserving approximation of the last section. The structure of the RPA is such that, the gauge field propagator replaces the scattering matrix Γ , and the two channels $\tilde{\Gamma}_{01;01}$, $\tilde{\Gamma}_{10;10}$ correspond to $\langle a\bar{a} \rangle$, $\langle \bar{a}a \rangle$. Diagrammatically, *the second bubble term in Fig. 2.5 is exactly the ladder sum in Fig. 2.3(b)*.

Another way to test the effective theory is by integrating out the fermions. Since there are ordinary fermions filling ν_{eff} Landau levels, we expect a Chern-Simons term in the effective action for \mathbf{a} .

The RPA prescription in Fig. 2.4 implies that

$$\mathcal{L}[\mathbf{a}] = -\frac{1}{2m^{*2}} \sum_{i,j} a_i \langle g_i g_j \rangle_0 a_j + \frac{\bar{p}}{2m^*} \sum_i a_i a_i , \quad (2.98)$$

The diamagnetic piece combines with the bare bubble amplitude in equation (2.95) to give $\frac{\bar{p}}{m^*} \frac{\omega_n^2}{\Delta^2 + \omega_n^2} a_i a_i$. In the limit $\omega \rightarrow 0$, this diagonal term vanishes. On the other hand, the cross term is proportional to ω_n in the same limit, leaving

$$\mathcal{L}[\mathbf{a}] = -\frac{\nu_{\text{eff}}}{4\pi} \epsilon^{ij} a_i \omega_n a_j ,$$

where ϵ^{ij} is the Levi-Civita symbol. Since the original problem was gauge invariant, the complete Lagrangian must contain the scalar potential a_0 :

$$\mathcal{L}[a] = -\frac{\nu_{\text{eff}}}{4\pi} i \epsilon^{\mu\nu\lambda} a_\mu \partial_\nu a_\lambda , \quad (2.99)$$

where $\mu, \nu, \lambda = t, x, y$ and $\partial_t \equiv i\omega_n$. This form is correct to leading order in \mathbf{q} , ω and shows the correct Hall conductivity of the composite fermions.

Chapter 3

Lowest Landau Level II: Composite Bosons

In the previous chapter, we considered composite fermions. In this one, we will consider composite bosons. In the former case, we derived an effective theory from first principles. However, this is not possible for more than one attached vortex and we follow a phenomenological approach instead. The main feature that we find is the magneto-roton excitation, which was predicted and analyzed by several authors [55, 58]. Our analysis provides a physical picture of this excitation.

3.1 Formalism

In this section we generalize the Haldane-Pasquier formalism by considering p objects attached to the underlying particle. The physical picture that will emerge is similar, with the composite particle being a bound state of p vortices and one particle. We specialize to $\nu = 1/p$ so that each vortex carries charge $1/p$ to maintain neutrality and the magnetic lengths are related by

$$\ell_{BR}^2 = p\ell_{BL}^2 . \tag{3.1}$$

3.1.a Fock Space

For fractional fillings ν the number of vortices in the composite particle is p . The matter operators are now $p + 1$ rank tensors $c_{m; n_1 \dots n_p}$, with

$$[c_{m; n_1 \dots n_p}, c_{n'_1 \dots n'_p; m'}^\dagger]_\pm = \delta_{mm'} \delta_{n_1 n'_1} \dots \delta_{n_p n'_p} \quad (3.2)$$

m runs from 1 to N_ϕ and the n 's from 1 to N . The left (physical) density is obtained by tracing over all the right indices

$$\rho_{mm'}^L = \sum_{n_1 \dots n_p} c_{n_1 \dots n_p; m}^\dagger c_{m; n_1 \dots n_p} \quad (3.3)$$

However, there are now p right densities:

$$\rho_{nn'}^{R_a} = \sum_{m; n_j, \hat{n}_a} c_{n_1 \dots n_{i-1} n n_{i+1} \dots n_p; m}^\dagger c_{m; n_1 \dots n_{i-1} n' n_{i+1} \dots n_p} , \quad (3.4)$$

where $a = 1, \dots, p$ and \hat{n}_a implies that there is no sum over n_a . Similarly, there are p copies of the constraints in eqn. (2.32), which require $|\Psi_{\text{phys}}^{m_1 \dots m_N}\rangle$ to be a singlet in each of the p right indices. A straightforward extension of the $p = 1$ case (eqn. (2.33)) shows that the basis is

$$|\Psi_{\text{phys}}^{m_1 \dots m_N}\rangle = \sum_{\alpha_i \beta_i \dots \gamma_i} \epsilon^{\alpha_1 \beta_1 \dots \gamma_1} \dots \epsilon^{\alpha_p \beta_p \dots \gamma_p} c_{\alpha_1 \dots \alpha_p; m_1}^\dagger c_{\beta_1 \dots \beta_p; m_2}^\dagger \dots c_{\gamma_1 \dots \gamma_p; m_N}^\dagger |0\rangle , \quad (3.5)$$

where there are N Greek indices of the type $\alpha\beta\dots\gamma$. The Levi-Civita symbols and anticommutation relations of the c 's ensure symmetry under the interchange of any pair of physical indices $m_i \leftrightarrow m_j$, and we are left with a bosonic Fock space of N particles in N_ϕ orbitals. Again, had we started with bosonic c 's, we would have ended up with a Fock space of composite Fermions.

3.1.b Physical Operators and Constraints

The field operator has p right coordinates η_i ,

$$c(z, \bar{\eta}_1, \dots, \bar{\eta}_p) = \sum_{m, n_i} u_m^L(z) \overline{u_{n_1}^R(\eta_1)} \dots \overline{u_{n_p}^R(\eta_p)} c_{m; n_1 \dots n_p} . \quad (3.6)$$

It is convenient to change the vortex coordinates to the so-called “center-of-mass” (or Jacobi) coordinates, which have been used in few-body problems in the context of atomic

physics [59]. This reduces the p -complex to one center-of-mass coordinate $\xi_{cm} = \frac{1}{p}(\eta_1 + \dots + \eta_p)$ and $p - 1$ relative coordinates ξ_α ($\alpha = 1, \dots, p - 1$), which are linear combinations of the η_i . We will denote the linear transformation by

$$\xi_\alpha = R_{\alpha i} \eta_i , \quad (3.7)$$

where $\alpha = 0, \dots, p - 1$ and $\alpha = 0$ stands for cm . Generally, Greek indices will be used for the ξ 's and Latin indices for the η 's.

One of the nice properties of Jacobi coordinates is that $\sqrt{p}R$ is orthogonal:

$$|\xi_{cm}|^2 + |\xi_1|^2 + \dots + |\xi_{p-1}|^2 = \frac{1}{p}(|\eta_1|^2 + \dots + |\eta_p|^2) \quad (3.8)$$

For the special where each vortex carries charge $1/p$ ($\nu = 1/p$), we can use this property to set the magnetic length of each ξ to $\ell_{BL}^2 \equiv \ell_{BR}^2/p$. The utility of this transformation is that *all coordinates now have only one magnetic length, ℓ_{BL} .*

The particular way in which Jacobi coordinates are constructed is well-illustrated by two special cases, $p = 2$ and $p = 3$, both of which we will utilize below. For two vortices there is only one relative coordinate, so the Jacobi system is

$$\begin{aligned} \xi_{cm} &= \frac{1}{2}(\eta_1 + \eta_2) \\ \xi_1 &= \frac{1}{2}(\eta_1 - \eta_2) \end{aligned} \quad (3.9)$$

The normalizations are chosen so as to preserve the normalization in eqn. (3.8). Specifically, the $1/2$ factor in ξ_1 is the reduced “mass”, m (with $1/m = 1/m_1 + 1/m_2$) of the two vortices—each vortex is taken to have unit “mass” ($m_i = 1$).

For $p = 3$, the coordinates are arranged so that ξ_1 is a vector from η_1 to η_2 , and ξ_2 connects η_3 to the center of mass of η_1 and η_2 . Each ξ is normalized by the square root of the reduced mass of the two objects which it connects. Fig. 3.1 illustrates this construction. The particular linear combinations are

$$\begin{pmatrix} \xi_{cm} \\ \xi_1 \\ \xi_2 \end{pmatrix} = \frac{1}{\sqrt{3}} \begin{pmatrix} \frac{1}{\sqrt{3}} & \frac{1}{\sqrt{3}} & \frac{1}{\sqrt{3}} \\ \frac{1}{\sqrt{2}} & -\frac{1}{\sqrt{2}} & 0 \\ \frac{1}{\sqrt{6}} & \frac{1}{\sqrt{6}} & -\sqrt{\frac{2}{3}} \end{pmatrix} \begin{pmatrix} \eta_1 \\ \eta_2 \\ \eta_3 \end{pmatrix} . \quad (3.10)$$

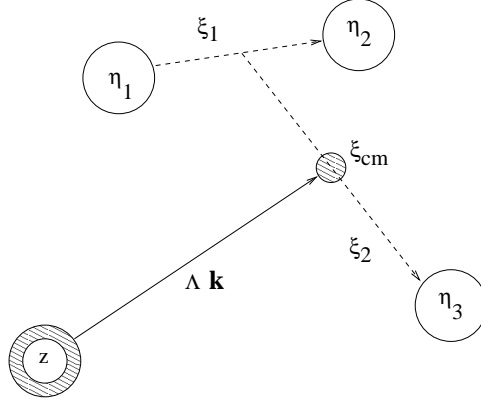


Figure 3.1: The composite with three vortices attached. The underlying particle is at z with charge $+1$, and the vortices are at η_i with charge $-1/3$. The (unnormalized) Jacobi vectors are dotted lines. z and the center of mass of the vortices, ξ_{cm} , are connected by $\wedge \mathbf{k}$, which we will later interpret as a dipole moment. Since the composite is neutral, it drifts with momentum \mathbf{k} .

There is a certain degree of freedom inherent in assigning the ξ . For instance, we could have chosen ξ_1 to connect η_1 to η_3 , and ξ_2 to connect η_2 to the center of mass of $\eta_{1,2}$. However, each choice obeys the normalization condition in eqn. (3.8). Viewed classically, $|\xi_{cm}|^2$ is a constant in the absence of external forces, so the normalization implies that $|\xi_1|^2 + \dots + |\xi_{p-1}|^2$ is fixed and that all choices of Jacobi sets can be transformed into each other by a member of $\text{SO}(p-1)$. Although this is a fundamental and generally useful property of the coordinate system, we will not use it in this thesis, but point it out for completeness. The most important property for us is that eqn. (3.8) scales the ξ in such a way that all coordinates have the same magnetic length.

For higher values of p , the Jacobi coordinates can be constructed recursively by grouping the vortices into pairs and connecting the centers of mass, and then repeating the process with the centers of mass. The details of the general procedure are described elsewhere [59]; however, here we only need the $p = 2, 3$ cases.

Now, the combination of the particle at z and the center of mass of the vortices at ξ_{cm} is just like a particle and vortex of equal but opposite charge, which can be treated by the

noncommutative Fourier transform (Appendix). The transformed field operators become

$$c_{\mathbf{k}}(\{\bar{\xi}\}) = \int d^2z \prod_{i=1}^p d^2\eta'_i c(z, \bar{\eta}'_1 \cdots \bar{\eta}'_p) \tau_{\mathbf{k}}(\xi'_{cm}, \bar{z}) \prod_{\alpha=1}^{p-1} \delta(\xi'_{\alpha}, \bar{\xi}_{\alpha}) . \quad (3.11)$$

The δ -functions implement the Jacobi coordinate transformation of eqn. (3.7) through $\xi'_{\alpha} = R_{\alpha i} \eta'_i$. Since the ξ_{α} themselves are coordinates with a magnetic length ℓ_{B_L} , the field can be cast into the complementary “spin” basis

$$c_{\mathbf{k}}(\{\bar{\xi}\}) = \sum_{\sigma_{\alpha}} c_{\mathbf{k} \sigma_1 \cdots \sigma_p} \overline{u_{\sigma_1}^L(\xi_1)} \cdots \overline{u_{\sigma_{p-1}}^L(\xi_{p-1})} . \quad (3.12)$$

The quantum numbers σ_{α} are nonnegative integers. They are angular momenta of the relative coordinates, but we will refer to them simply as “spin”. In this chapter we consider spinless fermions and bosons so there should be no chance for confusion.

The left density is integrated over all right coordinates and has the same momentum structure as in the $p = 1$ case:

$$\hat{\rho}_{\mathbf{q}}^L = \int \frac{d^2\mathbf{k}}{(2\pi)^2} \sum_{\sigma_{\alpha}} e^{\frac{1}{2}i\mathbf{k} \wedge \mathbf{q} \ell_{B_L}^2} c_{\mathbf{k} - \frac{1}{2}\mathbf{q}, \sigma_1 \cdots \sigma_{p-1}}^{\dagger} c_{\mathbf{k} + \frac{1}{2}\mathbf{q}, \sigma_1 \cdots \sigma_{p-1}} . \quad (3.13)$$

The right densities are more complicated,

$$\begin{aligned} \hat{\rho}_{\mathbf{q}}^{R_i} = & \quad (3.14) \\ & \int \frac{d^2\mathbf{k}}{(2\pi)^2} \int \prod_{\alpha=1}^{p-1} d^2\xi_{\alpha} d^2\xi'_{\alpha} \tau_{\mathbf{q}}(\xi'_{cm} - \eta'_i, \bar{\xi}_{cm} - \bar{\eta}_i) e^{\frac{1}{2}i\mathbf{k} \wedge \mathbf{q} \ell_{B_L}^2} c_{\mathbf{k} - \frac{1}{2}\mathbf{q}}^{\dagger}(\{\xi\}) c_{\mathbf{k} + \frac{1}{2}\mathbf{q}}(\{\bar{\xi}'\}) \end{aligned}$$

Notice the magnetic translation in $\xi_{cm} - \eta_i$, which is the vector from the center-of-mass to the i 'th vortex.

Finally, the Hamiltonian looks just like the unequally charged case, eqn. (2.44), in the previous chapter,

$$H = \frac{1}{2} \int \frac{d^2\mathbf{q}}{(2\pi)^2} V(\mathbf{q}) e^{-|\mathbf{q}|^2/2\ell_{B_L}^2} : \hat{\rho}_{\mathbf{q}}^L \hat{\rho}_{-\mathbf{q}}^L : \quad (3.15)$$

Again, only “left” operators appear since H is a physical quantity and $\hat{\rho}_{\mathbf{q}}^{R_i}$ are constants of the motion.

3.1.c Remarks on Many-Particle Wavefunctions

In this section, we augment the physical picture of the composite fermions and bosons by outlining the many-body wavefunctions that they can describe. In particular, we recover Laughlin's function at $\nu = 1/p$ [4].

Consider first N bosons at $\nu = 1/p$. There are N particle coordinates z_i and pN vortex coordinates $\bar{\eta}_{s,i}$ with $s = 1, \dots, p$ and $i = 1, \dots, N$. The constraints (Section 3.1.b) require that the $\bar{\eta}_{s,i}$ dependence of the wavefunction be that of a full Landau level for each s [18],

$$\Psi_{\text{phys}}(z_1, \bar{\eta}_{1,1}, \dots, \bar{\eta}_{p,1}, \dots, z_N, \bar{\eta}_{1,N}, \dots, \bar{\eta}_{p,N}) = f(z_1, \dots, z_N) \prod_{s; i < j} (\bar{\eta}_{s,i} - \bar{\eta}_{s,j})$$

The last factor is the product of p Laughlin-Jastrow factors (the Gaussian factors have been left off). Another way of writing it is the product of p Slater determinants of the matrices $m_{ij}^s = \{u_j^R(\bar{\eta}_{s,i})\}$. Each determinant is a Vandermonde determinant and is the unique totally antisymmetric wavefunction annihilated by the corresponding constraint.

The simplest ground state of composite bosons at zero temperature is the single-particle condensate

$$\langle c_{\mathbf{k} \sigma_1 \dots \sigma_{p-1}} \rangle = \sqrt{\bar{\rho}} \delta_{\mathbf{k},0} \prod_{\alpha} \delta_{\sigma_{\alpha},0} . \quad (3.16)$$

In coordinate space this can be rewritten suggestively as

$$\langle \psi_0(z, \bar{\eta}_1, \dots, \bar{\eta}_p) \rangle = \prod_s \tilde{\delta}(z, \bar{\eta}_s) , \quad (3.17)$$

where $\tilde{\delta}$ is the delta function with the magnetic length of the vortices, ℓ_{BR} . This puts the vortices on top of the particle, as one would expect from the lowest state due to electrostatic attraction. Projection onto the physical basis gives

$$f(z_1, \dots, z_N) = \int \prod_{s,i} d^2 \eta_{s,i} e^{-|\eta_{s,i}|^2 / 4\ell_{BR}^2} \prod_{s; i < j} (\eta_{s,i} - \eta_{s,j}) \prod_i^N \langle \psi_0(z_i, \bar{\eta}_{1,i}, \dots, \bar{\eta}_{p,i}) \rangle . \quad (3.18)$$

Using the condensate wavefunction (3.17), f is the product of p identical factors,

$$f(z_1, \dots, z_N) = \left[\int \prod_i d^2 \eta_i e^{-|\eta_i|^2 / 4\ell_{BR}^2} \prod_{i < j} (\eta_i - \eta_j) \prod_i \tilde{\delta}(z_i, \bar{\eta}_i) \right]^p . \quad (3.19)$$

Each factor is a Slater determinant of the matrix $m_{ij} = \{u_i^R(z_j)\}$, which is the same as a Vandermonde determinant of the matrix $v_{ij} = z_j^i$ times an overall factor. The end result is exactly the Laughlin state at $\nu = 1/p$,

$$f_p(z_1, \dots, z_N) = \prod_{i < j} (z_i - z_j)^p \prod_i e^{-|z_i|^2/4\ell_{BL}^2}. \quad (3.20)$$

Thus, we reinterpret the Laughlin state as a composite boson condensate.

However, there is a slight surprise if f_p is the unique characteristic of a Laughlin state. It turns out that the condensate is not required to carry the spin $\sigma_\alpha = 0$; any linear combination of the internal states $\{u_{\sigma_\alpha}^L(\bar{\xi}_\alpha)\}$ will project onto the same f_p . In other words, the simple condensate in eqn. (3.16) is generalized to

$$\langle c_{\mathbf{k}}(\bar{\xi}_1, \dots, \bar{\xi}_{p-1}) = \sqrt{\bar{\rho}} \delta_{\mathbf{k},0} u(\bar{\xi}_1, \dots, \bar{\xi}_{p-1}) \prod_{\alpha} e^{-|\xi_\alpha|^2/4\ell_{BL}^2}, \quad (3.21)$$

where u is a suitably normalized anti-analytic function of the $\bar{\xi}_\alpha$. In terms of composite bosons, the Laughlin state is infinitely degenerate (for all $p \neq 1$). We will come back to this question in Section 3.2 when we impose the constraints and model the fluctuations around the ground state.

Despite the infinitely degenerate ground state, the fundamental quasiholes can be represented unambiguously. We modify one delta function in equation (3.17) by $\tilde{\delta}(z, \bar{\eta}_s) \rightarrow \sum_m u_{m+1}^L(z) \overline{u_m^R(\eta_s)}$, moving the particle at z radially from the origin by one angular momentum unit. The effect on f_p is an overall factor of $\prod_i z_i$, which is the form of the quasihole wavefunction given by Laughlin [4]. This can be seen by writing one of the factors in eqn. (3.19) as a Slater determinant; the shifts $u_m^L(z_i) \rightarrow u_{m+1}^L(z_i)$ are equivalent to multiplying every column i by z_i and rescaling every row m by an overall numerical factor (due to the normalization of u_m), which only changes the determinant by an overall constant. Quasiholes can be moved around by applying magnetic translations $\hat{\tau}$, which are described in the Appendix.

3.2 Energy Functional

Section 3.1.c explained how the Laughlin wavefunction is a condensate of composite bosons. The salient feature was the degeneracy of the ground state. Let us rephrase this in terms

of the Hamiltonian (3.15), which is a function of only the left density. $\hat{\rho}^L$ is

$$\hat{\rho}_{\mathbf{q}}^L = \int \frac{d^2 \mathbf{k}}{(2\pi)^2} \sum_{\sigma_\alpha} e^{\frac{1}{2} i \mathbf{k} \wedge \mathbf{q} \ell_{B_L}^2} c_{\mathbf{k} - \frac{1}{2} \mathbf{q}, \sigma_1 \dots \sigma_{p-1}}^\dagger c_{\mathbf{k} + \frac{1}{2} \mathbf{q}, \sigma_1 \dots \sigma_{p-1}} \quad . \quad (3.22)$$

In eqn. (3.21) of the previous section, we pointed out that the condensate is infinitely degenerate because the Laughlin state does not depend on the wavefunction of the internal vortex coordinates. In other words, the expectation value of the Hamiltonian is unaffected by the internal “spin” state as long as the condensate is $\langle c_{\mathbf{k}, \sigma_1 \dots \sigma_{p-1}} \rangle \propto \delta_{\mathbf{k}, 0}$, which is enough to give $\langle \hat{\rho}_{\mathbf{k}}^L \rangle = \bar{\rho}$. Unlike the composite fermion case in Chapter 2, there is no unique mean field ground state to expand around. This degeneracy should disappear once the constraints are imposed.

Here we will follow an alternate route which allows us to include the constraints at the outset. We will construct a phenomenological Lagrangian that respects all the symmetries and include the constraints as Lagrange multipliers. The resulting Landau-Ginzburg theory can then be systematically expanded about a unique mean field solution.

The simplest rotationally invariant contribution to the Lagrangian consists of a momentum and a spin piece

$$\mathcal{L}_M + \mathcal{L}_J = - \sum_{\mathbf{k}, \sigma_\alpha} \left(\frac{1}{2M} |\mathbf{k}|^2 + \frac{J}{2} \sigma \right) c_{\mathbf{k} \sigma_1 \dots \sigma_{p-1}}^\dagger c_{\mathbf{k} \sigma_1 \dots \sigma_{p-1}} \quad , \quad (3.23)$$

where M, J are constants and $\sigma = \sum_{\alpha=1}^{p-1} \sigma_\alpha$. We may guess that the full Lagrangian should be

$$\mathcal{L} = \sum_{\mathbf{k}, \sigma_\alpha} c_{\mathbf{k} \sigma_1 \dots \sigma_{p-1}}^\dagger \partial_\tau c_{\mathbf{k} \sigma_1 \dots \sigma_{p-1}} + \mathcal{L}_M + \mathcal{L}_J + \mathcal{L}_{\text{constr}} \quad , \quad (3.24)$$

where the first term is the usual time derivative [53] and $\mathcal{L}_{\text{constr}}$ is the Lagrange multiplier term that imposes the constraints. However, this expression is not gauge invariant. \mathcal{L} must be invariant under the symmetries of c , which preserve the commutators of eqn. (3.2),

$$c \mapsto U_L c \prod_{i=1}^p U_{R_i} \quad , \quad (3.25)$$

where U_{R_i} is a unitary matrix acting on the i 'th right index and U_L acts on the left index of the matrix $c_{m; n_1 \dots n_p}$. We will find that in order to preserve these symmetries, it is necessary to introduce p gauge potentials that act on the right indices. The bare term $\mathcal{L}_M + \mathcal{L}_J$ will

acquire the vector components a_μ^i , $\mu = x, y$, and the Lagrange multipliers, λ^i , will play the role of the scalar potential a_0^i . Since the mass and spin terms are decoupled in $\mathcal{L}_M + \mathcal{L}_J$, we will consider their gauge invariant forms separately in the following two subsections.

3.2.a Mass Term

To write the mass term in coordinate space we need the transform of $i\mathbf{k}$, which is the analog of ∇ in ordinary space. To this end, define the LLL coordinate operators, Z and \bar{Z}

$$Z = z\delta(z, \bar{\xi}_{cm}) \quad \text{and} \quad \bar{Z} = \delta(z, \bar{\xi}_{cm})\bar{\xi}_{cm} , \quad (3.26)$$

which are adjoints of each other, $Z^\dagger = \bar{Z}$. In Cartesian coordinates $Z = Z_x + iZ_y$ and $Z_\mu^\dagger = Z_\mu$. It is straightforward to verify that the $\hat{\tau}_{\mathbf{k}}$ are eigenoperators of Z, \bar{Z} , that is

$$[Z * \hat{\tau}_{\mathbf{k}}] = -ik \hat{\tau}_{\mathbf{k}} \quad \text{and} \quad [\bar{Z} * \hat{\tau}_{\mathbf{k}}] = i\bar{k} \hat{\tau}_{\mathbf{k}} , \quad (3.27)$$

where the $*$ -commutator is defined in eqn. (7.4). As usual, $k = k_x + ik_y$ and $\bar{k} = k_x - ik_y$, so that $-\epsilon^{\mu\nu} [Z_\nu * \hat{\tau}_{\mathbf{k}}] = k_\mu \hat{\tau}_{\mathbf{k}}$. Therefore, $-i\epsilon^{\mu\nu} Z_\nu$ is the analog of the ordinary derivative operator ∂_μ when acting on $\hat{\tau}$. To see how Z acts on the matter field, we need to consider the Fock space operators in more detail.

In general, $c_{m; n_1, \dots, n_p}$ can be transformed on the left by some matrix $M_{mm'}$ or on the right by some matrix $\Lambda_{n'_i n_i}$ that acts on the i 'th right index. In coordinate space, $M = M(z, \bar{z}')$ and $\Lambda = \Lambda_i(\eta'_i, \bar{\eta}_i)$. We will continue to use the $*$ -operator, but its meaning must be clarified when acting on the right coordinates since there are p of them. We define

$$(c * \Lambda_i)(z, \bar{\eta}_1, \dots, \bar{\eta}_p) = \int d^2\eta'_i c(z, \bar{\eta}_1, \dots, \bar{\eta}'_i, \dots, \bar{\eta}_p) \Lambda_i(\eta'_i, \bar{\eta}_i) . \quad (3.28)$$

The index on the operator will always indicate the coordinate on which it acts, rendering this notation unambiguous. An example is $c * Z$, where Z acts on the center of mass coordinate:

$$\begin{aligned} (c * Z)(z, \bar{\eta}_1, \dots, \bar{\eta}_p) &= \frac{1}{p} \int d^2\eta'_1 c(z, \bar{\eta}'_1, \dots, \bar{\eta}_p) \eta'_1 \tilde{\delta}(\eta'_1, \bar{\eta}_1) + \dots \\ &+ \frac{1}{p} \int d^2\eta'_p c(z, \bar{\eta}_1, \dots, \bar{\eta}'_p) \eta'_p \tilde{\delta}(\eta'_p, \bar{\eta}_p) \end{aligned} \quad (3.29)$$

Let us define the coordinate operator from the right, v^i , by

$$v^i = \eta_i \tilde{\delta}(\eta_i, \bar{\eta}'_i) \quad \text{and} \quad \bar{v}^i = \tilde{\delta}(\eta_i, \bar{\eta}'_i) \bar{\eta}'_i , \quad (3.30)$$

such that

$$c * Z = \frac{1}{p} \sum_i c * v^i . \quad (3.31)$$

The Cartesian components of the v 's are Hermitian, $v_\mu^{i\dagger} = v_\mu^i$. Acting on the left, $Z * c$ is the same as before,

$$\begin{aligned} (Z * c)(z, \bar{\eta}_1, \dots, \bar{\eta}_p) &= \int d^2 z' z \delta(z, \bar{z}') c(z', \bar{\eta}_1, \dots, \bar{\eta}_p) \\ &\equiv z c(z, \bar{\eta}_1, \dots, \bar{\eta}_p) . \end{aligned} \quad (3.32)$$

Now, the Fourier transform, eqn. (3.11), together with the property in eqn. (3.27) afford a definition of the “derivative” operator

$$\bar{\partial} c = -\frac{1}{2} [Z * , c] \quad \text{and} \quad \partial c = \frac{1}{2} [\bar{Z} * , c] . \quad (3.33)$$

We translate this definition into Cartesian coordinates by using the conventional relations $\partial = (\partial_x - i\partial_y)/2$ and $\bar{\partial} = (\partial_x + i\partial_y)/2$,

$$\partial_\mu c = -i\epsilon^{\mu\nu} [Z_\nu * , c] , \quad (3.34)$$

where $\epsilon^{\mu\nu}$ is the Levi-Civita symbol. The non-commutative Fourier transform of $\partial_\mu c$ is $-ik_\mu c$. Further like ordinary derivatives, ∂_μ obeys the Leibnitz property $\partial(a * b) = \partial a * b + a * \partial b$, which follows easily from the Jacobi identity $[A, [B, C]] + [C, [A, B]] + [B, [C, A]] = 0$.

The unitary symmetry in eqn. (3.25) requires that the derivative operators are covariant. The infinitesimal version of the transformation on the right is obtained from the product of expanding each $U_{R_i} = 1 + i\Lambda_i$,

$$\begin{aligned} c &\mapsto c + ic * \Lambda \\ c^\dagger &\mapsto c^\dagger - i\bar{\Lambda} * c^\dagger , \end{aligned} \quad (3.35)$$

where Λ is a Hermitian operator,

$$\Lambda = \sum_i \Lambda_i(\eta'_i, \bar{\eta}_i) \quad (3.36)$$

and its conjugate is $\bar{\Lambda} = \sum_i \Lambda_i(\eta_i, \bar{\eta}'_i)$. A standard procedure from field theory can be used to make $\partial_\mu c$ covariant [60]. Since $Z_\mu * c$ is already covariant under right transformations, let

us consider each term in $c * Z_\mu$ separately, which are of the form $c * v_\mu^i$. First, we introduce a gauge potential $a_\mu^i(\eta'_i, \overline{\eta}_i)$ which transforms according to

$$a_\mu^i \mapsto a_\mu^i - \partial_\mu \Lambda_i + i[a_\mu^i * \Lambda_i] . \quad (3.37)$$

The derivative of Λ_i is constructed like $\partial_\mu c$,

$$\partial_\mu \Lambda_i = -i\epsilon^{\mu\nu}[v_\nu^i * \Lambda_i] . \quad (3.38)$$

Then the combination $c * (\epsilon^{\mu\nu} v_\nu^i + a_\mu^i)$ transforms according to the rules in eqns. (3.35) and (3.37):

$$\begin{aligned} c * (\epsilon^{\mu\nu} v_\nu^i + a_\mu^i) &\mapsto (c + ic * \Lambda_i) * (\epsilon^{\mu\nu} v_\nu^i + a_\mu^i + i\epsilon^{\mu\nu}[v_\nu^i * \Lambda_i] + i[a_\mu^i * \Lambda_i]) \\ &= c * (\epsilon^{\mu\nu} v_\nu^i + a_\mu^i) + ic * (\epsilon^{\mu\nu} v_\nu^i + a_\mu^i) * \Lambda_i + \mathcal{O}(\Lambda_i^2) \end{aligned} \quad (3.39)$$

showing that it is covariant.

The total contribution of the gauge potentials to $\epsilon^{\mu\nu} Z_\nu = \frac{1}{p} \sum_i \epsilon^{\mu\nu} v_\nu^i$ is just the sum of the individual gauge potentials, which we term a^{cm} ,

$$a_\mu^{cm} = \frac{1}{p} \sum_i a_\mu^i . \quad (3.40)$$

The covariant derivative becomes

$$\begin{aligned} D_\mu c &= \partial_\mu c - ic * a_\mu^{cm} \\ (D_\mu c)^\dagger &= \partial_\mu c^\dagger + ia_\mu^{cm} * c^\dagger . \end{aligned} \quad (3.41)$$

These derivatives obey $[D_\mu, D_\nu] = iG_{\mu\nu}$, where $G_{\mu\nu} = \partial_\mu a_\nu^{cm} - \partial_\nu a_\mu^{cm} - i[a_\mu^{cm} * a_\nu^{cm}]$ is the field strength [60]. By analogy to standard non-Abelian gauge theory, we will choose the transverse gauge for each a^i

$$\partial_\mu a_\mu^i = 0 . \quad (3.42)$$

The derivative is again defined by eqn. (3.38). Using the non-commutative Fourier transform, the gauge condition is exactly $\mathbf{q} \cdot a_{\mathbf{q}}^i = 0$.

The fully covariant mass term can now be written in coordinate space as

$$\begin{aligned} \mathcal{L}_M &\rightarrow -\frac{1}{2M} \text{Tr} \left[(D_\mu c)^\dagger * D_\mu c \right] \\ &= -\frac{1}{2M} \text{Tr} \left(\partial_\mu c^\dagger + ia_\mu^{cm} * c^\dagger \right) * \left(\partial_\mu c - ic * a_\mu^{cm} \right) . \end{aligned} \quad (3.43)$$

At mean field, the saddle point of the full Lagrangian

$$\begin{aligned}\langle a_\mu^{cm} \rangle &= 0 \\ \langle c_{\mathbf{k}, \sigma_1, \dots, \sigma_{p-1}} \rangle &= \sqrt{\bar{\rho}} \delta_{\mathbf{k}, 0} \prod_{\alpha} \delta_{\sigma_{\alpha}, 0} .\end{aligned}\tag{3.44}$$

After quadratically expanding \mathcal{L}_M about the saddle point, we find that the terms linear in a_μ^{cm} are proportional to $\partial_\mu a_\mu^{cm}$, which vanishes by the gauge choice. The quadratic term in a_μ^{cm} decouples from the matter fluctuations, and we are left with

$$\delta\mathcal{L}_M = -\frac{1}{2M} \text{Tr} \left(\partial_\mu c^\dagger * \partial_\mu c + \bar{\rho} a_\mu^{cm} * a_\mu^{cm} \right) .\tag{3.45}$$

In the next section, we will find a similar decoupling of the matter and gauge fluctuations in the spin term. Even if the ordinary kinetic energy $\mathbf{k}^2/2M$ is generalized to an arbitrary polynomial in \mathbf{k} , the same decoupling would hold at the Gaussian level. Gauge fields will be felt, however, as Lagrange multipliers in the constraint terms.

3.2.b Spin Term

Turning now to the spin term, we will suppress the left index in this subsection.

The preceeding subsection defined the operators $v^i = \eta_i \tilde{\delta}(\eta_i, \bar{\eta}'_i)$, whose sum was related to the center of mass coordinate operator. For the relative coordinates, the natural basis is

$$w^\alpha = -i \sum_j R_{\alpha,j} v^j \quad \text{and} \quad \bar{w}^\alpha = i \sum_j R_{\alpha,j} \bar{v}^j ,\tag{3.46}$$

where R is the Jacobi transformation $\xi_\alpha = \sum_j R_{\alpha,j} \eta_j$ that was constructed in Section 3.1.b. The i prefactor ensures that, in Cartesian coordinates, w_μ^α is related to $\epsilon^{\mu\nu} v_\nu^j$. This also has the effect of making the w_μ^α anti-Hermitian, $w_\mu^{\alpha\dagger} = -w_\mu^\alpha$, because v_μ^j is Hermitian.

In the single particle basis $u_\sigma^L(\xi_\alpha)$, w^α and \bar{w}^α act like $\xi_\alpha/\sqrt{2}\ell_{B_L}$ and $(\ell_{B_L}/\sqrt{2})\partial_{\xi_\alpha}$, respectively—see eqn. (2.16) and the immediately following discussion. Therefore, the quadratic form $\bar{w}^\alpha * w^\alpha$ is exactly $\sigma/2$, and the spin term can be written as

$$\begin{aligned}\mathcal{L}_J &= -J \sum_{\alpha} \text{Tr} \left(\bar{w}^\alpha * c^\dagger * c * w^\alpha \right) \\ &= -J \sum_{\alpha} \text{Tr} \left(w_\mu^\alpha * c^\dagger * c * w_\mu^\alpha \right) .\end{aligned}\tag{3.47}$$

Cyclicity of the trace was used to separate $w * \bar{w}$ in the first line. By changing to Cartesian coordinates in the second line, we ignore a constant term in the energy. This contribution is from the commutator $[\bar{w}^\alpha * w^\beta] = -2\delta_{\alpha\beta}$ to $w_\mu^\alpha * w_\mu^\alpha = (w^\alpha * \bar{w}^\alpha + \bar{w}^\alpha * w^\alpha)/2$.

Just as the ∂ 's were not covariant in the last subsection, the w^α are not, either. Recall from that discussion that each $c * \epsilon^{\mu\nu} v_\nu^i$ is made covariant by $\epsilon^{\mu\nu} v_\nu^i \mapsto \epsilon^{\mu\nu} v_\nu^i + a_\mu^i$. We thus introduce $p - 1$ gauge potentials a_μ^α ,

$$a_\mu^\alpha = \sum_i R_{\alpha,i} a_\mu^i \quad (3.48)$$

and the covariant operators W_μ^α ,

$$\begin{aligned} c * W_\mu^\alpha &= c * w_\mu^\alpha + c * a_\mu^\alpha \\ W_\mu^{\alpha\dagger} * c^\dagger &= -w_\mu^\alpha * c^\dagger + a_\mu^\alpha * c^\dagger. \end{aligned} \quad (3.49)$$

As in the previous section, we work in the Cartesian basis $\mu = x, y$ with $W_x = (W + \bar{W})/2$ and $W_y = (W - \bar{W})/2i$. The correct spin term is now

$$\begin{aligned} \mathcal{L}_J &\rightarrow -J \sum_\alpha \text{Tr} \left(W_\mu^{\alpha\dagger} * c^\dagger * c * W_\mu^\alpha \right) \\ &= J \sum_\alpha \text{Tr} \left(w_\mu^\alpha * c^\dagger - a_\mu^\alpha * c^\dagger \right) * \left(c * w_\mu^\alpha + c * a_\mu^\alpha \right). \end{aligned} \quad (3.50)$$

The part linear in a_μ^α is equal to

$$-J \text{Tr} c^\dagger * c * [w_\mu^\alpha * a_\mu^\alpha]. \quad (3.51)$$

The commutator is a sum of terms of the form $\epsilon^{\mu\nu} [v_\nu^i * a_\mu^j] \equiv i\partial_\mu a_\mu^i$ because $[v_\nu^i * a_\mu^j] = 0$ unless $i = j$. According to the transverse gauge choice, all terms in eqn. (3.51) vanish. In fact we can prove a more general statement for a polynomial spin dispersion. Any term in the energy of the form σ_α^n can be written as

$$\sigma_\alpha^n c_{\sigma_1 \dots \sigma_{p-1}}^\dagger c_{\sigma_1 \dots \sigma_{p-1}} = \text{Tr} c^\dagger * c * (W_\mu^{\alpha\dagger} * W_\mu^\alpha)^n. \quad (3.52)$$

The linear piece in a_μ^α always looks like (3.51) and vanishes in the transverse gauge. For our purposes, we will stick with the simplest non-trivial example, $J\sigma$.

The saddle point is

$$\begin{aligned} \langle a_\mu^\alpha \rangle &= 0 \\ \langle c_{\sigma_1 \dots \sigma_{p-1}} \rangle &= \prod_\alpha \delta_{\sigma_\alpha, 0} \end{aligned} \quad (3.53)$$

where the left coordinates are suppressed. Quadratic expansion about the saddle point gives the perturbation of \mathcal{L}_J as

$$\delta\mathcal{L}_J = -J \sum_{\alpha} \text{Tr} \left(w_{\mu}^{\alpha} * c^{\dagger} * c * w_{\mu}^{\alpha} + \bar{p} a_{\mu}^{\alpha} * a_{\mu}^{\alpha} \right) . \quad (3.54)$$

The second term is also proportional to $\sum_i \text{Tr} \left(a_{\mu}^i * a_{\mu}^i \right)$ because $\sqrt{p}R$ is orthogonal. It remains to treat the constraints gauge invariantly, the subject of the next section.

3.3 Constraints

We will treat the constraints by including p Lagrange multipliers, $\lambda^i(\eta_i, \bar{\eta}'_i)$. The Lagrangian then includes the term

$$\mathcal{L}_{\text{constr}} = i \sum_{i=1}^p \text{Tr} \lambda^i * \rho^{R_i} . \quad (3.55)$$

The ρ^{R_i} were constructed in eqn. (3.15). Gauge invariance under the transformation in eqn. (3.35) requires that

$$\lambda^i \mapsto \lambda^i + i[\Lambda_i * \lambda^i] .$$

The saddle point for λ^i is

$$\langle \lambda^i(\eta_i, \bar{\eta}'_i) \rangle = \tilde{\delta}(\eta_i, \bar{\eta}'_i) \quad (3.56)$$

or $\langle \lambda_{\mathbf{q}}^i \rangle = \delta_{\mathbf{q},0}$ in momentum space. Expansion of the fluctuations is analytically feasible if the $\rho_{\mathbf{q}}^{R_i}$ are expanded in powers of \mathbf{q} . It can be done exactly for $p = 2$, but we will also consider $p = 3$ to finite order.

At $p = 2$ there is only one relative coordinate, $\xi = (\eta_1 - \eta_2)/2$. The saddle point is

$$\begin{aligned} \langle c_{\mathbf{q}}(\bar{\xi}) \rangle &= \sqrt{\bar{p}} \delta_{\mathbf{q},0} \overline{u_0^L(\xi)} \\ \langle \lambda_{\mathbf{q}}^i \rangle &= \delta_{\mathbf{q},0} \end{aligned} \quad (3.57)$$

The displacement of the vortices from the center of mass was $\xi_{cm} - \eta_1 = -\xi$ and $\xi_{cm} - \eta_2 = \xi$ according to the Jacobi mapping in eqn. (3.9). Plugging this into the right densities, eqn.

(3.15), and expanding in powers of c about the saddle point we get

$$\begin{aligned}
\delta\rho_{\mathbf{q}}^{R_1} &= \sqrt{\frac{\bar{\rho}}{2\pi}} \int d^2\xi c_{\mathbf{q}}(\bar{\xi}) e^{-\frac{1}{4}|\xi|^2 - \frac{i}{2}\bar{q}\xi - \frac{1}{4}|q|^2} \\
&+ \sqrt{\frac{\bar{\rho}}{2\pi}} \int d^2\xi c_{-\mathbf{q}}^\dagger(\xi) e^{-\frac{1}{4}|\xi|^2 - \frac{i}{2}q\bar{\xi} - \frac{1}{4}|q|^2} , \\
\delta\rho_{\mathbf{q}}^{R_2} &= \sqrt{\frac{\bar{\rho}}{2\pi}} \int d^2\xi c_{\mathbf{q}}(\bar{\xi}) e^{-\frac{1}{4}|\xi|^2 + \frac{i}{2}\bar{q}\xi - \frac{1}{4}|q|^2} \\
&+ \sqrt{\frac{\bar{\rho}}{2\pi}} \int d^2\xi c_{-\mathbf{q}}^\dagger(\xi) e^{-\frac{1}{4}|\xi|^2 + \frac{i}{2}q\bar{\xi} - \frac{1}{4}|q|^2} ,
\end{aligned} \tag{3.58}$$

where c is the fluctuation about $\langle c \rangle$ and $\delta\rho^R \equiv \rho^R - \bar{\rho}$. $\ell_{B_L}^2$ is set to one above, and in what follows. If we make use of the identity

$$\frac{1}{2\pi} e^{-\frac{1}{4}|\xi|^2 - \frac{i}{2}\bar{q}\xi - \frac{1}{4}|q|^2} = \delta(\xi, -i\bar{q}) \equiv \sum_{\sigma=0}^{\infty} u_{\sigma}(\xi) \overline{u_{\sigma}(iq)} , \tag{3.59}$$

then

$$\begin{aligned}
\delta\rho_{\mathbf{q}}^{R_1} &= \sqrt{\bar{\rho}} \sum_{\sigma} c_{\mathbf{q}\sigma} u_{\sigma}(-i\bar{q}) + c_{-\mathbf{q}\sigma}^\dagger u_{\sigma}(-iq) , \\
\delta\rho_{\mathbf{q}}^{R_2} &= \sqrt{\bar{\rho}} \sum_{\sigma} c_{\mathbf{q}\sigma} u_{\sigma}(i\bar{q}) + c_{-\mathbf{q}\sigma}^\dagger u_{\sigma}(iq) .
\end{aligned} \tag{3.60}$$

This is an explicit expansion in powers of q since $u_{\sigma}(q) \sim q^{\sigma}$ (aside from an overall Gaussian factor). The superscript L has been dropped from u as we are setting $\ell_{B_L} = 1$.

Moving on to $p = 3$, there are two relative coordinates, $\xi_{1,2}$ that are given by eqn. (3.10). The matter field is $c_{\mathbf{q}}(\bar{\xi}_1, \bar{\xi}_2)$ with expectation value

$$\langle c_{\mathbf{q}}(\bar{\xi}_1, \bar{\xi}_2) \rangle = \sqrt{\bar{\rho}} \delta_{\mathbf{q},0} \overline{u_0(\xi_1)} \overline{u_0(\xi_2)} .$$

As in the $p = 2$ case, we obtain $\xi_{cm} - \eta_i$ in terms of the Jacobi coordinates from eqn. (3.10), put the result into the definition of ρ^{R_i} in eqn. (3.15) and expand about the saddle point in powers of c . For example, $\xi_{cm} - \eta_1 = -\sqrt{\frac{3}{2}}\xi_1 - \sqrt{\frac{1}{2}}\xi_2$, which gives

$$\begin{aligned}
\delta\rho_{\mathbf{q}}^{R_1} &= \\
&\int d^2\xi_1 d^2\xi_2 c_{\mathbf{q}}(\bar{\xi}_1, \bar{\xi}_2) u_0(\xi_1) u_0(\xi_2) e^{-\frac{1}{4}|\sqrt{\frac{3}{2}}\xi_1 + \sqrt{\frac{1}{2}}\xi_2|^2 - \frac{1}{2}\bar{q}(\sqrt{\frac{3}{2}}\xi_1 + \sqrt{\frac{1}{2}}\xi_2) - \frac{1}{4}|q|^2} + h.c. \\
&= 2\pi \int d^2\xi_1 d^2\xi_2 c_{\mathbf{q}}(\bar{\xi}_1, \bar{\xi}_2) \delta(\xi_1, -i\bar{q}\sqrt{3/2}) \delta(\xi_2, -i\bar{q}\sqrt{1/2}) + h.c. ,
\end{aligned} \tag{3.61}$$

where we used the delta function identity, eqn. (3.59). The procedure is analogous for $\rho^{R_{2,3}}$, and we obtain in spin space

$$\begin{aligned}
\delta\rho_{\mathbf{q}}^{R_1} &= \sqrt{p} \sum_{\sigma_1\sigma_2} c_{\mathbf{q}\sigma_1\sigma_2} u_{\sigma_1}(-i\bar{q}\sqrt{3/2}) u_{\sigma_2}(-i\bar{q}\sqrt{1/2}) + \\
&\quad \sqrt{p} \sum_{\sigma_1\sigma_2} c_{-\mathbf{q}\sigma_1\sigma_2}^\dagger u_{\sigma_1}(-iq\sqrt{3/2}) u_{\sigma_2}(-iq\sqrt{1/2}) ; \\
\delta\rho_{\mathbf{q}}^{R_2} &= \sqrt{p} \sum_{\sigma_1\sigma_2} c_{\mathbf{q}\sigma_1\sigma_2} u_{\sigma_1}(i\bar{q}\sqrt{3/2}) u_{\sigma_2}(-i\bar{q}\sqrt{1/2}) + \\
&\quad \sqrt{p} \sum_{\sigma_1\sigma_2} c_{-\mathbf{q}\sigma_1\sigma_2}^\dagger u_{\sigma_1}(iq\sqrt{3/2}) u_{\sigma_2}(-iq\sqrt{1/2}) ; \\
\delta\rho_{\mathbf{q}}^{R_3} &= \sqrt{2\pi p} \sum_{\sigma_2} c_{\mathbf{q}0\sigma_2} u_{\sigma_2}(i\bar{q}\sqrt{2}) + \sqrt{2\pi p} \sum_{\sigma_2} c_{-\mathbf{q}0\sigma_2}^\dagger u_{\sigma_2}(iq\sqrt{2}) .
\end{aligned}$$

3.4 Density Response and the Magnetoroton

The results of the last three sections add into the fluctuations of the Lagrangian density,

$$\delta\mathcal{L} = \text{Tr} (c^\dagger * \partial_\tau c) - \delta\mathcal{L}_M - \delta\mathcal{L}_J - i \sum_{i=1}^p \delta\lambda_{-\mathbf{q}}^i \delta\rho_{\mathbf{q}}^{R_i} , \quad (3.62)$$

where the first term is the usual Berry phase, τ being complex time, and the other pieces are given by eqns. (3.45), (3.54), and (3.55).

We can drop the fluctuations in the vector potentials, a^{cm} and a^i since they are decoupled and will not affect the physical quantities. Then in momentum space, $\delta\mathcal{L}_J + \delta\mathcal{L}_M$ become

$$\delta\mathcal{L}_M + \delta\mathcal{L}_J = \sum_{\sigma_\alpha} E_{\mathbf{k},\sigma} c_{\mathbf{k}\sigma_1\cdots\sigma_{p-1}}^\dagger c_{\mathbf{k}\sigma_1\cdots\sigma_{p-1}} , \quad (3.63)$$

where

$$\begin{aligned}
E_{\mathbf{k},\sigma} &= \varepsilon_{\mathbf{k}} + J_\sigma \\
\varepsilon_{\mathbf{k}} &= \frac{k^2}{2M} \\
J_\sigma &= J\sigma .
\end{aligned} \quad (3.64)$$

As observed previously, both $\varepsilon_{\mathbf{k}}$ and J_σ can be arbitrary polynomials in \mathbf{k} and σ , respectively, but the present form suffices for our purposes.

Let us rewrite the Lagrangian as

$$\delta\mathcal{L} = \delta\phi_k^\dagger \mathbf{G}_k^{-1} \delta\phi_k \quad (3.65)$$

$$\delta\phi_k = \begin{pmatrix} \delta\lambda_k^i \\ c_{-k\sigma}^\dagger \\ c_{k\sigma} \end{pmatrix} \quad (3.66)$$

The propagator matrix \mathbf{G} carries the physical information, including the correlation functions and the spectrum of excitations via the zeros of its determinant. We consider the $p = 2, 3$ cases in the following sections.

3.4.a The case $p = 2$

It is a lengthy, but straightforward, calculation to obtain the determinant by Gauss-Jordan elimination. It proves convenient to use the basis $\lambda^\pm = \lambda^1 \pm \lambda^2$, and we find,

$$\text{Det } \mathbf{G}^{-1} = P_{\text{even}} P_{\text{odd}}, \quad (3.67)$$

where

$$\begin{aligned} P_{\text{even}} &= \left\{ \prod_{\sigma=0}^{\infty} [E_{\mathbf{k},2\sigma}^2 - \omega_n^2] \right\} \left\{ \sum_{\sigma=0}^{\infty} \frac{|u_{2\sigma}|^2 E_{\mathbf{k},2\sigma}}{E_{\mathbf{k},2\sigma}^2 - i\omega_n^2} \right\} \\ P_{\text{odd}} &= \left\{ \prod_{\sigma=0}^{\infty} [E_{\mathbf{k},2\sigma+1}^2 - \omega_n^2] \right\} \left\{ \sum_{\sigma=0}^{\infty} \frac{|u_{2\sigma+1}|^2 E_{\mathbf{k},2\sigma+1}}{E_{\mathbf{k},2\sigma+1}^2 - i\omega_n^2} \right\} \end{aligned} \quad (3.68)$$

and $u_\sigma \equiv u_\sigma(k)$.

The general features of the spectrum emerge already if we keep only the terms up to $\sigma = 3$. We find that the lowest mode is

$$i\omega_n = \left[E_{\mathbf{k},0} E_{\mathbf{k},2} \left(\frac{\mathbf{k}^4 E_{\mathbf{k},0} + 8E_{\mathbf{k},2}}{\mathbf{k}^4 E_{\mathbf{k},2} + 8E_{\mathbf{k},0}} \right) \right]^{1/2}, \quad (3.69)$$

which is plotted in fig. 3.2. In keeping with an incompressible fluid, there is a finite gap at $\mathbf{k} = 0$. In general, the modes have energy gaps equal to σJ with $\sigma \geq 2$. The lowest mode is a mixture of only σ =even channels, the next one up is a mixture of σ =odd, and so forth, alternating in even/odd mixtures. Because the gap would vanish if the constraints were not included, or if $J \rightarrow 0$, the low energy physics is dominated by the internal vortex excitations of σ . The main feature in fig. 3.2 is the dip. According to the approximation in eqn. (3.69) it appears whenever $J > 1/M$. We have plotted the spectrum by including terms up to $\sigma = 4$, i.e. to $\mathcal{O}(q^8)$, and the shape is virtually identical to fig. 3.2. In proper units, the dip

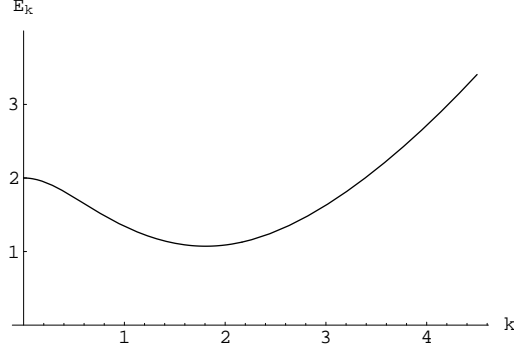


Figure 3.2: Lowest mode at $\nu = 1/2$ obtained from the action expanded to $\mathcal{O}(k^3)$. \mathbf{k} is in units of inverse magnetic length. The parameters are $m = 3$ and $J = 1$.

is always located at $|\mathbf{k}^*| \sim 1/\ell_{BL}$. It would seem to correspond to the magnetoroton that has been proposed by several authors [55, 58]. However, ours is the first analytical observation of this phenomena; earlier predictions relied on numerics. Based on the composite fermion picture, \mathbf{k} is proportional to the dipole moment, or separation between the particle and the center of mass of the vortices. It is tempting to conclude that the dip is an electrostatic-like feature, occurring when the relative orbit radius of the vortices is equal to the distance from the particle to their center of mass, i.e. $\xi/2 \sim \xi_{cm}$.

The density-density response function, $\chi^{LL}(q)$ can be calculated within the above framework as well. The connected part of this correlation function is

$$\chi^{LL}(q) = \langle \delta\rho_q^L \delta\rho_{-q}^L \rangle , \quad (3.70)$$

where $q = (\mathbf{q}, i\omega_n)$ and $\delta\rho^L$ is the fluctuating part of ρ^L (eqn. (3.22)). Expanding about the condensate in eqn. (3.57) gives,

$$\delta\rho_q^L = \sqrt{p}(c_{\mathbf{q},0}u_0 + c_{-\mathbf{q},0}^\dagger u_0) . \quad (3.71)$$

One way to get the lowest order term in χ is to substitute the expansions for $\rho^{R_{1,2}}$. A simple linear combination from eqn. (3.60) yields

$$\begin{aligned} \frac{1}{2}(\delta\rho_{\mathbf{q}}^{R_1} + \delta\rho_{\mathbf{q}}^{R_2}) &= \sqrt{p} \sum_{\sigma=0,2,4,\dots} \left(c_{\mathbf{q}\sigma} u_\sigma(-i\bar{q}) + c_{-\mathbf{q}\sigma}^\dagger u_\sigma(-iq) \right) \\ &= \delta\rho_{\mathbf{q}}^L + \sqrt{p} \sum_{\sigma=2,4,\dots} \left(c_{\mathbf{q}\sigma} u_\sigma(-i\bar{q}) + c_{-\mathbf{q}\sigma}^\dagger u_\sigma(-iq) \right) . \end{aligned} \quad (3.72)$$

On the average, the left-hand side is zero because the constraints vanish at mean field, $\langle \delta \rho_q^R \rangle = 0$, so that $\delta \rho_q^L \sim \mathcal{O}(|\mathbf{q}|^2)$ and

$$\chi^{LL}(q) = \mathcal{O}(|\mathbf{q}|^4) \quad (3.73)$$

just as we had before in the composite fermion case.

The same result can be obtained by an explicit calculation that extracts the field correlators from eqn. (3.66). An expansion in minors (Cramer's rule) of the propagator matrix \mathbf{G} leads to

$$\begin{aligned} \langle c_{\mathbf{k},0}^\dagger c_{\mathbf{k},0} \rangle &= -\frac{(i\omega_n + \varepsilon_{\mathbf{k}}) Q + |u_0|^2}{(\omega_n^2 + \varepsilon_{\mathbf{k}}^2) Q + 2|u_0|^2 \varepsilon_{\mathbf{k}}} \\ \langle c_{\mathbf{k},0}^\dagger c_{-\mathbf{k},0}^\dagger \rangle &= \frac{|u_0|^2}{(\omega_n^2 + \varepsilon_{\mathbf{k}}^2) Q + 2|u_0|^2 \varepsilon_{\mathbf{k}}} \end{aligned} \quad (3.74)$$

where

$$Q = \sum_{\sigma=2,4,6,\dots} \frac{2|u_\sigma|^2 E_{\mathbf{k},\sigma}}{\omega_n^2 + E_{\mathbf{k},\sigma}}. \quad (3.75)$$

Plugging these correlators into $\chi^{LL}(k) = \bar{\rho} \langle (c_{\mathbf{k},0} + c_{-\mathbf{k},0}^\dagger)^2 \rangle$, we find

$$\lim_{\mathbf{k} \rightarrow 0} \chi^{LL}(\mathbf{k}, i\omega_n = 0) = -\frac{|\mathbf{k}|^4}{16J}. \quad (3.76)$$

This result is consistent with an incompressible quantum Hall fluid [55]. Note that the limit is independent of M and is valid so long as $J \neq 0$, which is consistent with the vortex excitations dominating the long distance physics.

3.4.b The case $p = 3$

The expansions of the constraints, eqn. (3.62), is prohibitive in general. To get an idea of the spectrum, we cut the expansion off after $\sigma_{1,2} = 2$. The spectrum, as obtained from the zeros of \mathbf{G} is

$$i\omega_n = \begin{cases} \left[E_{\mathbf{k},0} E_{\mathbf{k},2} \left(\frac{\mathbf{k}^4 E_{\mathbf{k},0} + 4E_{\mathbf{k},2}}{\mathbf{k}^4 E_{\mathbf{k},2} + 4E_{\mathbf{k},0}} \right) \right]^{1/2} \\ \left[E_{\mathbf{k},1} E_{\mathbf{k},2} \left(\frac{\mathbf{k}^4 E_{\mathbf{k},1} + 4E_{\mathbf{k},2}}{\mathbf{k}^4 E_{\mathbf{k},2} + 4E_{\mathbf{k},1}} \right) \right]^{1/2} \end{cases}. \quad (3.77)$$

The second branch in eqn. (3.77) is doubly degenerate. Presumably this degeneracy would be lifted in a better approximation. The two modes are shown in fig. 3.3. With the help

of MATHEMATICA, we have analyzed the spectrum in more detail and find that the gaps are $J\sigma$, $\sigma \geq 2$. A non-zero gap, of course, is consistent with an incompressible fluid. Once

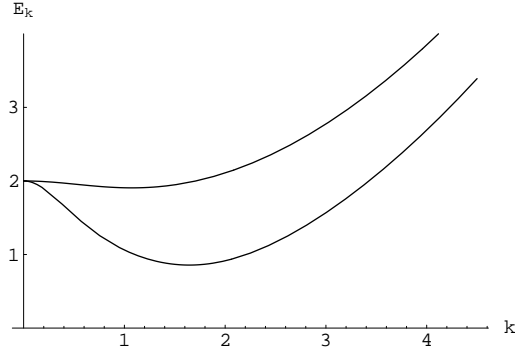


Figure 3.3: Lowest two modes at $\nu = 1/3$ obtained by expanding the action to $\mathcal{O}(k^2)$. The higher mode is doubly degenerate. \mathbf{k} is in units of inverse magnetic length. The parameters are $m = 3$ and $J = 1$.

again, the main feature is the magnetoroton gap. It seems to be a general feature for all p , provided that J is large enough relative to $1/M$.

Chapter 4

Paired States of Bosons in Two Dimensions

In this chapter we analyze p- and d-wave pairing of bosons from two points of view. First as an exact ground state of a particular Hamiltonian in the FQHE, where the bosons are really composite bosons. And second, in the framework of BCS theory of paired states of ordinary bosons.

We find that the permanent is an anti-Skyrmion texture sitting on the transition between ferromagnetic and helical ordering, both of which are single-particle condensates. The transition is of second order so that we can write a continuum quantum ferromagnet action [61] for the local magnetization in its vicinity. An analogous description on a lattice is straightforward and will be discussed briefly. The results are compared to numerics with excellent agreement.

In Section 4.2 we move on to the Haffnian. As we did for the permanent, we first construct a three-body Hamiltonian for which the trial wavefunction is exact, and from which numerical diagonalization techniques can extract the spectrum. Unfortunately in this case we cannot calculate the spectrum analytically and we resort to an effective BCS-type hamiltonian at the outset. A mean field analysis suggests three possible phases in the presence of an attractive channel at $l = -2$: (i) a single particle condensate, or Laughlin state, (ii) a pure pair state and (iii) a charge-density-wave phase. We conjecture that

the Haffnian lies on the special point separating (i) from (ii). In support, our numerical evidence suggests that the Haffnian is compressible and that it may contain incipient long range correlations in the density.

4.1 The Permanent: p-wave Pairing

4.1.a Analytic Structure of the Ground State

Before discussing the actual calculations, we briefly summarize the relevant properties of the permanent state. Detailed analysis and related states may be found elsewhere [28, 30, 62]. For the moment we begin by choosing to put the system on a sphere with a magnetic monopole in the center [14].

For $\nu = 1/q$, the permanent state is a spin-singlet ground state of spin-1/2 fermions for q =odd and of spin-1/2 bosons for q =even. The former case is the relevant one here, the simplest being $q = 1$. At this filling factor, the microscopic three-body Hamiltonian is the projection onto the manifold of states spanned by the closest approach of three fermions. It takes an especially compact form on the sphere, where each particle in the lowest Landau level (LLL) has orbital angular momentum $N_\phi/2$:

$$H = V \sum_{i < j < k} P_{ijk} \left(\frac{3}{2} N_\phi - 1, \frac{1}{2} \right). \quad (4.1)$$

The arguments $(3N_\phi/2 - 1, 1/2)$ are the total orbital angular momentum and z -component of spin, respectively, of three fermions at closest approach. P_{ijk} is the projection operator onto these states for each triplet of particles. Note that the angular momentum is allowed to be half integral because the relevant single particles states are monopole harmonics [63]. Due to symmetry, three fermions can never have total orbital angular momentum $3N_\phi/2$, so H is properly regarded as a projection onto triplet states of momentum *greater than or equal to* $3N_\phi/2 - 1$. To specify a unique ground state, the total flux, N_ϕ , through the sphere must be fixed. At $N_\phi = (N - 1) - 1$, the permanent is the densest zero-energy eigenstate of H . The densest state being the one with the smallest N_ϕ . For our purposes, it is most convenient to project stereographically onto the plane, where the i 'th particle has the complex coordinate $z_i = x_i + iy_i$. Denoting the spin component of the i 'th particle by

$\sigma_i = \uparrow_i, \downarrow_i$, casts the permanent into the form:

$$\Psi_{\text{perm}}(z_1 \sigma_1, \dots, z_{N/2} \sigma_{N/2}) = \sum_P \prod_{i=1}^{N/2} \frac{\uparrow_{P(2i-1)} \downarrow_{P(2i)} - \downarrow_{P(2i-1)} \uparrow_{P(2i)}}{z_{P(2i-1)} - z_{P(2i)}} \prod_{i < j} (z_i - z_j). \quad (4.2)$$

The prefactor is the permanent of an $N \times N$ matrix, which is a determinant with the sign of the permutation omitted, and P stands for all permutations of N objects. The second factor is the usual Laughlin-Jastrow ansatz with the Gaussian factors omitted. The BCS pairing structure of the prefactor is manifest in the above form; the spatial part of the pair wavefunction is in an orbital angular momentum $l = -1$ eigenstate and the spin part is a singlet. Therefore the prefactor is totally symmetric, representing a paired wavefunction of bosonic coordinates, which are non other than the composite bosons.

The factors in the denominator ensure that the relative angular momentum of each disjoint pair $(z_i - z_j)$ is reduced such that each projection by P_{ijk} gives zero. In other words, H penalizes those states which do not appear in the wavefunction. Addition of one flux quantum preserves this property and there is a space of zero energy states including the Laughlin state. Equivalently, reducing the flux by one quantum through the Laughlin state creates an anti- Skyrmion, which is a uniform spin configuration on the sphere (a “hedgehog”) costing zero energy. Stated in yet another way, extra flux in the permanent creates quasiholes (or edge states), which belong to a degenerate manifold of zero-energy states [30, 64]. The advantage of the $q = 1$ Laughlin state is that it is a Slater determinant of single particle states, which in this case is a Vandermonde determinant:

$$\Psi_L(z_1, \dots, z_N) = \prod_i \begin{pmatrix} 1 \\ 0 \end{pmatrix}_i \prod_{i < j} (z_i - z_j), \quad (4.3)$$

where $(1 \ 0)_i$ is the spin state of the i 'th particle, so that the total z - component of spin is $S_z = N/2$. The spin-wave states correspond to superpositions of the degenerate states defined by $S_z = N/2 - 1$. Notice that the prefactor of the Laughlin-Jastrow factor is trivially constant and symmetric under particle interchange. By analogy to the permanent (4.2), we interpret the prefactor as a wavefunction of composite bosons.

In the following subsection we switch to the plane and construct the spin wave excitations in the LLL using magnetic translation operators, with which we obtain the exact spin wave

spectrum at all wavevectors. We do not utilize the composite boson picture yet and all results in the next section are completely exact.

4.1.b Magnetic Translations on the Plane

A single magnon mode with momentum \mathbf{k} is represented in terms of spin density operators by $\hat{S}_{\mathbf{k}}^- = \sum_{j=1}^N e^{-i\mathbf{k}\cdot\mathbf{r}_j} \hat{\sigma}_j^-$, which periodically flips one spin of a completely polarized state. However, all operators must not have any components in the higher Landau levels. To impose this constraint, it proves necessary to project all operators into the LLL using the Bargmann-Fock representation [69, 65]. As a consequence, a magnon is composed of flipped spins along the direction *perpendicular* to \mathbf{k} .

The fundamental operator that we will need is the projected one-body density operator $\overline{\rho}_{\mathbf{k}}(\mathbf{r}_i) = \overline{e^{-i\mathbf{k}\cdot\mathbf{r}_i}}$. Here and throughout this chapter the overbar denotes projection into the LLL. This operator is discussed in detail in the Appendix. Because translations no longer commute in the LLL due to broken time translation symmetry in the presence of a magnetic field, a charged particle picks up an Aharonov-Bohm phase as it traverses a closed circuit. However, there is a one-to-one correspondence between the ordinary translations in zero field and the magnetic translations. In zero field, $\rho_{\mathbf{k}}(\mathbf{r}_i)$ translates the i 'th particle by a distance \mathbf{r} , and the corresponding magnetic translation, $\tau_{\mathbf{k}}(i)$, is a translation by $l_B^2 \hat{\mathbf{z}} \times \mathbf{k}$, where l_B is the magnetic length and $\hat{\mathbf{z}}$ is the direction of the magnetic field. The cross-product appears as a consequence of the Lorentz force. The explicit relation is

$$\tau_{\mathbf{k}}(i) = e^{\frac{k^2}{4}} \overline{\rho}_{\mathbf{k}}(\mathbf{r}_i), \quad (4.4)$$

where the magnetic length has been set to unity—as it will be throughout the chapter. The ubiquitous Gaussian factor can be thought of as the momentum space version of the most localized wavepacket in the LLL, or the projected delta function. The total spin and charge density operators are easily obtained from (4.4):

$$\overline{\rho}_{\mathbf{k}} = \sum_{i=1}^N e^{-\frac{k^2}{4}} \tau_{\mathbf{k}}(i) \quad (4.5)$$

$$\overline{S}_{\mathbf{k}}^a = \sum_{i=1}^N e^{-\frac{k^2}{4}} \tau_{\mathbf{k}}(i) \sigma_i^a, \quad (4.6)$$

where σ^a is the a 'th Pauli matrix. The projected spin density flips one spin and translates the resulting state by $\hat{\mathbf{z}} \times \mathbf{k}$, which is a quasihole-quasiparticle pair. The limit of large \mathbf{k} corresponds to a large pair so we expect that the spin wave spectrum approaches an asymptotic value in this limit.

The Laughlin state (4.3) is a Slater determinant, which allows the density-density correlation to be determined analytically [1] at $\nu = 1$. In terms of the magnetic translations in (4.5), the pair correlation function (projected onto the LLL) is:

$$\langle \Psi_L | : \overline{\rho_{\mathbf{q}} \rho_{-\mathbf{k}}} : | \Psi_L \rangle = \sum_{i \neq j} e^{-\frac{q^2}{4}} e^{-\frac{k^2}{4}} \langle \tau_{\mathbf{q}}(i) \tau_{-\mathbf{k}}(j) \rangle = -\langle \rho \rangle^2 \delta_{\mathbf{k}\mathbf{q}} e^{-\frac{q^2}{2}},$$

or

$$\sum_{i \neq j} \langle \tau_{\mathbf{q}}(i) \tau_{-\mathbf{k}}(j) \rangle = -\langle \rho \rangle^2 \delta_{\mathbf{k}\mathbf{q}}, \quad (4.7)$$

where the colons remove self-correlations by normal ordering. Equation (4.7) is the building block for much of the subsequent analytical results.

The non-commutativity of magnetic translations is irrelevant in (4.7) because the products involve different particles. However, the translations do not commute for the same particle. Rather, they form a representation of the magnetic translation group with the algebra:

$$[\tau_{\mathbf{q}}(i), \tau_{\mathbf{k}}(j)] = 2i \delta_{ij} \tau_{\mathbf{q}+\mathbf{k}}(i) \sin \frac{\mathbf{q} \wedge \mathbf{k}}{2} \quad (4.8)$$

$$\tau_{\mathbf{q}}(i) \tau_{\mathbf{k}}(i) = \tau_{\mathbf{q}+\mathbf{k}}(i) e^{\frac{i}{2} \mathbf{q} \wedge \mathbf{k}}, \quad (4.9)$$

where the wedge product stands for $(\mathbf{q} \times \mathbf{k}) \cdot \hat{\mathbf{z}}$.

Using the projected spin density operator we can easily construct a single magnon by applying the spin density operator (4.6) to the Laughlin state: $\Psi_{\mathbf{k}} = \bar{S}_{\mathbf{k}} \Psi_L$.

4.1.c Spin-Waves and Instability; Exact Results

The translationally invariant version of the three-body Hamiltonian (4.1) on the plane can be written as:

$$H = V \sum_{i \neq j \neq k} \nabla_i^2 \delta(\mathbf{r}_i - \mathbf{r}_j) \delta(\mathbf{r}_i - \mathbf{r}_k) \quad (4.10)$$

Of course, all observables are to be calculated after projection into the LLL. Since the Hamiltonian conserves the total spin, as well as being translationally invariant, the state

with one magnon is an exact eigenstate of \overline{H} with energy given by the usual expression [66]:

$$\omega_{\mathbf{k}} = \frac{\langle \Psi_L | \overline{S}_{\mathbf{k}}^+ [\overline{H}, \overline{S}_{\mathbf{k}}^-] | \Psi_L \rangle}{\langle \Psi_L | \overline{S}_{\mathbf{k}}^+ \overline{S}_{\mathbf{k}}^- | \Psi_L \rangle} . \quad (4.11)$$

Within the expectation value of \overline{H} , the two gradients reduce the orbital angular momentum of a triplet in $\Psi_{\mathbf{k}}$ and in $\Psi_{\mathbf{k}}^*$ by one, hence the identity with the spherical Hamiltonian (4.1).

\overline{H} can be rewritten in terms of the real-space density operator $\rho(\mathbf{r}) = \sum_i \delta(\mathbf{r} - \mathbf{r}_i)$ in a similar manner:

$$\begin{aligned} \overline{H} &= V \int d^2\mathbf{x} d^2\mathbf{x}' d^2\mathbf{x}'' : \nabla_{\mathbf{x}}^2 \overline{\rho}(\mathbf{x}) \overline{\rho}(\mathbf{x}') \overline{\rho}(\mathbf{x}'') : \delta(\mathbf{x} - \mathbf{x}') \delta(\mathbf{x}' - \mathbf{x}'') \\ &= -V \sum_{\mathbf{q}, \mathbf{p}} q^2 e^{-\frac{q^2}{4}} e^{-\frac{(\mathbf{q}-\mathbf{p})^2}{4}} e^{-\frac{p^2}{4}} \sum_{i \neq j \neq k} \tau_{-\mathbf{q}}(i) \tau_{\mathbf{q}-\mathbf{p}}(j) \tau_{\mathbf{p}}(k) . \end{aligned} \quad (4.12)$$

The last line is obtained by a Fourier transform and by the relation between the density and magnetic operators (4.5). Substitution of the last line into the energy expression (4.11) and use of the magnetic operator algebra (4.8) and (4.9) reduces the dispersion to:

$$\begin{aligned} \omega_{\mathbf{k}} &= -V \sum_{\mathbf{q}, \mathbf{p}} q^2 e^{-\frac{q^2}{2}} e^{-\frac{(\mathbf{q}-\mathbf{p})^2}{2}} e^{-\frac{p^2}{2}} \times \\ &\quad \sum_{i \neq j \neq k} \langle \tau_{-\mathbf{q}}(i) \tau_{\mathbf{q}-\mathbf{p}}(j) \tau_{\mathbf{p}}(k) \rangle_L \left(e^{i\mathbf{p} \wedge \mathbf{k}} + e^{i(\mathbf{q}-\mathbf{p}) \wedge \mathbf{k}} + e^{-i\mathbf{q} \wedge \mathbf{k}} - 3 \right) . \end{aligned} \quad (4.13)$$

Rather than calculating the triple-density correlator directly, observe that everything inside the expectation value is already in the LLL. Thus, the magnetic translations can be replaced by density operators according to the rule in (4.5). After Fourier transforming back into real space, we are left with terms like $\langle : \nabla_{\mathbf{x}}^2 \rho(\mathbf{x}) \rho(\mathbf{x}') \rho(\mathbf{x}'') : \rangle \delta(\mathbf{x} - \mathbf{x}') \delta(\mathbf{x}' - \mathbf{x}'' + \mathbf{k} \times \hat{\mathbf{z}})$, which can be evaluated by writing the density operator in second quantization, $\rho(\mathbf{x}) = \langle \hat{\psi}^\dagger(\mathbf{x}) \hat{\psi}(\mathbf{x}) \rangle$, and using Wick's theorem. For the spin-polarized $\nu=1$ state, the Green's function is known exactly [1], being, in the symmetric gauge,

$$\langle \hat{\psi}^\dagger(\mathbf{x}) \hat{\psi}(\mathbf{x}') \rangle_L = \langle \rho \rangle e^{-\frac{1}{4}|\mathbf{x}-\mathbf{x}'|^2} e^{\frac{i}{2}\mathbf{x} \wedge \mathbf{x}'} . \quad (4.14)$$

The end-result is the *exact* spin wave spectrum:

$$\omega_{\mathbf{k}} = C \left[1 - e^{-k^2/2} \left(\frac{k^2}{2} + 1 \right) \right] , \quad (4.15)$$

where Ω is the area of the system, $\langle \rho \rangle = 1/2\pi\ell_B^2$, and the asymptotic value is $C = 16V\langle \rho \rangle\Omega$. Equation (4.15) is the central result of this section. It should be borne in mind that,

although it was obtained for the Laughlin state (4.3), it is also valid for the permanent (4.2), since the two are degenerate in the presence of our three-body interaction (4.1). The comparison to exact numerics is shown in Fig. 4.1.

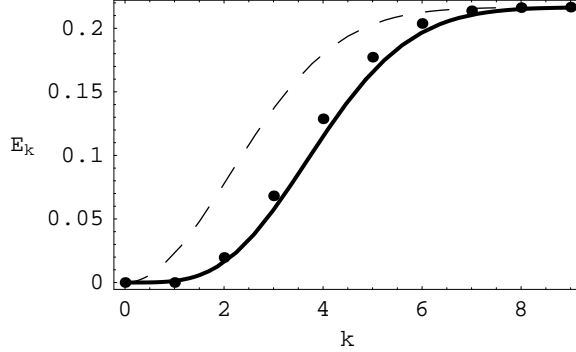


Figure 4.1: Spin-Wave Dispersion: Points are numerical data for $N = 10, N_\phi = 9$ (computed by E. Rezayi). Solid line is the spectrum in (4.15), with C determined by matching to the data at the highest k . For comparison, the dotted line is the spectrum for a two body interaction (4.16) with $V_2 = 0$.

At large \mathbf{k} , $\omega_{\mathbf{k}}$ approaches an asymptotic value as expected. This is the energy of a widely separated quasihole-quasiparticle pair, as in earlier work on two-body interactions [67]. However, the novel feature of (4.15) emerges at small \mathbf{k} , where $\omega_{\mathbf{k}} \sim k^4$, in contrast to the usual quadratic dependence. In other words, the spin stiffness is exactly zero when the interaction is the three-body Hamiltonian (4.10). This is precisely what was conjectured earlier based on numerical evidence [30]. Here, however, we have an exact calculation verifying that claim, and the comparison with the original data is quite good, as shown in Fig. 4.1. Therefore, the permanent is poised on the brink of an instability because $\omega_{\mathbf{k}}$ becomes negative as soon as the spin stiffness dips below zero.

The degeneracy of the *polarized* Laughlin state and the *unpolarized* permanent can also be understood in light of the long wavelength behavior of the spectrum. At zero spin stiffness, it should cost no energy to create a slowly varying spin texture of unbounded size. In fact numerical calculations of the spin-spin correlator $\langle S_z(\mathbf{x})S_z(\mathbf{y}) \rangle$ on the sphere confirm that the spins are approximately anti-aligned at antipodal points, indicating an anti-Skyrmion texture with long range order (Fig. 4.2). In the next subsection we will see

that pairing of composite bosons predicts precisely this ordering. Skyrmions are not new in the FQHE [68, 69] and are typically associated with excitations when extra flux is added. Here, however, they appear at one *fewer* flux quantum.

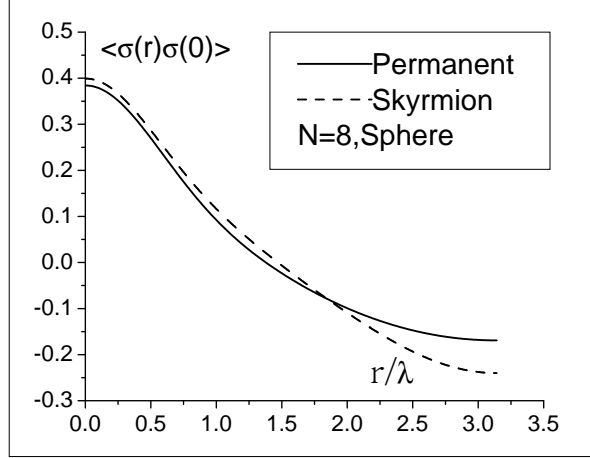


Figure 4.2: $\langle S_z S_z \rangle$ of the Permanent and, for comparison, of the Laughlin state with one fewer flux. λ is the magnetic length. (Computed by E. Rezayi)

The three-body spectrum obtained above cannot exhibit an instability because it is always stable—i.e. projection operators generally have no negative eigenvalues. However, a negative quadratic term can be restored by including a short-range, two-body interaction. For concreteness, we model such a potential by the simplest, non-trivial expansion,

$$H_2 = \sum_{i \neq j} V_0 \delta(\mathbf{x}_i - \mathbf{x}_j) + \frac{1}{2} V_2 \nabla_i^2 \delta(\mathbf{x}_i - \mathbf{x}_j) , \quad (4.16)$$

in place of H . There is no restriction on the sign of V_2 , but V_0 should be positive. Except for the special case $V_2 = 0$, for which H_2 is the pseudopotential [1] at $\nu = 1$, the Laughlin state is no longer an eigenstate. However, due to translational invariance, the state with one magnon is an eigenstate, so that its spectrum may be calculated exactly once again. Projecting H_2 onto the LLL and following the same procedure as before yields:

$$\omega_{\mathbf{k}} = -\frac{1}{2} \sum_{\mathbf{q}} V_q e^{-q^2/2} \left(e^{i\mathbf{q} \wedge \mathbf{k}} + e^{-i\mathbf{q} \wedge \mathbf{k}} - 2 \right) , \quad (4.17)$$

where $V_q = V_0 + \frac{1}{2} V_2 q^2$. Eqn. (4.17) agrees with earlier calculations using many-body

techniques [67]. Unlike the three-body case, the coefficient of the quadratic term in the dispersion does not vanish in general. However, by tuning the interaction parameters, the stiffness can be forced to zero, and the two- and three-body interactions will behave similarly at large distance. For example, the ratio $V_2/V_0 = -2/3$ mimics the three-body spectrum (4.15) at small \mathbf{k} .

When $V_2/V_0 < -2/3$, $\omega_{\mathbf{k}}$ looks like the familiar “Mexican Hat” potential, with a minimum at the wavevector $Q^2 = |V_0/V_2|$. At zero temperature, all the magnons (or quasiparticle-quasihole pairs) condense into the momentum \mathbf{Q} . Nonetheless, the total velocity of the superfluid is zero because the up-spins condense into $\mathbf{Q}/2$ and the down-spins into $-\mathbf{Q}/2$. We illustrate this explicitly by a Hartree-Fock function in the LLL with the variational parameter \mathbf{Q} . At this point this is more of an ansatz than anything else, but we will justify this in the next subsection. For the moment, consider the single particle orbitals

$$\phi_m(\mathbf{r}) = \frac{1}{\sqrt{2}} \begin{pmatrix} e^{\frac{i}{2}\mathbf{Q}\cdot\mathbf{r}} \\ e^{-\frac{i}{2}\mathbf{Q}\cdot\mathbf{r}} \end{pmatrix} z^m e^{|z|^2/2} \equiv \begin{pmatrix} \rho_{\mathbf{Q}/2}(\mathbf{r}) \\ \rho_{-\mathbf{Q}/2}(\mathbf{r}) \end{pmatrix} z^m e^{|z|^2/2}, \quad (4.18)$$

where $\rho_{\mathbf{Q}/2}(\mathbf{r})$ is the one-body density operator that is to be projected into the LLL according to the rule in (4.4). The Slater determinant, $\tilde{\Psi}_{\mathbf{Q}}$, of these orbitals exhibits helical spin order and reduces to Ψ_L at $\mathbf{Q} = 0$. In terms of the magnetic operators, $\tilde{\Psi}_{\mathbf{Q}}$ is:

$$\tilde{\Psi}_{\mathbf{Q}}(z_1, \dots, z_N) = \prod_i \frac{1}{\sqrt{2}} e^{-Q^2/4} \begin{pmatrix} \tau_{\mathbf{Q}/2}(i) \\ \tau_{-\mathbf{Q}/2}(i) \end{pmatrix}_i \prod_{i < j} (z_i - z_j) e^{-\sum_i |z_i|^2/4}. \quad (4.19)$$

Let us rewrite $\tilde{\Psi}_{\mathbf{Q}}$ as the spinor operator times the purely spatial part, $\tilde{\Psi}_{\mathbf{Q}} = T_{\mathbf{Q}} \Psi_0$. The energy $E_{\mathbf{Q}}$ of $\tilde{\Psi}_{\mathbf{Q}}$ can be calculated in exactly the same way as the spin-wave energy (by using (4.11)). We find that $E_{\mathbf{Q}}$ is identical to $\omega_{\mathbf{Q}}$, i.e.

$$\begin{aligned} \omega_{\mathbf{Q}} &= \frac{\langle \bar{S}_{\mathbf{Q}}^+ [\bar{H}_2, \bar{S}_{\mathbf{Q}}^-] \rangle_L}{\langle \bar{S}_{\mathbf{Q}}^+ \bar{S}_{\mathbf{Q}}^- \rangle_L} = \\ E_{\mathbf{Q}} &= \frac{\langle \bar{T}_{\mathbf{Q}}^\dagger [\bar{H}_2, \bar{T}_{\mathbf{Q}}] \rangle_0}{\langle \bar{T}_{\mathbf{Q}}^\dagger \bar{T}_{\mathbf{Q}} \rangle_0}. \end{aligned} \quad (4.20)$$

In fact, this identity holds generally for *any* translationally invariant interaction that can be expressed as a product of charge density operators. In particular, it is true for both of

the three- and two-body interactions, illustrating that our picture of a magnon condensate is internally consistent.

The wavevector \mathbf{Q} plays the role of an order parameter which increases continuously from zero as one crosses over from the ferromagnetic into the helical phase. On the other hand, the magnetization undergoes a first order transition. The boundary between the two phases is defined by $\rho_s = 0$. In the following subsection, we prove that helical order is incipient in the ground states of the permanent by adopting the composite boson point of view. A similar procedure on the sphere will show that the analog of the helical ordering is exactly the anti-Skyrmion, as was suggested by the numerical data in Fig. 4.2.

4.1.d Spin Order of the Permanent

Let us begin by recalling the general theory of paired bosons in zero magnetic field [23]. An effective Hamiltonian which captures this physics is of the BCS type:

$$K_{eff} = \sum_{\mathbf{k}\sigma} \left[\xi_{\mathbf{k}} c_{\mathbf{k}\sigma}^\dagger c_{\mathbf{k}\sigma} + \frac{1}{2} \left(\Delta_{\mathbf{k}}^* c_{-\mathbf{k}\downarrow} c_{\mathbf{k}\uparrow} + \Delta_{\mathbf{k}} c_{\mathbf{k}\uparrow}^\dagger c_{-\mathbf{k}\downarrow}^\dagger \right) \right] \quad (4.21)$$

where $\xi_{\mathbf{k}} = \varepsilon_{\mathbf{k}} - \mu$ and $\varepsilon_{\mathbf{k}}$ is the single-particle kinetic energy and $\Delta_{\mathbf{k}}$ is the gap function. In the fractional quantum Hall effect, the quasiparticles entering K_{eff} are the composite bosons, $c_{\mathbf{k}\sigma}$, which see no magnetic field. We assume that $\varepsilon_{\mathbf{k}} \simeq k^2/2m^*$ at small \mathbf{k} , where m^* is an effective mass of the composite (see for example Chapter 2). For p-wave pairing, we take $\Delta_{\mathbf{k}}$ to be an eigenfunction of rotations in \mathbf{k} of eigenvalue $l = -1$. At small \mathbf{k} the generic form of the gap function is thus

$$\Delta_{\mathbf{k}} \simeq \hat{\Delta}(k_x - ik_y) \quad (4.22)$$

where $\hat{\Delta}$ is a constant. Although there is no explicit single particle condensate in K_{eff} , it will be emerge naturally below as being equivalent to pure p-wave order.

More rigorously, one must solve the self-consistent gap equation when the interaction contains an attractive $l = -1$ channel. Consider a non-singular interaction which has a power series expansion at short distance: $V(\mathbf{k}) = a_0 + a_2 k^2 + \dots$. The gap equation is

$$\Delta_{\mathbf{k}} = -\frac{1}{2} \sum_{\mathbf{k}'} V(\mathbf{k} - \mathbf{k}') \frac{\Delta_{\mathbf{k}'}}{E_{\mathbf{k}'}}. \quad (4.23)$$

where the quasiparticle energy is

$$E_{\mathbf{k}} = \sqrt{\xi_{\mathbf{k}}^2 - |\Delta_{\mathbf{k}}|^2} \quad (4.24)$$

Note the minus sign in contrast with the familiar fermion case. This is a complicated non-local integral equation, but it separates if we assume that the gap function contains only one angular momentum channel: $\Delta_{\mathbf{k}} = |\Delta_{\mathbf{k}}|e^{il\phi}$, where ϕ is the polar angle of \mathbf{k} . The interaction expands similarly into angular momenta:

$$V(\mathbf{k} - \mathbf{k}') = \sum_{m=-\infty}^{\infty} V_m(k, k')e^{-im(\phi-\phi')} \quad (4.25)$$

where the coefficients $V_l(k, k')$ depend only on the magnitudes of \mathbf{k} and \mathbf{k}' . It is straightforward to show that the leading order behavior of V_l in \mathbf{k} is

$$V_l(k, k') \simeq k^l \quad (4.26)$$

Substituting the expansion (4.25) into the gap equation (4.23) yields precisely the p-wave gap (4.22) at leading order in \mathbf{k} whenever $V_{-1}(k, k')$ is negative and $V_l = 0$ for $l \neq -1$. For general l -wave pairing the gap is proportional to $(k_x - ik_y)^l$ at long distance.

The quasiparticle energy $E_{\mathbf{k}}$ contains important physical information. When $\mu < 0$ and $\hat{\Delta}$ is small enough, the gap is $E_0 = \mu$ and $2E_0$ is the energy needed to break a condensed pair. On the other hand, as the gap closes the paired state ceases to exist and a single particle condensate appears [23]. Precisely at $\mu = 0$ the spectrum is unstable for any finite $\hat{\Delta}$. However, as we will show shortly, the pure pair state is really a single particle condensate and the solution of K_{eff} is fully consistent when we expand about this new minimum.

In the absence of any single particle condensates, a pure pair state of spin-1/2 bosons is

$$|\Omega\rangle = \frac{1}{\mathcal{N}} \exp \left\{ \frac{1}{2} \sum_{\mathbf{k}} g_{\mathbf{k}} c_{\mathbf{k}\uparrow}^{\dagger} c_{-\mathbf{k}\downarrow}^{\dagger} \right\} |0\rangle \quad (4.27)$$

where \mathcal{N} is the normalization given by

$$\mathcal{N} = \prod_{\mathbf{k}} \frac{1}{1 - |g_{\mathbf{k}}|^2}. \quad (4.28)$$

To ensure that $|\Omega\rangle$ is normalizable it is necessary that $|g_{\mathbf{k}}|^2 < 1$ for all \mathbf{k} and p-wave order requires that $g_{\mathbf{k}}$ is antisymmetric in momentum space: $g_{\mathbf{k}} = -g_{-\mathbf{k}}$. Therefore, due to

bosonic statistics, the lowest allowed spin state of a pair is the spin singlet $\uparrow_i \downarrow_j - \downarrow_i \uparrow_j$ so $|\Omega\rangle$ has total spin $S = 0$.

In real space, the (unnormalized) component of the pair wavefunction with N particles (N even) is

$$\Psi(\mathbf{r}_1\sigma_1, \dots, \mathbf{r}_N\sigma_N) = \sum_P \prod_{i=1}^{N/2} g(\mathbf{r}_{P(2i-1)} - \mathbf{r}_{P(2i)}) \left(\uparrow_{P(2i-1)} \downarrow_{P(2i)} - \downarrow_{P(2i-1)} \uparrow_{P(2i)} \right) \quad (4.29)$$

where $g(\mathbf{r})$ is the inverse Fourier transform of $g_{\mathbf{k}}$ and P runs over all permutations of N objects. This is the form of a permanent of an $N \times N$ matrix, which looks like a determinant, but with the sign of P omitted. In fact, it is the analog of the Pfaffian (which is the determinant of an antisymmetric matrix) for paired fermions.

If we are dealing with the FQHE, then the bosonic operators $c_{\mathbf{k}\sigma}$ really originated as composite bosons. During projection to the LLL, one typically picks up a cutoff factor on $g_{\mathbf{k}}$ of $\exp(-\ell_B^2 |\mathbf{k}|^2/2)$, where ℓ_B is the magnetic length. We will neglect this factor in all that follows with the understanding that K_{eff} and $g_{\mathbf{k}}$ are valid at long distance. With this caveat, it is easy to see that if

$$g_{\mathbf{k}} = \frac{\lambda}{(k_x + ik_y)} \quad (4.30)$$

with λ a constant, then the asymptotic behavior at long distance of the inverse Fourier transform is

$$g(\mathbf{r}) \simeq \frac{1}{z}. \quad (4.31)$$

Comparing this with (4.29), we find that at long distance, the pair wavefunction is precisely the permanent prefactor of the LLL state defined by Ψ_{perm} (4.2).

While the Laughlin-Jastrow factor is taken care of by the transformation to composite bosons, it should be borne in mind that the price of this projection is an extra constraint or a fluctuating (Chern-Simons) gauge field. We are neglecting these effects at the mean field level. Analogous questions for pairing of composite fermions have been raised recently [72].

Now let us consider the occupation number at wavevector \mathbf{k} : $\langle n_{\mathbf{k}} \rangle = \langle c_{\mathbf{k}\uparrow}^\dagger c_{\mathbf{k}\uparrow} \rangle + \langle c_{\mathbf{k}\downarrow}^\dagger c_{\mathbf{k}\downarrow} \rangle$. From the form of $|\Omega\rangle$ (4.15) this can be written as a function of $g_{\mathbf{k}}$ only,

$$\langle n_{\mathbf{k}} \rangle = \frac{|g_{\mathbf{k}}|^2}{1 - |g_{\mathbf{k}}|^2}. \quad (4.32)$$

Substituting the asymptotic behavior (4.30), we can write the total number of particles as

$$N = \sum_{\mathbf{k}} \langle n_{\mathbf{k}} \rangle = \sum_{\mathbf{k}} \frac{|\lambda|^2}{|\mathbf{k}|^2 - |\lambda|^2} \quad (4.33)$$

The occupation numbers fall off algebraically at small \mathbf{k} and even more quickly (exponentially) on the scale of $k > 1/\ell_B$. The condition of normalisability of the ground state guarantees that $|\lambda/k|^2 < 1$ for all \mathbf{k} —in other words, $|\lambda|$ must be less than the minimum wavevector, $|\mathbf{k}_{min}|$. To make sense of this expression we now impose boundary conditions that compactify the plane into a torus. For simplicity, consider an $L \times L$ torus in the xy -plane; generalization to $L_x \times L_y$ and modular parameter τ is straightforward.

On the torus there are four degenerate ground states for the permanent Hamiltonian (4.2) corresponding to periodic $(++)$ or antiperiodic, $(+-)$, $(-+)$, $(--)$, boundary conditions in each of the two directions. When both directions are periodic $(++)$ the minimum reciprocal lattice vector allowed is $\mathbf{k}_{min} = 0$ and N becomes sharply peaked (in fact it is a delta function) at n_0 . One of the spin directions (say, \uparrow) is singled out by the correlations and we are left with nothing other than a Bose condensate with

$$\langle c_{\mathbf{k}\sigma} \rangle = \sqrt{N} \delta_{\mathbf{k},0} \delta_{\sigma,\uparrow} \quad (4.34)$$

which is the spin-polarized Laughlin state. On the other hand, in the antiperiodic sector, $(+-)$ or $(-+)$, $|\mathbf{k}_{min}| = \pi/L$. Inverting (4.33), we find that $|\lambda| = |\mathbf{k}_{min}| - \mathcal{O}(1/N)$ and in the thermodynamic limit one of these two sectors is macroscopically occupied. For example, in the $(+-)$ direction, $\mathbf{k}_{min} = (\pi/L, 0)$. Since the total momentum of the condensate must be zero, we occupy $(+\pi/L, 0)$ and $(-\pi/L, 0)$ with equal probability:

$$\langle c_{\mathbf{k}\uparrow} \rangle = \sqrt{\frac{N}{2}} \delta_{\mathbf{k},\mathbf{k}_{min}} \text{ and } \langle c_{\mathbf{k}\downarrow} \rangle = \sqrt{\frac{N}{2}} \delta_{\mathbf{k},-\mathbf{k}_{min}} \quad (4.35)$$

In real space this is precisely the helical winding with $\mathbf{Q} = 2\mathbf{k}_{min}$ which corresponds to the spins winding exactly once over the length of the system L in the \hat{x} direction. For the remaining antiperiodic sector, $(--)$, $|\mathbf{k}_{min}| = \sqrt{2}\pi/L$ and the winding is along the diagonal.

In any case, we have shown that three of the ground states of the permanent Hamiltonian are really single particle condensates with helical spin order and the remaining one is the

Laughlin spin polarized state. As we tune through the transition, one or the other long range order takes over. This justifies our Hartree-Fock ansatz (4.20). In the following subsection 4.1.e we shall expand about the single particle minimum by using an effective Landau-Ginzburg theory instead of K_{eff} .

Finally, we repeat the analog of the above on a sphere, which provides a nice intuitive picture of the anti-Skyrmion texture. Recall that the permanent state on the sphere has one fewer flux quantum than the Laughlin state. Thus, composite bosons live on the surface of a sphere with a magnetic monopole of strength one. The appropriate single particle states are monopole harmonics, $Y_{L,M}(\theta, \phi)$, with angular momentum $L \geq 1/2$ and M is the magnetic quantum number in the range $-L \leq M \leq L$ [63]. A pair wavefunction must be rotationally invariant just as it is translationally invariant on the torus or the plane. The unique bilinear scalar is

$$\sum_{L=-1/2}^{\infty} \sum_{M=-L}^L Y_{L,M}(\theta, \phi) Y_{L,-M}(\theta', \phi') f_L \langle 0, 0 | L, M; L, -M \rangle, \quad (4.36)$$

where $\langle 0, 0 | L, M; L, -M \rangle$ is the Clebsch-Gordan coefficient for coupling $|L, M\rangle$ and $|L, -M\rangle$ into the orbital singlet $|0, 0\rangle$ and f_L is a function of L only. This particular Clebsch-Gordan coefficient is equal to a function of L times $(-1)^{L-M}$, i.e. the only M -dependence is in the phase factor $(-1)^M$ [74]. If we combine all of the L dependence of f_L and the angular momentum coupling into a single pair amplitude, $g_L(-1)^M$, then we can write the many-body paired state as

$$|\Omega\rangle = \frac{1}{\mathcal{N}} \exp \left\{ \sum_{L,M} g_L (-1)^M c_{L,M\uparrow}^\dagger c_{L,-M\downarrow}^\dagger \right\} |0\rangle. \quad (4.37)$$

Note that M is half-integral so the pairing amplitude $g_L(-1)^M$ is antisymmetric under $M \rightarrow -M$ which is consistent with bosonic statistics and with the planar symmetry $\mathbf{k} \rightarrow -\mathbf{k}$. The relationship of angular momentum to linear momentum is $L = |\mathbf{k}|R$, where R is the radius of the sphere (Haldane in ref. [1]). Therefore, by analogy to (4.30), we expect that $g \simeq 1/L$ at small L , although we have no explicit proof of this statement. Fortunately, the exact form of g_L is not important for the following.

The lowest Landau level of the composite bosons has only two available states: $|1/2, \pm 1/2\rangle$. By analogy to the torus, the spins ought to condense into these two lowest states with equal

probability. In real space this says that

$$\begin{aligned}\langle c_{\downarrow}(\theta, \phi) \rangle &= Y_{1/2, -1/2}(\theta, \phi) = -e^{i\phi} \sqrt{1 - \cos \theta} \\ \langle c_{\uparrow}(\theta, \phi) \rangle &= Y_{1/2, 1/2}(\theta, \phi) = \sqrt{1 + \cos \theta}\end{aligned}\tag{4.38}$$

The expression for the first few monopole harmonics may be found in ref. [63], and a factor of $\sqrt{N/2}$ has been omitted from the right hand sides of (4.38). With the above condensate it is easy to calculate the expectation of the spin density $\langle S_i \rangle = \langle c_{\alpha}^{\dagger} \sigma_i^{\alpha\beta} c_{\beta} \rangle$, where $\sigma_i^{\alpha\beta}$ is the i 'th Pauli matrix with spin indices α and β :

$$\begin{aligned}\langle S_z \rangle &= -\cos \theta \\ \langle S_x \rangle &= -\sin \theta \cos \phi \\ \langle S_y \rangle &= -\sin \theta \sin \phi\end{aligned}\tag{4.39}$$

This is precisely an anti-Skyrmion spin ordering as the numerical data in Fig. 4.2 shows.

In summary, the mean field theory of composite bosons is completely consistent with the analytical and numerical results of the previous subsection. Furthermore, it seems that pure p-wave pairing of bosons in two dimensions should be viewed as a single particle condensate.

4.1.e Effective Field Theory Near the Transition

An effective continuum quantum ferromagnetic action (CQFM) for the polarized FQHE has been proposed recently by Read and Sachdev [61]. The idea is to write a sigma model for the local magnetization [66], $\hat{\mathbf{n}}$. Their model includes terms up to momentum squared, the higher order terms being irrelevant in the renormalization group sense. We modify this CQFM by stabilizing it in the helical region ($\rho_s < 0$) by adding terms that are quartic in momentum. At the end of this subsection, we will briefly discuss this theory on a lattice.

The CQFM Lagrangian density is

$$\mathcal{L}_0[\hat{\mathbf{n}}] = i\mathcal{A}(\hat{\mathbf{n}}) \cdot \partial_{\tau} \hat{\mathbf{n}} + \frac{\rho_s}{2} (\nabla \hat{\mathbf{n}})^2 ,\tag{4.40}$$

where τ is complex time and the time derivative term is the Berry phase. \mathcal{A} is the monopole vector potential such that $\nabla_{\hat{\mathbf{n}}} \times \mathcal{A} = \hat{\mathbf{n}}$. Although the model defined by \mathcal{L}_0 is unstable when the stiffness is negative, higher order derivative terms can stabilize this region. The symmetry broken helical phase contains an $SO(2) \times SU(2)$ residual symmetry; $SO(2)$ for

rotations of \mathbf{Q} in the plane and $SU(2)$ for the spins. There are three terms at leading non-trivial order that obey this requirement:

$$\partial_a n_i \partial_a n_i \partial_b n_j \partial_b n_j, \quad \partial_a n_i \partial_b n_i \partial_a n_j \partial_b n_j, \quad \partial_a^2 n_i \partial_b^2 n_i,$$

where $a, b = 1, 2$ and $i, j = 1, 2, 3$ and repeated indices are summed over. A renormalization group analysis shows that mode elimination in \mathcal{L}_0 generates a combination of only the first two terms: $\mathcal{L}_J = J(2\partial_a n_i \partial_b n_i \partial_a n_j \partial_b n_j - \partial_a n_i \partial_a n_i \partial_b n_j \partial_b n_j)$, which is associated with spin wave scattering [61]. The third term, $\mathcal{L}_K = K(\nabla^2 \hat{\mathbf{n}})^2$, is associated with a second-nearest neighbor interaction on a lattice. If only these two terms are retained, then the total CQFHM Lagrangian is given by

$$\mathcal{L}[\hat{\mathbf{n}}] = \mathcal{L}_0[\hat{\mathbf{n}}] + \mathcal{L}_J[\hat{\mathbf{n}}] + \mathcal{L}_K[\hat{\mathbf{n}}].$$

Although \mathcal{L}_J cannot introduce any k^4 terms into the dispersion since it arises from mode elimination, it will emerge that \mathcal{L}_K is sufficient to reproduce all of the long wavelength features found in the previous subsection. We choose to keep \mathcal{L}_J at this point for added generality.

Using spherical angles, $\hat{\mathbf{n}}$ can be parameterized by ϕ , its direction in the plane and θ , the fluctuation out of the plane. Small deviations (ϑ, φ) from helical ordering with wavevector \mathbf{Q} are given by $\theta = \vartheta$, $\phi = \mathbf{Q} \cdot \mathbf{x} + \varphi$. The fluctuations in the spherical angles should obey $|\nabla \varphi|, |\nabla \vartheta| \ll |\mathbf{Q}|$. In these coordinates, $\hat{\mathbf{n}} = (\cos \vartheta \cos(\mathbf{Q} \cdot \mathbf{x} + \varphi), \cos \vartheta \sin(\mathbf{Q} \cdot \mathbf{x} + \varphi), -\sin \vartheta)$, and the ferromagnetic phase is recovered when $\mathbf{Q} = 0$. The Berry phase reduces to the simple expression, $i\vartheta \partial_\tau \varphi$.

The mean field energy density of the helical state is given by

$$E_0(Q^2) = \frac{1}{2} \left[\rho_s Q^2 + (J + K) Q^4 \right], \quad (4.41)$$

which has the desired shape when the stiffness is negative. The spectrum of \mathcal{L} can be found by including fluctuations to second order in φ and ϑ . The Green's functions $\langle \varphi(-\mathbf{k}, -\omega) \varphi(\mathbf{k}, \omega) \rangle$ and $\langle \vartheta(-\mathbf{k}, -\omega) \vartheta(\mathbf{k}, \omega) \rangle$ both have poles at

$$i\omega_{\mathbf{k}} = \begin{cases} \frac{1}{2} \{ [4J(\mathbf{Q} \cdot \mathbf{k})^2 + K(k^2 - Q^2)^2] [4(J + K)(\mathbf{Q} \cdot \mathbf{k})^2 + Kk^4] \}^{1/2} & \rho_s \leq 0 \\ \left(\frac{1}{2} \rho_s k^2 + \frac{1}{2} K k^4 \right) & \rho_s \geq 0, \end{cases} \quad (4.42)$$

where \mathbf{Q} is the momentum which minimizes E_0 . For certain ranges of the parameters (J, K) , the spectrum is always positive, and \mathcal{L} describes a stable system. For simplicity, consider the helical state with $J = 0$ and K positive. Then the spin wave energy of the CQFHM simplifies to

$$i\omega_{\mathbf{k}} = \frac{K}{2}|k^2 - Q^2|\sqrt{4(\mathbf{Q} \cdot \mathbf{k})^2 + k^4} \quad (4.43)$$

As required, $\omega_{\mathbf{k}} \sim k^4$ when ρ_s zero. The three-body spectrum obtained in the previous subsection can be reproduced by identifying $K/2$ with the coefficient of the k^4 term in (4.43). On the other hand, when ρ_s is negative, we obtain the reasonable behavior, at small k :

$$i\omega_{\mathbf{k}} \sim \begin{cases} k^2 & \text{if } \mathbf{k} \perp \mathbf{Q} \\ k & \text{if } \mathbf{k} \parallel \mathbf{Q} \end{cases} \quad (4.44)$$

This may be expected because the spins are aligned ferromagnetically perpendicular to $\hat{\mathbf{Q}}$ but anti-ferromagnetically parallel to $\hat{\mathbf{Q}}$.

4.1.f Lattice Model

Before leaving the spin waves and moving on to the charged excitations, we briefly summarize a lattice model of spin-1/2 bosons that exhibits the helical transition. We represent the spin sector by two types of hard-core bosons hopping on a lattice with a short-range, spin-dependent interaction.

Defining $b_{i\sigma}$ to be the bosonic destruction operator on site i , consider the following Hamiltonian:

$$H_{lat} = -t \sum_{\langle ij \rangle, \sigma} b_{i\sigma}^\dagger b_{j\sigma} - \mu \sum_i n_i + U \sum_i n_i(n_i - 1) + J \sum_{\langle ij \rangle} \left(\mathbf{S}_i \cdot \mathbf{S}_j - \frac{1}{4} n_i n_j \right), \quad (4.45)$$

where n_i is the total number of bosons per site, and $\langle ij \rangle$ denotes the sum over nearest neighbors. The U -term is required since we are dealing with hard-core bosons; the singular gauge transformation which mapped the fermions to bosons maintains the repulsion at the same site. The final, antiferromagnetic, term is very much like the fermion $t - J$ interaction [66]. In the continuum limit, it reduces to the rotationally invariant interaction, $|\epsilon^{\sigma\tau} \hat{\psi}_\sigma \nabla \hat{\psi}_\tau|^2$. We will not discuss H_{lat} further, save to point out its mean-field features.

This two-component model is similar to the *one*-component lattice boson model considered earlier by M. Fisher et al. [75]. In the superfluid regime, which is characterized by large t/U or special values of μ where H_{lat} has particle-hole symmetry, one is free to consider bose condensation of the particle fields. If one also makes the self-consistent restriction $t/U < Jn/2U$, n being the average number of bosons per site, then the free energy of the helical phase is lower than that of the ferromagnetic phase. As in the continuum, this winding is described by the condensation:

$$\begin{aligned}\langle b_{i\uparrow}^\dagger \rangle &= \sqrt{\frac{N_\uparrow}{N_L}} e^{i\mathbf{Q}\cdot\mathbf{x}_i} \\ \langle b_{i\downarrow}^\dagger \rangle &= \sqrt{\frac{N_\downarrow}{N_L}} e^{-i\mathbf{Q}\cdot\mathbf{x}_i},\end{aligned}\tag{4.46}$$

where $N_\uparrow = N_\downarrow = N/2$ and N_L is the number of lattice sites. The optimal condensate wavevector lies along the diagonal of the lattice: $\mathbf{Q} = Q\hat{\mathbf{x}} + Q\hat{\mathbf{y}}$ with Q determined by the solution of $\cos Q = 2t/Jn$ (in units of the inverse lattice constant).

As the hopping decreases, provided that one is in a given region of μ/U , the ground state crosses over into a Mott insulator and it is no longer valid to argue based on Bose condensation. However, at points of particle-hole symmetry, the superfluid persists down to infinitesimal hopping. For the Hall liquid, the insulating phase is most relevant since the charge excitations must be gapped. It would be interesting to map out in detail the phase diagram of this magnetic superfluid to insulator transition.

4.2 The Haffnian: d-wave Pairing

The previous section has analyzed the spin sector of the permanent in some detail. Its spin-wave dispersion was shown to be soft, allowing a magnetic transition. We now want to ask the question whether there is a ground state wavefunction whose density sector exhibits an analogous behavior. To this end, we introduce a d-wave paired wavefunction, or ‘‘Haffnian’’, describing hard-core, spinless *bosons* at filling factor $\nu = 1/2$. In the FQHE, it is a d-wave paired state of composite bosons. We will then argue that the Haffnian is compressible and sits on the phase boundary between incompressibility and non-uniform charge density order. At present we have no effective field theory that captures this behavior.

Although d-wave paired states have been proposed in a different context by Wen and Wu [32], their Haffnian wavefunctions describe *incompressible* states of *fermions*. As our proposal is somewhat different, in the following subsection we present the relevant constructions in some detail, mainly along the lines used to investigate non-abelian statistics [30].

4.2.a Analytic Structure of the Haffnian

The Haffnian builds in pairing into the Laughlin state, much like the Pfaffian of Moore and Read [28]:

$$\Psi_{Hf} = \sum_P \frac{1}{(z_{P(1)} - z_{P(2)})^2 \cdots (z_{P(N-1)} - z_{P(N)})^2} \prod_{i < j} (z_i - z_j)^2. \quad (4.47)$$

This describes an even number, N , of spinless bosons at half-filling and flux $N_\phi = 2(N - 1) - 2$ (on the sphere). The prefactor is known as a Haffnian in linear algebra and is also the permanent of the $N \times N$ ($N > 2$) matrix $M_{ij} = 1/(z_i - z_j)^2$ ($i \neq j$, $M_{ii} = 0$). The Haffnian, Pfaffian and determinant are related by several identities, which may be found in, for instance, Greiter et al. [31]

To construct the parent Hamiltonian for Ψ_{Hf} , it is convenient to work on the sphere, where each particle has orbital angular momentum $N_\phi/2$. Using the same notation as in the permanent (4.1), H_{Hf} is a sum of three-body projection operators:

$$H_{Hf} = \sum_{i \neq j \neq k} V_0 P_{ijk}(3N_\phi/2) + V_2 P_{ijk}(3N_\phi/2 - 2) + V_3 P_{ijk}(3N_\phi/2 - 3). \quad (4.48)$$

Ψ_{Hf} is the unique zero-energy eigenstate of H_{Hf} at N_ϕ flux. The proof of this statement proceeds by showing that the maximum angular momentum of any triplet in Ψ_{Hf} is $3N_\phi/2 - 4$; the details are in Section 4.2.b. Note that projection onto angular momentum $3N_\phi/2 - 1$ is absent. This is a consequence of the symmetries of Clebsch-Gordan coupling; three spinless bosons of angular momentum L cannot be in a total angular momentum state of $3L - 1$.

Alternatively, Ψ_{Hf} can be rewritten explicitly as a paired state of composite bosons. By analogy with the permanent, the order parameter (on the plane or torus) is an eigenstate of angular momentum with eigenvalue $l = -2$, i.e. $\Delta \simeq \hat{\Delta}(k_x - ik_y)^2$ to leading order in \mathbf{k} . Likewise the many-body state is a BCS wavefunction of d-wave bosons in two dimensions

and the asymptotic behavior of the pair state reproduces the $1/z^2$ nature of the Haffnian prefactor (4.47).

4.2.b The Haffnian Hamiltonian on the Sphere

To see that Ψ_{Hf} does not contain any triplets of total angular momentum greater than $3N_\phi/2 - 4$, we generalize Haldane's original argument for two-body interactions [14]. This argument is easily applicable to n -body interactions. The factors $(z_i - z_j)$ on the plane correspond to $(u_i v_j - u_j v_i)$ on the sphere, with (u_i, v_i) being the spinor coordinates of z_i . The total angular momentum of a triplet (ijk) on the sphere is *one-half* of the maximum of the coherent state operator $\mathbf{S}_{ijk} = \hat{\Omega} \cdot (\mathbf{L}_i + \mathbf{L}_j + \mathbf{L}_k)$, where $\hat{\Omega}(\phi, \theta)$ is any direction on the sphere and \mathbf{L}_i is the angular momentum of the i 'th particle. $(\mathbf{L}_i + \mathbf{L}_j + \mathbf{L}_k)$ commutes with any factor involving only particles i, j, k ; i.e. all factors $(u_a v_b - u_b v_a)$ with $a, b \in \{i, j, k\}$. Translating this to the plane, we can find the maximum of \mathbf{S}_{ijk} acting on Ψ_{Hf} almost by inspection. When all factors involving *exactly one of* z_i, z_j or z_k are multiplied out, the result will be a polynomial with terms of the form $z_i^A z_j^B z_k^C$. The maximum value of $1/2(A + B + C)$ is exactly the maximum value of the total angular momentum of the triplet (ijk) . In particular, this maximum is $3N_\phi/2 - 4$ for Ψ_{Hf} , so it is certainly a zero energy eigenstate of H_{Hf} .

It must still be shown that Ψ_{Hf} is the unique ground state. To this end, we will use the method in Appendix A of Milovanović and Read [64]. Consider the behavior of the Haffnian prefactor in (4.47) as three particles (ijk) approach each other, the other particles remaining far away from the three. The Laurent series must contain terms of the form $(z_i - z_j)^{q_{ij}} (z_j - z_k)^{q_{jk}} (z_k - z_i)^{q_{ki}}$ with q_{ab} positive or negative integers. By continuity, the total function must contain this Laurent factor for any position of the particles. In order for Ψ_{Hf} to be analytic, as it must be in the LLL, each q must not be smaller than -2 , or $Q \equiv q_{ij} + q_{jk} + q_{ki} \geq -6$. In particular, Ψ_{Hf} is annihilated by $P_{ijk}(3N_\phi/2)$ if the inequality is strict, $Q > -6$. Another way to see this is on the plane: $P_{ijk}(3N_\phi/2)$ is the projection onto the closest approach of a triplet—all three particles are clumped at the north pole, taking the maximum L_z value—which takes the form $\delta^{(2)}(z_i - z_j) \delta^{(2)}(z_j - z_k)$ on the plane. Thus, if $Q = -6$, the delta function interaction does not annihilate Ψ_{Hf} . Reducing the total angular

momentum (on the sphere) by one corresponds to restricting further the particles' closest approach, or increasing the lower limit of Q by one. In this way, we obtain the requirement $Q > -3$ in order for $P_{ijk}(L)$ to annihilate the ground state whenever $L > 3N_\phi/2 - 4$. The extreme case $Q = -2$ corresponds to the densest eigenstate. There are four possible such factors:

$$\frac{1}{(z_i - z_j)^2}, \frac{1}{(z_i - z_j)(z_k - z_j)}, \frac{(z_i - z_j)^2}{(z_j - z_k)^2(z_k - z_i)^2}, \frac{(z_i - z_j)}{(z_j - z_k)^2(z_k - z_i)}.$$

Symmetrizing these factors with respect to (ijk) leaves only terms like the first one. Therefore H_{Hf} automatically requires a pairing structure of its ground state that is given by the Haffnian.

Other zero-energy eigenstates are obtained by multiplying in factors symmetric in the particle coordinates, being formally allowed since they can only increase Q . These states describe quasiholes and edge excitations and are less dense than the ground state since they contain added flux. They are enumerated explicitly in the Section 4.2.c; here we verify that they are indeed zero-energy eigenstates of H_{Hf} . Without loss of generality, pick a definite triplet, $(ijk) = (123)$, for convenience. There are several cases to check, corresponding to the possible terms appearing in some quasihole state (4.50): (i) the pair (z_1, z_2) is broken, (ii) the pair involving z_3 and another particle, say z_4 , is broken, (iii) both pairs (z_1, z_2) and (z_3, z_4) are broken, and (iv) neither pair is broken. For illustration, we check case (ii), the others being done similarly. Applying the generalization of Haldane's argument, the maximum degree of the triplet (123) is $2(N - 3) + 2(N - 3) + 2(N - 3) + 2n + (n - 2)$. The first three contributions come from the terms $(z_i - z_a)$, where $i = 1, 2, 3$ and $a \neq 1, 2, 3$, the fourth term is due to the quasihole operator $\Phi(z_1, z_2, z_5, \dots)$, and the last takes into account the maximum orbital quantum number of the unpaired boson, z_3^{n-2} . Using the flux condition $N_\phi = 2(N - 1) - 2 + n$, leads to one-half the maximum degree (or maximum total orbital angular momentum of a triplet) being $3N_\phi/2 - 4$, which is consistent with requirement that it be less than $3N_\phi/2 - 3$. Note that it has tacitly been assumed that $n \geq 2$; if $n = 1$ then the unpaired boson is in the zeroth orbital and half of the maximum degree is $3N_\phi/2 - 3 - n/2$. The other three cases can be checked straightforwardly by such counting, proving that the quasihole states (4.50) are annihilated by H_{Hf} .

4.2.c Zero Energy Eigenstates

In addition to the Haffnian, there are other zero energy eigenstates of H_{Hf} generated by adding $n = 1, 2, \dots$ flux quanta. The structure of these excitations is more complex than that of the familiar Laughlin quasiholes, having an infinite degeneracy in the thermodynamic limit. In previous work [30], this degeneracy has been suggested to provide the necessary manifold of states for nonabelian statistics, which we discuss below. Proper construction of the zero energy states is useful for understanding the numerical spectrum of H_{Hf} , so we will go through them in some detail.

The quasihole in the paired state, like in the Laughlin state, is generated by one flux, but it is built of *two* vortices at w_1 and w_2 each carrying *one-half* flux quantum. Let n be the number of flux added to the Haffnian, i.e. $N_\phi = 2(N-1) - 2 + n$, with w_1, \dots, w_{2n} being the positions of the vortices. Denoting $B/2$ as the number of broken pairs in the Haffnian and $\{m_1, m_2, \dots, m_B\}$ as the quantum numbers of the orbitals into which the unpaired bosons are placed, the explicit form for the manifold of zero-energy eigenstates is

$$\Psi_{m_1, m_2, \dots, m_B}(z_1, z_2, \dots, z_N; w_1, w_2, \dots, w_{2n}) = \sum_{\sigma \in S_N} \prod_{k=1}^B z_{\sigma(k)}^{m_k} \prod_{l=1}^{(N-B)/2} \frac{\Phi(z_{\sigma(B+2l-1)}, z_{\sigma(B+2l)}; w_1, \dots, w_{2n})}{(z_{\sigma(B+2l-1)} - z_{\sigma(B+2l)})^2} \prod_{i < j} (z_i - z_j)^2. \quad (4.49)$$

Φ is the quasihole operator given by:

$$\Phi(z_1, z_2; w_1, \dots, w_{2n}) = \sum_{\tau \in S_{2n}} \prod_{r=1}^n (z_1 - w_{\tau(2r-1)})(z_2 - w_{\tau(2r)}). \quad (4.50)$$

It can be verified that the $\Psi_{m_1, m_2, \dots, m_B}(z_1, z_2, \dots, z_N; w_1, w_2, \dots, w_{2n})$ are in fact zero-energy eigenstates of H_{Hf} (Section 4.2.a). If no pairs are broken ($B = 0$), Φ builds in two vortices—each within half of the bosons—for each of the n flux. Hence the interpretation that the vortices carry charge $1/4$, or $1/2q$ for more general filling factors. The unpaired bosons are labeled by the orbital quantum numbers $\{m_1, \dots, m_B\}$, which must satisfy the condition $0 \leq m_1 \leq \dots \leq m_B \leq n - 2$. The upper limit follows from the constraint on N_ϕ and the ordering is simply to avoid overcounting upon symmetrization. This is equivalent to putting B bosons into $n - 1$ orbitals, for which the multiplicity is

$$\binom{B + n - 2}{B}. \quad (4.51)$$

Note that for $n = 2$ all of the bosons coming from broken pairs are in the lowest orbital, z^0 , and there are no unbroken pairs at $n = 1$.

There is an additional degeneracy coming from the positions of the quasiholes themselves, which is calculated by expanding Φ in the w 's using the elementary symmetric polynomials $e_m(w) = \sum_{i_1 < \dots < i_m} w_{i_1} \dots w_{i_m}$. The e_m have the property that, for $m = 0, \dots, j$, they form a basis for the algebra of all symmetric polynomials in j variables. Thus, zero-energy states may also be obtained as linear combinations of the e_m . When Φ is expanded in this way we obtain all the symmetric polynomials in w_1, \dots, w_{2n} in which the degree of any w is no greater than $(N - B)/2$. The total number of linearly independent states, for a fixed B and a fixed set of m_i 's, is at most the total number of linearly independent symmetric functions of w in the expansion of Φ , which establishes the upper bound on the positional degeneracy of the quasiholes. That this is also the correct degeneracy, without overcounting, is proven elsewhere [30]. We can now write down this number by regarding the vortices as some kind of bosonic particle, interpreting the $e_m(w)$ as the states for $2n$ bosons occupying the $(N - B)/2 + 1$ orbitals $\{1, \dots, w^{(N-B)/2}\}$ (recall that Φ appears $(N - B)/2$ times due to the product $\prod_{l=1}^{(N-B)/2}$ in (4.50)):

$$\binom{(N - B)/2 + 2n}{2n}. \quad (4.52)$$

Throughout this construction it has been tacitly assumed that N is even, so B is necessarily even as well. The construction for N odd proceeds with only slight modification, but the counting in (4.51) and in (4.52) does not change, since B has the same parity as N . In either case, the total number of linearly independent quasihole states is obtained by multiplying the two combinatorial factors and summing over the allowed values of B :

$$\sum_{B, (-1)^B = (-1)^N} \binom{B + n - 2}{B} \binom{(N - B)/2 + 2n}{2n}. \quad (4.53)$$

To complete this description, one should check that all states in (4.50) exhaust all zero-energy eigenstates at fixed N and n and that they are linearly independent. Since this is somewhat involved and is discussed at length elsewhere [30], we will omit it here.

As a special case, notice that for two added flux ($n = 2$) the Laughlin state, for bosons at $\nu = 1/2$, is recovered when all pairs are broken ($B = N$). Therefore, up to two flux quanta,

the Haffnian and the Laughlin states are degenerate eigenstates of H_{Hf} . It is convenient to adopt the composite boson interpretation of the quasihole positional degeneracy (4.52). Rewriting this combinatorial factor as

$$\binom{(N-B)/2 + 2n}{(N-B)/2}, \quad (4.54)$$

affords an interpretation as $(N-B)/2$ composite bosons in $2n+1$ orbitals. On the sphere at $n=2$ this is the correct degeneracy for an $L=2$ angular momentum multiplet, independently of both N and B . The unpaired bosons are all forced into the lowest orbital $m=0$, which is manifested by the degeneracy factor (4.51) reducing to unity. Thus, the manifold of degenerate states is composed of $N/2$ states (one for each of $B=0, 2, \dots, N-2$) carrying angular momentum $L=2$ and one Laughlin state (for $B=N$) carrying $L=0$, which is a rotationally invariant. The main point of the expression (4.54) is that the zero energy eigenstates of H_{Hf} contain *both* d-wave pairs *and* unpaired composite bosons in the $m=0$ orbital

The degeneracy at $L=2$ is a feature that is reminiscent of the permanent. In that case, an analogous argument at $n=1$ leads to a Laughlin state at $\nu=1$ and a set of $N/2$ states carrying $L=1$. The $(N-B)/2$ paired bosons were interpreted as spin waves [30], which we have established to condense into helical order (4.35). Spin wave excitations are, of course, gapless, but one may expect that the $L=2$ modes in the Haffnian are massive, being density excitations. However, we argue that this is not the case and H_{Hf} is compressible, indicating that it sits right on the transition from an incompressible state to one with non-uniform charge density order.

4.2.d d-wave Pairing of Spinless Bosons

In the previous subsection we showed that the lowest single particle orbital may be macroscopically occupied by breaking pairs (4.54). A proper description of this system must therefore include a single particle condensate at the outset. As soon as there is such a condensate there is also isotropic scattering out of the superfluid, which gives rise to an s-wave pair amplitude.

On the torus or plane, the full Hamiltonian is given by

$$K = \sum_{\mathbf{k}} \left(\frac{k^2}{2m^*} - \mu \right) c_{\mathbf{k}}^\dagger c_{\mathbf{k}} + \frac{1}{2} \sum_{\mathbf{k}, \mathbf{k}', \mathbf{q}} V(\mathbf{q}) c_{\mathbf{k}+\frac{1}{2}\mathbf{q}}^\dagger c_{\mathbf{k}'-\frac{1}{2}\mathbf{q}}^\dagger c_{\mathbf{k}-\frac{1}{2}\mathbf{q}} c_{\mathbf{k}'+\frac{1}{2}\mathbf{q}} \quad (4.55)$$

We assume that the lowest state $\mathbf{k} = 0$ is macroscopically occupied with an amplitude $\Phi = \langle c_0 \rangle$ and expand around this condensate: $c_{\mathbf{k}} \rightarrow \Phi + \tilde{c}_{\mathbf{k}}$. In addition there is the possibility of s- and d-wave pairing of the anomalous correlators $\langle \tilde{c}_{\mathbf{k}} \tilde{c}_{-\mathbf{k}} \rangle$. The resulting effective Hamiltonian is

$$K_{eff} = \sum'_{\mathbf{k}} \left[\xi_{\mathbf{k}} c_{\mathbf{k}}^\dagger c_{\mathbf{k}} + \frac{1}{2} \left(\Delta_{\mathbf{k}} c_{\mathbf{k}}^\dagger c_{-\mathbf{k}}^\dagger + \Delta_{\mathbf{k}}^* c_{-\mathbf{k}} c_{\mathbf{k}} \right) \right], \quad (4.56)$$

where the prime on the summation indicates that the $\mathbf{k} = 0$ term is to be omitted when $\Phi > 0$; otherwise the summation is over all wavevectors. The chemical potential is shifted by the $\langle c_0^\dagger c_0 \rangle$ contribution from expanding the interaction so that the single particle energy is now $\xi_{\mathbf{k}} \simeq \mathbf{k}^2/2m^* - \mu + 2V(0)|\Phi|^2$. For consistency, it is necessary that $V(0)$ is positive, which is a standard assumption in interacting Bose systems. It is also common to assume that the exchange contributions do not modify m^* significantly.

The pair order parameter must satisfy the self-consistent gap equation in the presence of a condensate:

$$\Delta_{\mathbf{k}} = \Phi^2 V(\mathbf{k}) - \frac{1}{2} \sum'_{\mathbf{k}'} V(\mathbf{k} - \mathbf{k}') \frac{\Delta_{\mathbf{k}'}}{E_{\mathbf{k}'}} \quad (4.57)$$

To make sense of this complicated integral equation, we shall assume that $\Delta_{\mathbf{k}}$ is dominated by the (s+d)-wave symmetry and, furthermore, that its leading order behavior is

$$\Delta_{\mathbf{k}} = \Delta_{\mathbf{k}}^s + \Delta_{\mathbf{k}}^d \quad \text{with} \quad \begin{cases} \Delta_{\mathbf{k}}^s \simeq \hat{\Delta}^s \\ \Delta_{\mathbf{k}}^d \simeq \hat{\Delta}^d (k_x - ik_y)^2 \end{cases} \quad (4.58)$$

where $\hat{\Delta}^{s,d}$ are constants. Recall that the interaction can be expanded into angular momentum eigenstates (4.26) and that each channel has the asymptotic behavior $V_l(k, k') \simeq k^l$. In other words, it is implicit in the above form (4.58) that the long distance property of each order parameter is dictated by its respective angular momentum channel.

The standard procedure is to diagonalize K_{eff} . This is the familiar Bogoliubov transformation that replaces the original particles and holes by quasiparticles $\alpha_{\mathbf{k}}$:

$$\alpha_{\mathbf{k}} = u_{\mathbf{k}}^* c_{\mathbf{k}} + v_{\mathbf{k}} c_{-\mathbf{k}}^\dagger \quad (4.59)$$

Commutation relations are preserved if $|u_{\mathbf{k}}|^2 - |v_{\mathbf{k}}|^2 = 1$ and symmetry requires that $u_{\mathbf{k}} = u_{-\mathbf{k}}$ and $v_{\mathbf{k}} = v_{-\mathbf{k}}$. The following solutions for $u_{\mathbf{k}}$ and $v_{\mathbf{k}}$ put K_{eff} into the form $K_{eff} = \sum_{\mathbf{k}} E_{\mathbf{k}} \alpha_{\mathbf{k}}^\dagger \alpha_{\mathbf{k}}$:

$$\begin{aligned} v_{\mathbf{k}}^2 &= \frac{1}{2} \left(\frac{\xi_{\mathbf{k}}}{E_{\mathbf{k}}} - 1 \right) \frac{\Delta_{\mathbf{k}}}{|\Delta_{\mathbf{k}}|} \\ u_{\mathbf{k}}^2 &= \frac{1}{2} \left(\frac{\xi_{\mathbf{k}}}{E_{\mathbf{k}}} + 1 \right) \end{aligned} \quad (4.60)$$

$$E_{\mathbf{k}}^2 = \xi_{\mathbf{k}}^2 - |\Delta_{\mathbf{k}}|^2. \quad (4.61)$$

There is a kind of gauge freedom in that both $u_{\mathbf{k}}$ and $v_{\mathbf{k}}$ can be multiplied by a \mathbf{k} -dependent phase factor, without changing the physics. We adopt the convention that $u_{\mathbf{k}}$ is real and positive, while $v_{\mathbf{k}}$ carries the possible d-wave phase factor.

If both s- and d-wave amplitudes are nonvanishing, an interesting feature emerges immediately. The quasiparticle spectrum contains an anisotropic piece coming from the cross terms in $|\Delta_{\mathbf{k}}|^2$,

$$E_{\mathbf{k}}^2 = \xi_{\mathbf{k}}^2 - |\hat{\Delta}^s + \hat{\Delta}^d k^2 e^{-2i\phi}|^2, \quad (4.62)$$

where k is the magnitude of and ϕ is the polar angle of \mathbf{k} . Choosing the constants $\hat{\Delta}^{s,d}$ to be real for the moment, the anisotropy is

$$- 2\hat{\Delta}^s \hat{\Delta}^d k^2 \cos 2\phi \quad (4.63)$$

which has two minima at $\phi = 0, \pi$. There is a relative $U(1)$ phase degree of freedom between the pairing amplitudes, which is equivalent to an $SO(2)$ rotation of the minima. In other words, the transformation $\hat{\Delta}^s \rightarrow e^{2i\alpha} \hat{\Delta}^s$ is the same as $\phi \rightarrow \phi + \alpha$. It is interesting that this anisotropy arises not from an attraction in $V(\mathbf{k})$, which is isotropic, but rather from the coexistence of two distinct pairing symmetries in momentum space.

A unique ground state wavefunction exists for each solution of the gap equations. Its generic form is like that of the permanent (4.15) but with an allowance for the single particle condensate

$$|\Omega\rangle = \frac{1}{\mathcal{N}} \exp \left\{ \Phi c_0^\dagger + \sum_{\mathbf{k}}' g_{\mathbf{k}} c_{\mathbf{k}}^\dagger c_{-\mathbf{k}}^\dagger \right\} |0\rangle. \quad (4.64)$$

The normalization is the same as in Eq. (4.28) but with an extra factor of $\exp(|\Phi|^2)$. The reciprocal space pair wavefunction, $g_{\mathbf{k}}$, can be expressed in terms of the Bogoliubov

parameters $u_{\mathbf{k}}$ and $v_{\mathbf{k}}$ as

$$g_{\mathbf{k}} = \frac{v_{\mathbf{k}}}{u_{\mathbf{k}}} \quad (4.65)$$

The generic form of the N -body paired wavefunction has already been discussed in Eq. (4.29) and the Haffnian exists only when $\Phi = 0$ since it is a pure paired state. Furthermore, the asymptotic behavior of the real space pair wavefunction $g(\mathbf{r}) \simeq 1/z^2$ is obtained when

$$g_{\mathbf{k}} = \lambda \frac{k_x^2 + k_y^2}{(k_x + ik_y)^2} . \quad (4.66)$$

The N -body state of composite bosons constructed in this way is exactly the Haffnian prefactor of Eq. (4.47). And, the same remarks following Eq. (4.31), concerning the validity of this mean field approximation, apply here.

Unfortunately, unlike the permanent case, the occupation number $\langle n_{\mathbf{k}} \rangle = \langle c_{\mathbf{k}}^\dagger c_{\mathbf{k}} \rangle$ does not contain any new information since it is constant:

$$\langle n_{\mathbf{k}} \rangle = \frac{|\lambda|^2}{1 - |\lambda|^2} .$$

However, the required form of $g_{\mathbf{k}}$ does constrain the parameters at which the Haffnian can exist. At small \mathbf{k} , the asymptotic behavior of $g_{\mathbf{k}}$ (4.66) is consistent with $\hat{\Delta}^s = 0$ only if $u_{\mathbf{k}}$ and $v_{\mathbf{k}}$ have the same asymptotic behavior.

To understand where this point lies we must understand the phase diagram as derived from the self-consistency condition (4.57). It is simplified by assuming the asymptotic expansion for $\Delta_{\mathbf{k}}$ in Eq. (4.58) and by expanding $V(\mathbf{k} - \mathbf{k}')$ into angular momentum eigenstates as before (4.25). This decomposition separates the BCS gap equation (4.57) into two coupled integral equations,

$$\hat{\Delta}^s = \Phi^2 V(\mathbf{k}) - \frac{1}{2} \sum'_{\mathbf{k}'} V_0(k, k') \frac{\hat{\Delta}^s + \hat{\Delta}^d k'^2 \cos 2\phi'}{E_{\mathbf{k}'}} \quad (4.67)$$

$$\hat{\Delta}^d k^2 = -\frac{1}{2} \sum'_{\mathbf{k}'} V_{-2}(k, k') \frac{\hat{\Delta}^s \cos 2\phi' + \hat{\Delta}^d k'^2}{E_{\mathbf{k}'}} . \quad (4.68)$$

The assumption that the s-wave amplitude is constant then implies that $\mathbf{k} = 0$ in the first equation to leading order. The coefficient $V_0(k, k')$ reduces to $V(\mathbf{k}')$ at $\mathbf{k} = 0$, and the leading order term of $V_{-2}(k, k')$ is proportional to k^2 so the second equation is consistent (c.f. Eq. (4.26)). Further simplification is possible by choosing a particular gauge for the

phases of the condensates. A convenient choice is to pick a real $\hat{\Delta}^d$ and to absorb the phase of $\hat{\Delta}^s$ into ϕ' ; this only rotates the inhomogeneity of the spectrum (4.63). Since the phase of Φ is locked to that of $\hat{\Delta}^s$, *all order parameters can be chosen to be real and positive*. Finally, since the inhomogeneity is even under parity, $\phi' \rightarrow -\phi'$, the odd terms $\sin 2\phi'$ in the numerator cancel and only $\cos 2\phi'$ appears.

The crudest criterion for the solutions of the gap equations is whether or not Φ vanishes. Consider first the situation when $\Phi = 0$ and the fluid consists of pure pairs. In principle both s- and d-wave pairing can coexist since the gap equations allow this generally. However, if we make the reasonable assumption that $V(\mathbf{k})$ is positive everywhere then only $\hat{\Delta}^d$ is allowed. This may be seen from a closer inspection of the ϕ' -dependent part of the integrand in (4.67). Let us split it into two disjoint pieces characterized by $\cos 2\phi'$ negative or positive. The corresponding $E_{\mathbf{k}'}$ is always larger in the former case because the inhomogeneity (4.63) has a negative sign. Therefore, the total contribution of the $\hat{\Delta}^d$ term to the right hand side is always negative. That is to say

$$\int_0^{2\pi} d\phi' V(\mathbf{k}') \frac{\cos 2\phi'}{E_{\mathbf{k}'}} \geq 0. \quad (4.69)$$

Since $\hat{\Delta}^s$ is also positive in our gauge there is no consistent solution of (4.67) when $\Phi = 0$. The only possibility is a pure d-wave gap that satisfies (4.68) with $\hat{\Delta}^s = 0$. In this phase $\mu < 0$ and $2E_0 = 2|\mu|$ is the gap to breaking a pair (see also [23]). Thus, when there is no single particle condensate the system is specified by the following gap equation and quasiparticle spectrum:

$$\begin{aligned} \hat{\Delta}^d k^2 &= -\frac{1}{2} \sum_{\mathbf{k}'} V_{-2}(k, k') \frac{\hat{\Delta}^d k'^2}{E_{\mathbf{k}'}} \\ E_{\mathbf{k}}^2 &= \mu^2 + \frac{|\mu|}{m^*} k^2 + \left[\left(\frac{1}{2m^*} \right)^2 - (\hat{\Delta}^d)^2 \right] k^4 \end{aligned} \quad (4.70)$$

$\hat{\Delta}^d$ is real in this gauge.

On the other hand, when $\Phi > 0$ there is a new set of considerations, which require $V_0(k, k') = 0$ for consistency. Firstly, in order for K_{eff} to be a stable approximation to the full Hamiltonian, $\langle c_0 \rangle$ must be a minimum of the free energy. The resultant constraint, sometimes known as the Gross-Pitaevsky equation, pins the chemical potential to the single particle condensate by $\mu = V(0)\Phi^2$ (in the gauge where Φ is real). Furthermore, the

spectrum is dominated by the gapless Goldstone phonon mode at low \mathbf{k} , requiring $E_0 = \xi_0^2 - |\Delta_0|^2$, or

$$-\mu + 2V(0)\Phi^2 = \hat{\Delta}^s. \quad (4.71)$$

In conjunction with the pinning condition $\mu = V(0)\Phi^2$, this implies that $\hat{\Delta}^s = V(0)\Phi^2$. But, using the positivity condition in Eq. (4.69), this is consistent with the gap equation (4.67) only if we reinstate the \mathbf{k} -dependence of $\hat{\Delta}^s$ or if $V_0(k, k')$ vanishes. We shall assume the latter as it is much more tractable. Ultimately, this condition is traced back to the asymptotic behavior of the gap function (4.58), which is somewhat restrictive. However, we now have a tractable and fully consistent system. Summarizing these results for $\Phi > 0$,

$$\begin{aligned} \hat{\Delta}^s &= V(0)\Phi^2 = \mu \\ \hat{\Delta}^d k^2 &= -\frac{1}{2} \sum'_{\mathbf{k}'} V_{-2}(k, k') \frac{\hat{\Delta}^s \cos 2\phi' + \hat{\Delta}^d k'^2}{E_{\mathbf{k}'}} \\ E_{\mathbf{k}}^2 &= 2\mu \left(\frac{1}{2m^*} - \hat{\Delta}^d \cos 2(\phi + \alpha) \right) k^2 + \left[\left(\frac{1}{2m^*} \right)^2 - (\hat{\Delta}^d)^2 \right] k^4. \end{aligned} \quad (4.72)$$

We have used the gauge in which all order parameters are real, which shifts ϕ by α , the phase of $\hat{\Delta}^s$. The single particle condensate constraint $\hat{\Delta}^s = \mu$ has also been used in the last expression.

We can now map out the phase diagram in the space of μ and $\hat{\Delta}^d$ by looking at the spectra in Eqs.(4.70) and (4.72). Fig. 4.3 illustrates the possible phases. The dotted line indicates the instability of both spectra when $\hat{\Delta}^d > 1/2m^*$. For clarity, in each of the four regions there is an inset of the typical spectrum $E_{\mathbf{k}}^2$. The spectrum in region (IV) is presumably stabilized at higher momenta (which is represented by the dashed curve) so that the instability is really a kind of “d-wave roton”. The spectrum in region (III) is clearly unstable, indicating a new phase. As μ increases from (IV) into (III), the pair gap and probably the roton gap, too, go to zero. Although we have no explicit calculations, it is probable that the phase in (III) is a charge-density-wave at the roton wavevector. On the other hand, there are no instabilities in regions (I) and (II). (I) is a pure, isotropic, d-wave condensate, in which the gap is half of the energy required to break a pair. As the gap closes, and we move into (II) at fixed $\hat{\Delta}^d$, a single particle condensate develops so that all three condensates, Φ , $\hat{\Delta}^s$, and $\hat{\Delta}^d$ exist; accordingly, there is a linear phonon mode and an

anisotropy due to the coexistence of both pairings. As $\hat{\Delta}^d$ increases from (II) to (III), the anisotropy is strong enough that the gap closes at finite momentum, in addition to $\mathbf{k} = 0$. This is consistent with the transition from (IV) to (III).

The Haffnian itself can only exist at $\mu = 0$, which can be seen from the asymptotics of $u_{\mathbf{k}}$ and $v_{\mathbf{k}}$. Since the pair amplitude $g_{\mathbf{k}}$ is a pure $l = -2$ eigenstate at $\mathbf{k} \rightarrow 0$ when the Haffnian is the asymptotic form of the many-body wavefunction, $\hat{\Delta}^s$ must vanish. Furthermore, the requirement that $|g_{\mathbf{k}}| = |v_{\mathbf{k}}/u_{\mathbf{k}}| \rightarrow 1$ as $\mathbf{k} \rightarrow 0$ restricts the relative behavior of $u_{\mathbf{k}}$ and $v_{\mathbf{k}}$, and the explicit solution in Eq. (4.61) implies that $\mu = 0$. The thick line in the figure marks the transition region, $\mu = 0$ with a stable spectrum ($\hat{\Delta}^d < 1/2m^*$), where the Haffnian represents the long range behavior. E. Rezayi [76] has analyzed numerically the

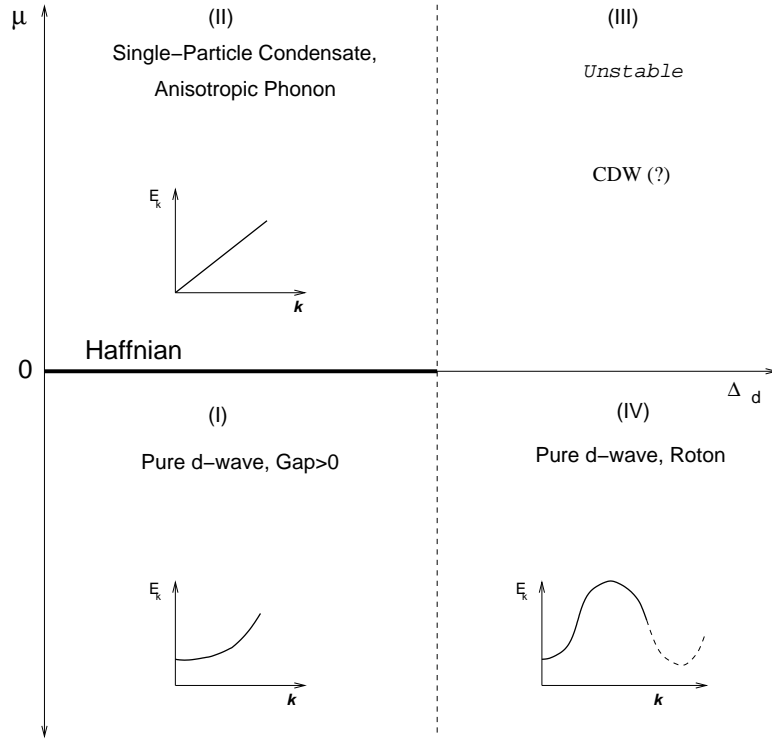


Figure 4.3: Phases of bosons in two dimensions.

Haffnian Hamiltonian in eqn. 4.47. He found that for V_0 negative the ground state is a paired state, while for V_0 positive it is a Laughlin state, which is a Bose condensate. This is consistent with the Haffnian being on a phase boundary.

Chapter 5

Fermion Pairing: Quantum Hall Effect for Spin

In this Chapter, we provide a detailed derivation of the Hall conductivity for spin transport in the d- and p-wave pairing of fermions. In the FQHE, the fermions are really composite fermions, and we ignore gauge field fluctuations. This is equivalent to showing that the induced action for the system in an external gauge field that couples to the spin is a Chern-Simons (CS) term. In the d-wave case, the system is spin-rotation invariant, so we obtain an SU(2) CS term, while in the p-wave case, there is only a U(1) symmetry, so we find a U(1) CS term. In both cases, the Hall spin conductivity is given by a topological invariant. Within the BCS mean field approach, using a conserving approximation, this topological invariant is the winding number of the order parameter in momentum space and is an integer, which is the statement of quantization. We argue that the quantization in terms of a topological invariant is more general than the approximation used.

5.1 BCS Hamiltonian

Considering first the spin-singlet paired states, we use the Nambu basis where the symmetries are transparent. Define

$$\Psi = \frac{1}{\sqrt{2}} \begin{pmatrix} c \\ i\sigma_y c^\dagger \end{pmatrix}, \quad (5.1)$$

with

$$c = \begin{pmatrix} c_{\uparrow} \\ c_{\downarrow} \end{pmatrix}, \quad (5.2)$$

so that Ψ transforms as a tensor product of particle-hole and spin-space spinors. We consider an interacting system and approximate it as in BCS theory, then with a minimal coupling to the gauge field, we use a conserving approximation to obtain the spin response. In Fourier space, we should note that

$$\Psi_{\mathbf{k}} = \frac{1}{\sqrt{2}} \begin{pmatrix} c_{\mathbf{k}} \\ i\sigma_y c_{-\mathbf{k}}^{\dagger} \end{pmatrix}. \quad (5.3)$$

In the Nambu basis, the kinetic energy becomes (with $K = H - \mu N$)

$$\begin{aligned} K_0 &= \sum_{\mathbf{k}} \xi_{\mathbf{k}}^0 (c_{\mathbf{k}\uparrow}^{\dagger} c_{\mathbf{k}\uparrow} + c_{\mathbf{k}\downarrow}^{\dagger} c_{\mathbf{k}\downarrow}) \\ &= \sum_{\mathbf{k}} \xi_{\mathbf{k}}^0 \Psi_{\mathbf{k}}^{\dagger} (\sigma_z \otimes I) \Psi_{\mathbf{k}}, \end{aligned} \quad (5.4)$$

where $\xi_{\mathbf{k}}^0 = |\mathbf{k}|^2/(2m) - \mu$ is the kinetic energy, containing the bare mass m , and the products in the spinor space are understood. Products like $\sigma_z \otimes I$ act on the Nambu spinors, with the first factor acting in the particle-hole factor, the second in the spin-space factor. The interaction term, for a spin-independent interaction V , is

$$K_{\text{int}} = \frac{1}{2} \sum_{\mathbf{k}\mathbf{k}'\mathbf{q}} V_{\mathbf{q}} : \Psi_{\mathbf{k}+\mathbf{q}}^{\dagger} (\sigma_z \otimes I) \Psi_{\mathbf{k}} \Psi_{\mathbf{k}'-\mathbf{q}}^{\dagger} (\sigma_z \otimes I) \Psi_{\mathbf{k}'} :. \quad (5.5)$$

Here the colons $: \dots :$ denote normal ordering, that is all the c^{\dagger} 's are brought to the left. In the BCS-extended Hartree-Fock approximation, the effective quasiparticle Hamiltonian (for later reference) is

$$\begin{aligned} K_{\text{eff}} &= \sum_{\mathbf{k}} \Psi_{\mathbf{k}}^{\dagger} [\xi_{\mathbf{k}} (\sigma_z \otimes I) + \text{Re } \Delta_{\mathbf{k}} (\sigma_x \otimes I) \\ &\quad - \text{Im } \Delta_{\mathbf{k}} (\sigma_y \otimes I)] \Psi_{\mathbf{k}}. \end{aligned} \quad (5.6)$$

This is for singlet pairing, where $\Delta_{-\mathbf{k}} = \Delta_{\mathbf{k}}$, and not just for d-wave. Here $\xi_{\mathbf{k}}$ is $\xi_{\mathbf{k}}^0$ plus the Hartree-Fock corrections. If we define a vector

$$\mathbf{E}_{\mathbf{k}} = (\text{Re } \Delta_{\mathbf{k}}, -\text{Im } \Delta_{\mathbf{k}}, \xi_{\mathbf{k}}) \quad (5.7)$$

then the quasiparticle energy $E_{\mathbf{k}} = |\mathbf{E}_{\mathbf{k}}|$, and

$$K_{\text{eff}} = \sum_{\mathbf{k}} \Psi_{\mathbf{k}}^{\dagger} (\mathbf{E}_{\mathbf{k}} \cdot \boldsymbol{\sigma} \otimes I) \Psi_{\mathbf{k}}. \quad (5.8)$$

5.2 Spin Response in a Conserving Approximation

In the Nambu notation, it is clear that $K = K_0 + K_{\text{int}}$, and K_{eff} , are invariant under global SU(2) rotations that act on the spin-space, that is the second factor in the tensor products. The spin density, the integral of which over all space is the total spin and generates such global transformations, and the spin current densities are given by

$$J_0^a(\mathbf{q}) = \frac{1}{2} \sum_{\mathbf{k}} \Psi_{\mathbf{k}-\mathbf{q}/2}^\dagger (I \otimes \sigma_a) \Psi_{\mathbf{k}+\mathbf{q}/2} \quad (5.9)$$

$$J_i^a(\mathbf{q}) = \frac{1}{2} \sum_{\mathbf{k}} \frac{k_i}{m} \Psi_{\mathbf{k}-\mathbf{q}/2}^\dagger (\sigma_z \otimes \sigma_a) \Psi_{\mathbf{k}+\mathbf{q}/2}, \quad (5.10)$$

where $i = x, y$ is the spatial index, and $a = x, y, z$ is the spin-space index. Spin conservation implies the continuity equation, as an operator equation,

$$\partial J_\mu^a / \partial x_\mu = 0, \quad (5.11)$$

where $\mu = 0, x, y$, and the summation convention is in force.

So far we have not introduced a gauge field for spin. Since the spin is conserved locally, we can turn the symmetry into a local gauge symmetry by introducing an SU(2) vector potential, and making all derivatives covariant. The effect on K is to add the integral of

$$A_\mu^a J_\mu^a + \frac{1}{8m} A_i^a A_i^a \Psi^\dagger (\sigma_z \otimes I) \Psi. \quad (5.12)$$

The gauge field is to be used solely as an external source, with which to probe the spin response of the system, and then set to zero.

If we now consider integrating out the fermions, then we can obtain an action in the external gauge fields, which can be expanded in powers of A_μ^a . The zeroth-order term is the free energy density, times the volume of spacetime, and the first-order term vanishes by spin-rotation invariance. The second-order term corresponds to linear response: the second functional derivative with respect to A_μ^a , at $A_\mu^a = 0$, yields the (matrix of) linear response functions. In particular, the spatial components yield the conductivity tensor in the usual way. Therefore we consider the imaginary-time time-ordered function,

$$\Pi_{\mu\nu}^{ab} = -i \langle J_\mu^a(q) J_\nu^b(-q) \rangle, \quad (5.13)$$

where time-ordering is understood, and from here on we use a convention that p , q , etc. stand for three-vectors $p = (p_0, \mathbf{p})$, and further $p_0 = i\omega$ is imaginary for imaginary time. For $\mu = \nu = i = x$ or y , an additional “diamagnetic” term $\bar{n}\delta^{ab}/4m$ is present in $\Pi_{\mu\nu}^{ab}$, which we do not show explicitly. As consequences of the continuity equation and the related gauge invariance, $\Pi_{\mu\nu}$ must be divergenceless on both variables, $q_\mu \Pi_{\mu\nu} = q_\nu \Pi_{\mu\nu} = 0$. To maintain these when using the BCS-Hartree-Fock approximation for the equilibrium properties, one must use a conserving approximation for the response function, which in this case means summing ladder diagrams (compare the charge case in Ref. [21], pp. 224–237). We used the identical method in treating composite bosons at $\nu \neq 1$ in Chapter 2, Chapter 2.

One begins with the BCS-Hartree-Fock approximation, which can be written in terms of Green’s functions as (we consider only zero temperature, and $\int dp_0$ is along the imaginary p_0 axis throughout)

$$G^{-1}(p) = p_0 - \xi_{\mathbf{p}}^0 \sigma_z \otimes I - \Sigma(p), \quad (5.14)$$

$$\Sigma(p) = i \int \frac{d^3 k}{(2\pi)^3} (\sigma_z \otimes I) G(k) (\sigma_z \otimes I) V(k - q). \quad (5.15)$$

Note that $G(p)$ and $\Sigma(p)$ are matrices acting on the tensor product space. The equations are solved by

$$G^{-1}(p) = p_0 - \mathbf{E}_{\mathbf{p}} \cdot \boldsymbol{\sigma} \otimes I, \quad (5.16)$$

(we write 1 for $I \otimes I$) as one can also see from the effective quasiparticle Hamiltonian K_{eff} , and $\Delta_{\mathbf{p}}$ obeys the standard gap equation.

In the response function, the ladder series can be summed and included by dressing *one* vertex, to obtain (again not showing the diamagnetic term)

$$\begin{aligned} \Pi_{\mu\nu}^{ab}(q) = & -i \int \frac{d^3 p}{(2\pi)^3} \text{tr} \left[\gamma_{\mu}^a(p, p+q) G(p+q) \right. \\ & \left. \times \Gamma_{\nu}^b(p+q, p) G(p) \right], \end{aligned} \quad (5.17)$$

where γ_{μ}^a is the bare vertex,

$$\gamma_0^a(p, p+q) = \frac{1}{2} I \otimes \sigma_a, \quad (5.18)$$

$$\gamma_i^a(p, p+q) = -\frac{(p + \frac{1}{2}q)_i}{2m} \sigma_z \otimes \sigma_a, \quad (5.19)$$

and Γ_μ^a is the dressed vertex satisfying

$$\begin{aligned}\Gamma_\nu^b(p+q, p) &= \gamma_\nu^b(p+q, p) + i \int \frac{d^3k}{(2\pi)^3} \sigma_z \otimes IG(k+q) \\ &\quad \times \Gamma_\nu^b(k+q, k) G(k) \sigma_z \otimes IV(p-k).\end{aligned}\tag{5.20}$$

At small q , we can obtain useful information about this function from the Ward identity that results from the continuity equation. The particular Ward identity we use here is an exact relation of the vertex function to the self-energy, and the conserving approximation (the ladder series) was constructed to ensure that it holds also for the approximated vertex and self energy functions.

Following Schrieffer's treatment [21], we consider the vertex function with external legs included:

$$\Lambda_\mu^a(r_1, r_2, r_3) = \langle J_\mu^a(r_3) \Psi(r_1) \Psi^\dagger(r_2) \rangle,\tag{5.21}$$

for spacetime coordinates r_1, r_2, r_3 . Applying $\partial/\partial r_{3\mu}$ to both sides and using the operator continuity equation, we obtain the exact identity in Fourier space

$$q_\mu \Gamma_\mu^a(p+q, p) = \frac{1}{2} I \otimes \sigma_a G^{-1}(p) - \frac{1}{2} G^{-1}(p+q) I \otimes \sigma_a.\tag{5.22}$$

Since G^{-1} is trivial in the spin-space indices, it commutes with $I \otimes \sigma_a$. Hence at $q \rightarrow 0$, the right-hand side vanishes, so $\Gamma(p+q, p)$ has no singularities as $q \rightarrow 0$. This differs from the charge case, for example, where this calculation (using the ladder series approximation) leads to the discovery of the collective mode [39]. Since the spin symmetry is unbroken, no collective mode is necessary to restore this conservation law, and so there is no singularity in the vertex function for spin.

One can verify that the Ward identity is satisfied using the BCS-Hartree-Fock G^{-1} and the ladder series for Γ . At $q = 0$, this yields the important results

$$\Gamma_\mu^a(p, p) = -\frac{1}{2} \partial_\mu G^{-1}(p) I \otimes \sigma_a,\tag{5.23}$$

or explicitly,

$$\begin{aligned}\Gamma_0^a(p, p) &= \frac{1}{2} I \otimes \sigma_a, \\ \Gamma_i^a &= -\frac{1}{2} \partial_i G^{-1}(p) I \otimes \sigma_a,\end{aligned}\tag{5.24}$$

where ∂_i and ∂_μ stand for $\partial/\partial p_i$, $\partial/\partial p_\mu$ from here on, and the extra minus in the first relation is consistent because implicitly $q_\mu \Gamma_\mu = q_0 \Gamma_0 - q_i \Gamma_i$.

We now calculate Π at small q . To zeroth order, use of the Ward identity shows that the J - J function gives zero, except when $\mu = \nu = i$. In that case, it reduces to a constant that cancels the diamagnetic term also present in just that case. Hence we require only the part first-order in q . In the expression for Π above, we first shift $p \rightarrow p - \frac{1}{2}q$, so that q no longer appears in any bare vertices, but does appear in the Green's functions on both sides of the ladder, between the rungs which are the interaction lines. Hence to first order, we obtain a factor $\pm \frac{1}{2} \partial_\mu G = \mp \frac{1}{2} G \partial G^{-1} G$ in place of G in one position in the ladder. Since there may be any number of rungs (including zero) between this and either of the vertices at the ends, the terms can be summed up into a ladder dressing each vertex, evaluated at $q = 0$. Hence we obtain to first order

$$\begin{aligned} \Pi_{\mu\nu}^{ab}(q) = & -\frac{i}{2} \int \frac{d^3 p}{(2\pi)^3} \text{tr} \left[\Gamma_\mu^a(p, p) q_\lambda \partial_\lambda G \Gamma_\nu^b(p, p) G(p) \right. \\ & \left. - \Gamma_\mu^a(p, p) G(p) \Gamma_\nu^b(p, p) q_\lambda \partial_\lambda G \right]. \end{aligned} \quad (5.25)$$

Using the Ward identity, this becomes

$$\begin{aligned} \Pi_{\mu\nu}^{ab}(q) = & \frac{i}{8} q_\lambda \int \frac{d^3 p}{(2\pi)^3} \text{tr} \left\{ (I \otimes \sigma_a) (I \otimes \sigma_b) G \partial_\mu G^{-1} \right. \\ & \left. \times [G \partial_\lambda G^{-1}, G \partial_\nu G^{-1}] \right\} \end{aligned} \quad (5.26)$$

Since the G 's are independent of the spin-space indices, the explicit σ 's factor off, and the result is δ^{ab} times a spin-independent part. The latter can be simplified using the BCS-Hartree-Fock form of G , by writing the latter as

$$G(p) = \frac{p_0 + \mathbf{E}_p \cdot \boldsymbol{\sigma} \otimes I}{p_0^2 - E_p^2}. \quad (5.27)$$

The spin-independent factor contains $\epsilon_{\mu\nu\lambda}$ since it is antisymmetric in these labels. Keeping track of the signs, we find for the quadratic term in the induced action

$$\frac{1}{4\pi} \frac{\mathcal{M}}{4} \int d^3 r A_\mu^a \frac{\partial A_\nu^a}{\partial r_\lambda} \epsilon_{\mu\nu\lambda}, \quad (5.28)$$

with \mathcal{M} given by the topological invariant

$$\mathcal{M} = \int \frac{d^2 p}{8\pi} \epsilon_{ij} \mathbf{E}_p \cdot (\partial_i \mathbf{E}_p \times \partial_j \mathbf{E}_p) / E_p^3. \quad (5.29)$$

The right hand side is exactly the Pontriagin winding number m , and is an integer as long as \mathbf{E} is a continuous, differentiable function of \mathbf{p} ; it is 2 for the d-wave case.

To ensure SU(2) gauge invariance, the CS term should include also a term cubic in A , with no derivatives. For this term we evaluate the triangle one-loop diagrams with three insertions of J , with each vertex dressed by the ladder series. Setting the external momenta to zero, the Ward identity can be used for all three vertices, and the result can be seen to be

$$\begin{aligned} \Pi_{\mu\nu\lambda}^{abc}(0,0) &= -\frac{1}{24} \int \frac{d^3p}{(2\pi)^3} \text{tr} \left[(I \otimes \sigma_a) G \partial_\mu G^{-1} \right. \\ &\quad \left. \times \{ (I \otimes \sigma_b) G \partial_\nu G^{-1}, (I \otimes \sigma_c) G \partial_\lambda G^{-1} \} \right]. \end{aligned} \quad (5.30)$$

The anticommutator $\{, \}$ arises since the result must be symmetric under permutations of the index pairs μ, a , etc. The product $\sigma_a \sigma_b \sigma_c$, when traced over the spin-space indices, yields a factor $2i\epsilon_{abc}$, which is antisymmetric, and so the remainder must contain $\epsilon_{\mu\nu\lambda}$ to maintain symmetry; the rest of the structure is the same as before. Hence the full result is the SU(2) CS term, which we write in terms of the 2×2 matrix vector potentials $A_\mu = \frac{1}{2} \sigma_a A_\mu^a$,

$$\frac{k}{4\pi} \int d^3x \epsilon_{\mu\nu\lambda} \text{tr} (A_\mu \partial_\nu A_\lambda + \frac{2}{3} A_\mu A_\nu A_\lambda). \quad (5.31)$$

Here k is the conventional notation for the coefficient of such a term, in this same normalization; if we wished to quantize the theory by functionally integrating over A , we would need $k = \text{an integer}$. In our case $k = \mathcal{M}/2 = 1$ for d-wave.

For the spin-triplet case with an unbroken U(1) symmetry, we must use the fact that $\Delta_{-\mathbf{k}} = -\Delta_{\mathbf{k}}$. For example, in the two-dimensional A-phase, as occurs in the 331 state in the double-layer FQHE system with zero tunneling, the pairs are in the isospin $S_z = 0$ triplet state $\uparrow_i \downarrow_j + \downarrow_i \uparrow_j$, and the U(1) symmetry generated by S_z is unbroken; we recall that the underlying Hamiltonian is not assumed to have a full SU(2) symmetry. The effective quasiparticle Hamiltonian becomes, in the Nambu-style notation,

$$\begin{aligned} K_{\text{eff}} &= \sum_{\mathbf{k}} \Psi_{\mathbf{k}}^\dagger [\xi_{\mathbf{k}}(\sigma_z \otimes I) + \text{Re } \Delta_{\mathbf{k}}(\sigma_x \otimes \sigma_z) \\ &\quad - \text{Im } \Delta_{\mathbf{k}}(\sigma_y \otimes \sigma_z)] \Psi_{\mathbf{k}}. \end{aligned} \quad (5.32)$$

The U(1) vector potential A_μ couples to S_z , and the vertex functions contain $I \otimes \sigma_z$, which commutes with the BCS-Hartree-Fock Green's function G . The tensors appearing in the

three terms in K_{eff} obey the same algebra as the three in that for the spin-singlet case (where they were trivial in the second factor), and as in that case commute with $I \otimes \sigma_z$. Consequently, the derivation for the induced action to quadratic order in A_μ is similar to that for the SU(2) singlet case above, and the traces in the Nambu indices can be carried out with the same result as before, to obtain the abelian CS term

$$\frac{1}{4\pi} \mathcal{M} \int d^3r A_\mu \frac{\partial A_\nu}{\partial r_\lambda} \epsilon_{\mu\nu\lambda}, \quad (5.33)$$

and no cubic term. In this case, \mathcal{M} is again given by the winding number m which is 0 or ± 1 in the p-wave strong and weak-pairing phases (respectively) discussed in this chapter.

5.3 Discussion and Generalizations

We note that the effect of the vertex corrections we included as ladder series is to renormalize the $q = 0$ vertices as shown in eq. (5.23) for the spin-singlet case, and use these in one-loop diagrams with no further corrections. This corresponds to the minimal coupling $p \rightarrow p - A$ in the action, as one would expect by gauge invariance. If we assume such a coupling, and treat the low-energy, long-wavelength theory near the weak-strong transition as Dirac fermions with relativistic dispersion and minimal coupling to the external gauge field, then the expression for \mathcal{M} as an integral over \mathbf{p} covers only half the sphere in \mathbf{n} space, and we would get ± 1 (d-wave), $\pm 1/2$ (p-wave). The missing part results from the ultraviolet regulator in the field theory version of the calculation [78], or from a second fermion with a fixed mass in some lattice models [77]. In our calculation, the remainder is provided by the ultraviolet region, where $\Delta_{\mathbf{k}} \rightarrow 0$ as $\mathbf{k} \rightarrow \infty$. At the transition, $\mu = 0$, the map is discontinuous and covers exactly half the sphere in the p-wave case, so $\mathcal{M} = 1/2$, as in other problems. In the d-wave case with rotational symmetry, the value of $|v_{\mathbf{k}}/u_{\mathbf{k}}|$ as $\mathbf{k} \rightarrow 0$ is nonuniversal, and hence so is the value of σ_{xy}^s at the transition. This is a consequence of the non-relativistic form of the dispersion relation of the low-energy fermions in this case. We may also note that for a paired system on a lattice, as in models of high T_c superconductors, a similar calculation will give an integral over the Brillouin zone, which is a torus T^2 , instead of the \mathbf{k} plane which can be compactified to S^2 . But maps from T^2 to S^2 are again classified by the integers, and the integer winding number is given by the

same expression, so quantization is unaffected.

We can also argue that the quantization result away from a transition is exact in a translationally-invariant system, at least in all orders in perturbation theory. For this we use the form in eq. (5.26) or (5.30), where the Ward identity for the vertex has been used. Diagrammatically, it is clear that the exact expression can be similarly written, using the exact (i.e., all orders in perturbation) Green's function and vertex function. (This is also true when the CS gauge field interaction is included.) The Ward identity that relates them is exact, and the result for σ_{xy}^s is of the same form as shown. The next step, the frequency integrals, cannot be done explicitly in this case, because the precise form of the Green's function is unknown, and the analogs of $\xi_{\mathbf{k}}$, $\Delta_{\mathbf{k}}$ (or of $u_{\mathbf{k}}$, $v_{\mathbf{k}}$) do not exist. The latter do not exist because in general the poles in the Green's function, which would represent the quasiparticles, are broadened by scattering processes, except for the lowest energies for kinematical reasons. However, the form in eq. (5.26) is itself a topological invariant, as we will now argue. As long as there is a gap in the support of the spectral function of G , $G(p)$ is continuous and differentiable on the *imaginary* frequency axis, and tends to $I \otimes I/p_0$ as $p_0 \rightarrow \pm i\infty$. Thus G^{-1} exists and never vanishes. Considering the spin-singlet case for convenience, the spin-space structure is trivial, so we may perform the corresponding traces, and then G or G^{-1} is a 2×2 matrix, with the same reality properties on the imaginary p_0 axis as in the BCS-Hartree-Fock approximation. (The spin-triplet case should work out similarly, because of the algebraic structure already mentioned.) It thus represents a real non-zero 4-component vector, in $\mathbf{R}^4 - 0$, which topologically is the same as S^3 . S^3 is obtained by dividing G by its norm, $(\text{tr} G^\dagger G)^{1/2}$, and the normalized G is a 2×2 unitary matrix with determinant -1 , so it lies in S^3 . The \mathbf{k} space can be compactified to S^2 as before, and the frequency variable can be viewed as an element of the interval $\mathcal{I} = (-1, 1)$, so the integral is over $S^2 \times \mathcal{I}$. However, since the limit of the Green's function as $p_0 \rightarrow \pm i\infty$ for fixed \mathbf{k} is independent of \mathbf{k} , we can view this as simply S^3 . Thus we are dealing with maps from S^3 to S^3 , the equivalence classes of which are classified by the homotopy group $\pi_3(S^3) = \mathbf{Z}$. The integral we have obtained simply calculates the integer winding number or Pontryagin index of the map, when properly normalized (G can be normalized to lie in $\text{SU}(2)$ without affecting the integral). This establishes the quantization of σ_{xy}^s in a translationally-invariant

system with a gap, at least to all orders in perturbation theory, and probably can be made fully non-perturbative (as the Ward identity is already).

Chapter 6

Adsorption on Carbon Nanotubes

In this chapter we switch gears into one dimension and consider adsorption on nanotubes as discussed in the introductory chapter, Section 1.3.

6.1 Nanotube geometry

Fig. 6.1 illustrates the way in which a nanotube is obtained by wrapping a graphite sheet. The hexagons are at positions $R_{n,m} = na_+ + ma_-$, where a_{\pm} are primitive lattice vectors of the honeycomb lattice. The standard convention is to identify $R_{0,0} \equiv R_{N,M}$, and to simply label the tube (N, M) . The case (N, N) is known as the armchair tube, $(N, 0)$ is the zig-zag, and all others are chiral. There is a geometric frustration whenever the wrapping destroys the tripartite nature of the infinite sheet, which occurs when $(N - M) \bmod 3$ is non-zero (this criterion is familiar in the context of electronic conductivity[44]). Thus, both zig-zag and chiral tubes can be frustrated geometrically, whereas armchair tubes cannot. The adsorption sites form a triangular lattice wrapped on the cylinder, which is shown in Fig. 6.2 for the $(7, 0)$ zig-zag. In the following section we specify the Hamiltonian and consider the simplest (classical) limit in which intersite tunneling of adatoms is prohibited. We will then turn on the hopping perturbatively (the quantum case).

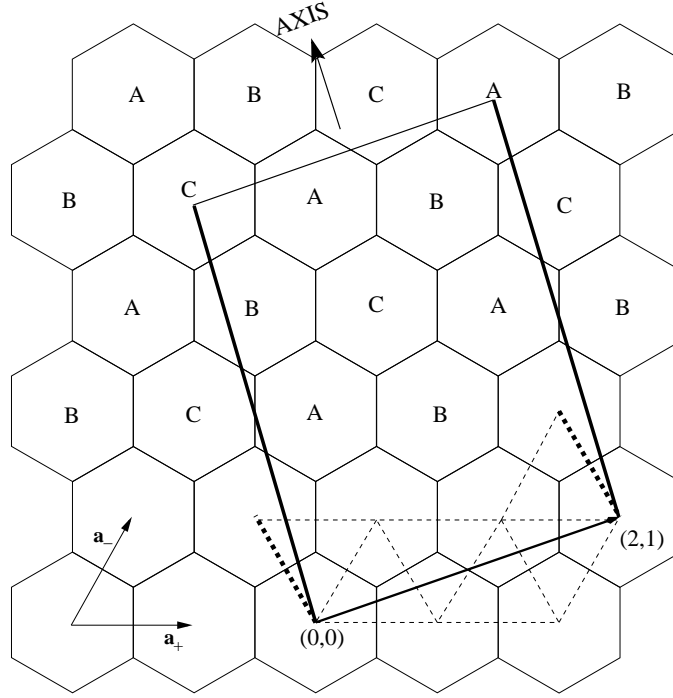


Figure 6.1: An example of wrapping of the graphite sheet to make a $(2,1)$ tube. \mathbf{a}_{\pm} are the primitive lattice vectors of the honeycomb lattice. The solid rectangle is the primitive cell of the tube. The tube can also be built up by stacking the dotted region along the axis with the solid dotted lines identified. Also shown is the tripartite lattice labeling A, B, C.

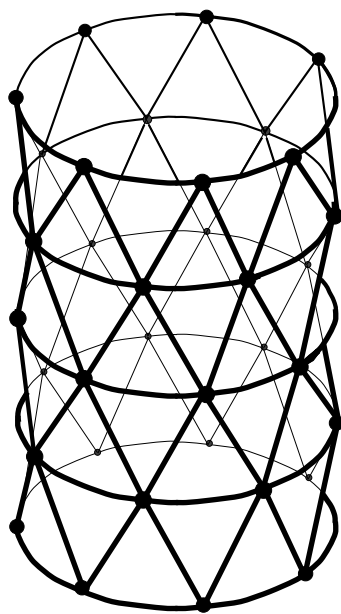


Figure 6.2: Adsorption sites on a $(7,0)$ zig-zag nanotube

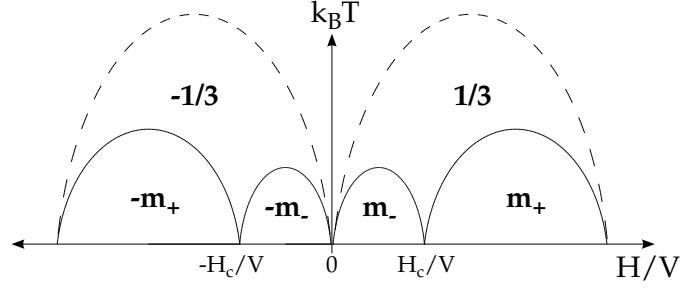


Figure 6.3: Phase diagram of the (N, M) tube

6.2 The Hamiltonian and Classical Limit

When the adsorbed gas is a hard-core boson, the lattice gas is defined by the Bose-Hubbard Hamiltonian[42, 66]

$$\mathcal{H} = -t \sum_{\langle ij \rangle} b_i^\dagger b_j + b_j^\dagger b_i + V \sum_{\langle ij \rangle} n_i n_j - \mu \sum_i n_i, \quad (6.1)$$

where n_i is the boson density at site i , V is the nearest neighbor repulsion and t is the hopping amplitude. The occupation numbers n_i are restricted to 0,1 by the hard-core condition. There is a familiar Heisenberg spin representation [81], which identifies $S_i^z = n_i - 1/2$, $S_i^+ = b_i^\dagger$, and $S_i^- = b_i$. The Hamiltonian is thus

$$\mathcal{H} = -2t \sum_{\langle ij \rangle} S_i^x S_j^x + S_i^y S_j^y + V \sum_{\langle ij \rangle} S_i^z S_j^z - H \sum_i S_i^z, \quad (6.2)$$

where $S_i^z = n_i - 1/2$ and $H = \mu - 3V$ is an effective external magnetic field. Throughout the paper we will use the spin and density representations interchangeably. The spin models obtained in this way are similar to recent examples of “spin tubes”[48].

The Ising limit of the spin models, $t = 0$ corresponds to the case when hopping is forbidden, and already contains many interesting features. We start the analysis in this regime, obtaining the phase diagram as a function of the magnetic field, and then consider quantum fluctuations perturbatively in t/V . We summarize our results first.

The phase diagram in the temperature-magnetic field plane of a typical tube is shown in Fig. 6.3. When the index $q = (N - M) \bmod 3$ is 1 or 2, we find four lobes (solid lines), corresponding to two plateaus with magnetizations $m_- < 1/3$ and $m_+ > 1/3$. Here,

we use the standard Ising notation in which spin is ± 1 . Note that the plateaus are real phases only at zero temperature because the tube is one-dimensional. At finite temperature, the boundaries should be interpreted as crossovers. Nonetheless, deep within a lobe, at $k_B T \ll V$, the magnetizations are well-defined. Specifically, for $q = 1$, we obtain the exact expressions

$$\begin{aligned} m_+ &= \frac{1}{3} \left(1 + \frac{2}{2M + N} \right) & m_- &= \frac{1}{3} \left(1 - \frac{2}{2N + M} \right) \\ H_c &= \left(4 - \frac{2M}{N + M} \right) V \end{aligned} \quad (6.3)$$

The complementary case of $q = 2$ is obtained by interchanging $N \leftrightarrow M$. On the other hand, those tubes without geometric frustration ($q = 0$) behave similarly to the flat sheet (dotted lines) which has only two lobes with magnetizations $\pm 1/3$ [41]. In the flat sheet, the dotted lines are second order phase transitions in the universality class of the Potts-3 models [82]. In our wrapped case, as the tube perimeter approaches the flat sheet limit, one expects that the geometric frustration becomes irrelevant. Indeed, as N or $M \rightarrow \infty$, m_+ and m_- squeeze $1/3$ as the inverse of the tube diameter and become indistinguishable. Beyond the lobes, where the field is strong enough to overcome all nearest neighbor bonds ($|H|/V > 6$ at $k_B T = 0$), the tube is fully polarized. The filling fractions are obtained from the magnetizations by $m = -2(n - 1/2)$. The phase diagram, however, is more easily visualized in terms of spin since spin reversal, $m \leftrightarrow -m$, corresponds to particle-hole symmetry, $n \leftrightarrow 1 - n$.

We have verified this prediction numerically by transfer matrix methods [81] for zig-zag tubes up to $N = 11$ and for the chiral tubes up to $N + M = 7$.^{*} The transfer matrix rows for a sample tube are delineated by dotted lines in Fig. 6.1. It should be noted that similar transfer matrix calculations have been carried out for the special case of unfrustrated zig-zag tubes ($q = 0$) [82]. The motivation in these earlier works was a finite size scaling analysis of the solid phases on flat graphite.

Although 7 is probably too small to be physical, we believe that the arguments in this paper generalize to any tube. In Fig. 6.4 we display sample data for two zig-zag tubes with

^{*}The programming used the GNU implementation of FORTRAN 77 on a PC. The main stumbling block is very large contributions to the partition function at low T ; the LAPACK routine library was used to handle numbers outside ordinary machine range.

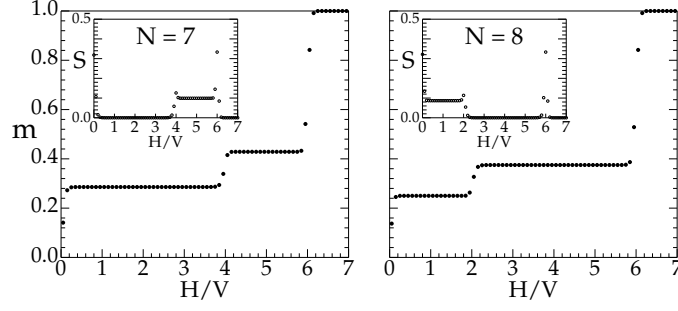


Figure 6.4: Magnetization and entropy per site at $k_B T = 0.05V$

different q : $(7,0)$ and $(8,0)$. The magnetization curves show clear plateaus whose values and transition fields match those predicted by Eq. (6.3). By increasing the temperature and following the evolution of the plateaus, we generate the phase diagram above.

We find that a rather interesting feature of the zig-zag $(N,0)$ tubes emerges, making them exceptional. The insets in Fig. 6.4 indicate an extensive entropy at zero temperature, which has plateaus, too. Upon enumerating the degenerate space explicitly (Section 6.3 below), we shall show that the entropy is exactly $s = (\ln 2)/N$ and that it occurs in m_+ for $q = 1$ and in m_- for $q = 2$. In the presence of hopping, the non-degenerate plateaus retain their gaps, whereas the degenerate ones become correlated states with a unique ground state and *gapless* excitations. More precisely, conformal invariance develops and the effective theory has central charge $c = 1$ with a compactification radius, R , quantized by the tube circumference, $R = N$.

In order to understand the magnetizations and nature of the geometric frustration, it is more intuitive to use the original bosonic picture. As a result of hard-core repulsion on the infinite graphite sheet, the $m = 1/3$ plateau corresponds to filling one of the three sublattices, A, B or C , of the triangular lattice. This configuration minimizes the repulsion, $V n_i n_j$, while maximizing the filling, μn . It is natural to try the same for nanotubes, as we illustrate in Fig. 6.5 for $(5,0)$. Upon wrapping, however, the thick vertical lines are identified and the lattice is no longer tripartite. In fact, the number of sublattice sites is no longer equal, and there is a mismatch along the thick line, which we term the “zipper”. On the left we fill the A sublattice, obtaining the filling fraction $n_+ = 2/5$, and on the right either B or C may be filled with the result that $n_- = 3/10$. For general $(N,0)$ there are $2N$ hexagons in

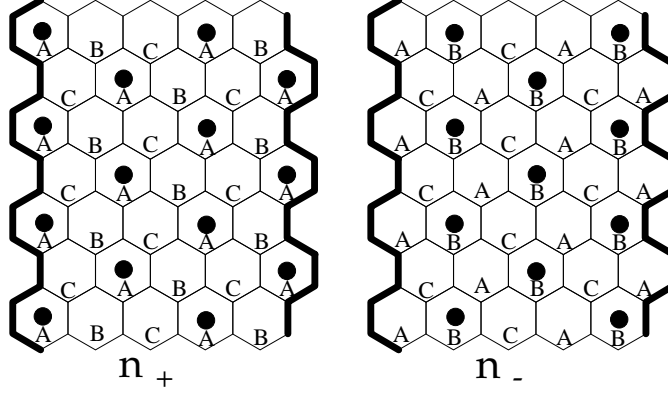


Figure 6.5: Fillings and zipper of the $(5,0)$ zig-zag tube. n_{\pm} corresponds to m_{\mp}

the unit cell, and the filling fractions are $n_+ = \lceil 2N/3 \rceil / 2N$ and $n_- = \lfloor 2N/3 \rfloor / 2N$, where $\lceil x \rceil$ and $\lfloor x \rfloor$ denote the larger and smaller of the two bounding integers of x , respectively. The magnetizations in Eq. (6.3) follow directly by using the correspondence $m = -2(n - 1/2)$. Furthermore, due to the sublattice mismatch, the number density of adjacent particles, n_b , may be non-zero. In the case of $(5,0)$, there are two broken bonds per unit cell in n_+ , and none in n_- . This result generalizes to any $q = 2$ zig-zag tube: $n_{b+} = 2/2N$ and $n_{b-} = 0$. For $q = 1$, the argument goes through as before, except that $n_{b+} = 1/2N$. We summarize this compactly by $n_{b+} = q/2N$.

Substituting these fillings into the Hamiltonian (6.1) yields two energies per site, $e_{\pm}(\mu) = Vn_{b\pm} - \mu n_{\pm}$. The transition occurs when these levels cross: $e_+ = e_-$, or

$$\frac{q}{2N} - \mu \frac{\lceil 2N/3 \rceil}{2N} = -\mu \frac{\lfloor 2N/3 \rfloor}{2N} \quad (6.4)$$

Solving for μ and using the correspondence $H = \mu - 3V$ gives precisely the critical field in Eq. (6.3). In particular, this explains why there are exactly two independent plateaus. Note that, for the special case of the zig-zags, the critical field depends only on q and not on N per se.

In the above analysis, we have made only one assumption, namely that the zipper runs parallel to the tube axis. In general, the zipper may wind helically around the tube or wiggle sideways. However, in all the cases that we considered, the straight zipper has the lowest energy, and moreover, our transfer matrix computations, which are blind to this assumption, are consistent with our analysis.

The chiral tubes are different. Due to their geometry the zipper is forced to wind, but, again, we find that the choice of the straightest possible zipper reproduces our numerics for $N + M$ up to 7. The determination of the fillings and level crossings is much more involved than that of the zig-zag, and we leave it for a more detailed paper. In any case, our analysis reveals that the plateaus in a chiral tube are not macroscopically degenerate, so that the zig-zags are at a special degenerate point.

6.3 Macroscopic Degeneracy and Quantum Fluctuations

Having understood in detail the Ising limit, we now turn on a small hopping, $t \ll V$, that introduces quantum fluctuations. Deep within a plateau, the substrate is maximally filled since adding a particle increases n_b . Consequently, all plateaus begin with a classical gap of order V , and we work in the Hilbert space of the classical ground states. Those plateaus which have only a discrete symmetry must retain their gaps, but the macroscopically degenerate plateaus are more complicated.

Let us reconsider the n_+ filling of the $(5, 0)$ tube in Fig. 6.5. Notice that a particle may hop laterally by one site without changing n_b , as we illustrate in Fig. 6.6, left. Imagine building a typical n_+ state layer-by-layer from top to bottom, with a total of L layers. Each new layer must add exactly two filled sites and one nearest-neighbor bond ($n_b = 1/5$). This constraint implies that no two adjacent sites may be occupied within a layer; if they were, then, to conserve n_b , two adjacent sites must be occupied in the next, and so on up the tube. However, this state is not connected to any other by a single hop. Similarly, the particles cannot hop from layer to layer because this adds another intra-layer bond. An allowed state can be represented as a string of occupied sites, $\sigma = \{\sigma_i\}$, $i = 1, \dots, L$, which in our example is $\sigma = \{\dots(5, 3)(5, 2)(5, 3)\dots\}$. At each layer, there are exactly two possibilities for the following one. For example, $(1, 4)$ can be followed by $(1, 4)$ or by $(2, 4)$. However, the total number of possibilities at any given level is five. Fig. 6.6 (right) summarizes this structure succinctly as a *square* lattice wrapped on the cylinder. A typical state, then, is a lattice path along the tube. There is a recent Hubbard model considered by Henley and Zhang [83] of spinless fermions on a square lattice in which the bookkeeping of states is

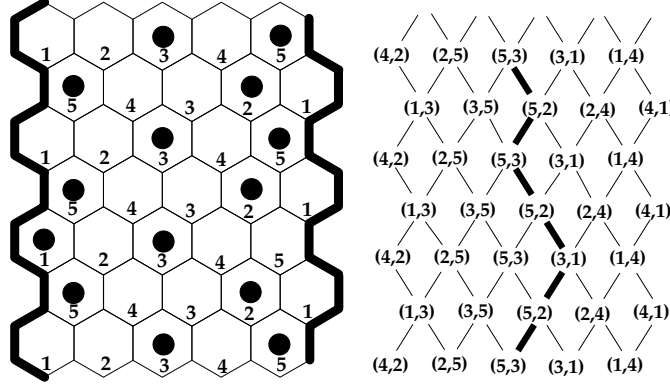


Figure 6.6: LEFT: Typical configuration in n_+ (or m_-) of the $(5,0)$ tube. Alternating numbering within layers allows a symmetric description from bottom-to-top or top-to-bottom. RIGHT: Allowed states as paths on a wrapped square lattice. The vertex labels may be dropped.

very similar.

Generalizing to $(N,0)$, we find N possible states in each layer and two in the succeeding one, and the structure of states is again that of a wrapped square lattice with N squares along the circumference. The dimension of the Hilbert space is the number of lattice paths, $N2^L$, so that in an infinitely long tube, the entropy per site is exactly $(\ln 2)/N$, as claimed earlier. Notice that constrained paths introduce correlations along the length of the tube, despite the absence of inter-layer hopping.

The matrix elements of the projected Hamiltonian connect only those states that differ by a single hop:

$$\langle \tau | \mathcal{H} | \sigma \rangle = \begin{cases} -2t & \text{if } \sum_i \delta_{\sigma_i \tau_i} = L - 1 \\ 0 & \text{otherwise} \end{cases} \quad (6.5)$$

It turns out that this Hamiltonian is exactly solvable, being closely related to a class of solid-on-solid models that were introduced by Pasquier [89]. In the following section we derive the continuum limit of \mathcal{H} , and we confirm the result numerically in the succeeding section.

6.3.a Continuum Limit

In the previous section, the paths σ were labeled, for clarity, by a string of occupied sites on the nanotube. A simpler representation is to work with the wrapped square lattice directly,

where the path is uniquely specified by an initial point and its direction in each layer. We will label the topmost layer by $i = 1$ with i increasing by 1 with each downward move. There are L layers of hexagons and we impose periodic boundary conditions, $L + 1 \equiv 1$. In order for the layers to match, L has to be even.

To specify the initial point on σ , we chose an “anchor” α on one of the N sites in the $i = 1$ layer ($\alpha = 1, \dots, N$). Now, represent a step to the right in layer i by a fermion, c_i^\dagger , and a step to the left by a hole, c_i . A state $|\sigma\rangle$ in the Hilbert space, S , is represented by

$$|\sigma\rangle = |\alpha\rangle \otimes c_{i_1}^\dagger c_{i_2}^\dagger \cdots c_{i_p}^\dagger |0\rangle, \quad (6.6)$$

where α is the anchor site in the first layer and $i_1 \cdots i_p$ are the layers where the path steps to the right. For instance, the portion of the path in fig. 6.6 is $|\sigma\rangle = |3\rangle \otimes c_1^\dagger c_3^\dagger c_4^\dagger \cdots |0\rangle$. The fermionic representation is convenient since there is exactly one step in each layer, but hard-core bosons can also be used. In any case, in one dimension they are equivalent. The number of particles (steps to the right) and holes (steps to the left) must add up to L in order for the path to close on itself along the length of the tube. Each path also has a topological character for the number of times that it winds around the tube, which must be a multiple of N for the path to close. These two conditions may be written as

$$N_p + N_h = L \quad (6.7)$$

$$N_p - N_h = bN, \quad (6.8)$$

where $N_{p,h}$ is the number of particles or holes, and b is an integer. If the particles are assigned a charge, then bN is the total charge. Note that $b = 0$ corresponds to half-filling, $N_p = N_h = L/2$.

Whenever it is allowed within a layer, a single hop changes the step sequence right-left to left-right and *vice versa*, which corresponds to $c_{i+1}^\dagger c_i$ or $c_i^\dagger c_{i+1}$. In a layer without a kink no hops are possible, and the hopping terms vanish by fermionic statistics. Since we are working in periodic boundary conditions, the boundary terms, $c_1^\dagger c_L$ and $c_L^\dagger c_1$, must be treated more carefully. A hop at this point is necessarily accompanied by a translation of the anchor point by $|\alpha\rangle \mapsto |\alpha \pm 1\rangle$. Let us represent this operation by

$$R_\pm |\alpha\rangle = |\alpha \pm 1\rangle \quad (6.9)$$

with $R_-^\dagger = R_+$. Cylindrical wrapping requires a \mathbf{Z}_N symmetry because $|\alpha \pm N\rangle \equiv |\alpha\rangle$, i.e. $R_\pm^N = R_\pm$. Putting the bulk and boundary hopping terms together, the Hamiltonian of eqn. (6.5) becomes

$$\mathcal{H} = -2t \left[\sum_{i=1}^{L-1} c_{i+1}^\dagger c_i + R_- \otimes c_1^\dagger c_L \right] + h.c. . \quad (6.10)$$

We can think of \mathcal{H} as describing free fermions on a periodic one dimensional chain with a \mathbf{Z}_N impurity on one of the bonds.

\mathcal{H} can be diagonalized exactly in momentum space. Going around the tube lengthwise contributes a phase e^{ikL} while going around the perimeter contributes $e^{i\phi}$, with $\phi = 2\pi a/N$ ($a = 1, \dots, N-1$). Therefore toroidal boundary conditions require

$$e^{ikL} e^{i\phi} = 1 . \quad (6.11)$$

Or,

$$k = \frac{2\pi v}{L} \left(n + \frac{a}{N} \right) , \quad (6.12)$$

where $v = 2t$ is the velocity and n is an integer. The Hamiltonian contains the usual free particle dispersion, but with the allowed k given by eqn. (6.12),

$$\mathcal{H} = -4t \sum_k \cos k c_k^\dagger c_k . \quad (6.13)$$

If the spectrum is linearized around the Fermi momentum, $|k_F|$ (at half-filling), then at small k , nonzero a states cost an additional energy of $(2\pi v/L)(a/N)^2$.

The a/N offset in k can be thought of as a minimally coupled vector potential such that the magnetic field is a δ -flux tube through the torus containing (a/N) flux quanta. In other words, one of the bonds along the chain (the “anchor”) had \mathbf{Z}_N symmetry, whose effect is equivalent to a flux tube. Fig. 6.7 illustrates this equivalence. The offset in k is like a total current in the fermion system.

At this point, one can see two topological effects of the torus. First is the \mathbf{Z}_N flux tube, or total current. As we have seen, its contribution to the energy near $|k_F|$ was $(2\pi v/L)(a/N)^2$. Second is the path winding along the length of the tube, or total charge, eqn. (6.7). Its

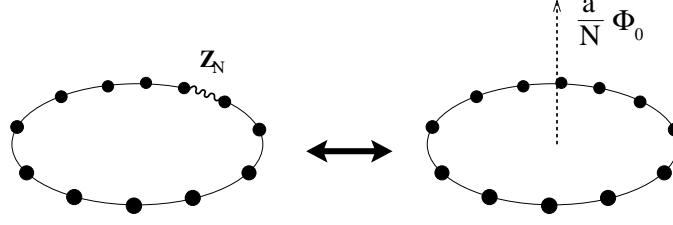


Figure 6.7: The left ring shows the \mathbf{Z}_N impurity on the anchor bond (wavy line). The right ring shows the equivalent alternative, where the impurity is replaced by a flux tube through the torus.

contribution to the energy near $|k_F|$ is similar, $(2\pi v/L)(bN/2)^2$. The total energy due to these topological sectors is

$$\Delta E_{a,b} = \frac{2\pi v}{L} \left(\frac{a^2}{N^2} + \frac{b^2 N^2}{4} \right). \quad (6.14)$$

This expression is familiar from the Luttinger liquid model of one-dimensional spinless Fermions [88].

We can now obtain the continuum limit of our model. It is well known that free fermions in one dimension are equivalent to free bosons. The corresponding Lagrangian is

$$\mathcal{L} = \frac{1}{8\pi} [v^{-1}(\partial_t \varphi)^2 - v(\partial_x \varphi)^2], \quad (6.15)$$

where φ is the bosonic field. \mathcal{L} is a conformally invariant theory with central charge $c = 1$. We conjecture that the topological effects that we described above come from compactifying φ on a circle of radius R ,

$$\phi \equiv \varphi + 2\pi R. \quad (6.16)$$

By compactifying the boson, topological modes (or zero modes) appear. In field theory, they are conventionally obtained from electric and magnetic monopoles. The energy of the zero modes is

$$E_{a,b}^0 = \frac{2\pi v}{L} \left(\frac{a^2}{R^2} + \frac{b^2 R^2}{4} \right), \quad (6.17)$$

where a and b are integers labeling the fundamental cycles on the torus. Comparing $E_{a,b}^0$ to $\Delta E_{a,b}$ (6.14), we find that $R = N$. The ordinary phonon, (oscillator) modes exist on

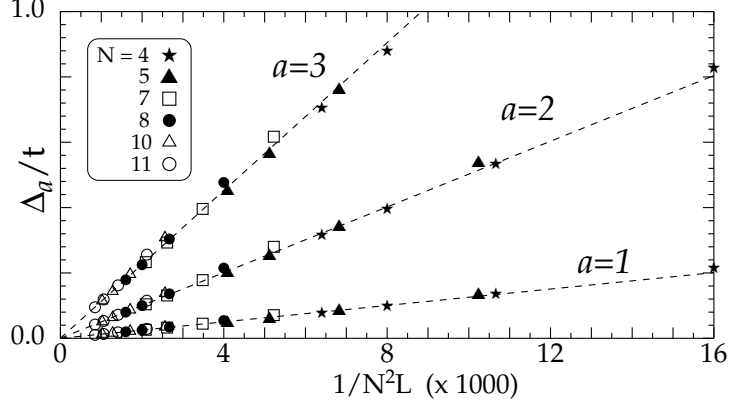


Figure 6.8: The gap scales as $1/N^2 L$.

top of each topological sector and simply contribute the usual phonon energy, so that the complete dispersion is

$$E = E_{a,b}^0 + \frac{2\pi}{L}|n|. \quad (6.18)$$

The overall picture of a compactified boson with central charge $c = 1$ is consistent with the solid-on-solid models of Pasquier [89].

6.3.b Numerics

We have diagonalized the original Hamiltonian, eqn. (6.5) numerically with periodic boundary conditions for system sizes up to $N = 11$ and $L = 10$. Due to the sparseness of \mathcal{H}_m we were also able to obtain the ground state energy up to $L = 16$. We will fix $2t = 1$ in what follows.

We find that the degeneracy is lifted and the ground state becomes unique and uniform. The ground state energy, $E_0(L)$, follows $E_0 \sim -0.61L - 0.31\pi c/L$. The lowest $N - 1$ excited states are given by $\Delta_a = a^2 \Delta / (N^2 L)$, with $\Delta = 12.9 \pm 0.5$, which is shown in Fig. 6.8 for $a = 1, 2, 3$. All of these levels are doubly degenerate. This ground state energy and spectrum are in perfect agreement with free bosons compactified on a radius $R = \zeta N$, as we described in the previous section.

Right- and left-moving oscillator modes of energy $\omega_n = v k_n$, where $k_n = 2\pi n/L$, appear in the spectrum, but for $a < N$ the zero modes are the lowest. Our spectrum in Fig. 6.8

corresponds to $E_{a,b}^0$ with $b = 0$. The modes with non-zero b are very high in energy and are washed out by our small system size. To fix ζ , we look at higher low-lying levels (which also scale like $1/L$). We find that the N 'th excitation energy is independent of N and quadruply degenerate. This can happen only if the N 'th zero mode, $E_{\pm N,0}^0 = 2\pi v/\zeta^2 L$, is degenerate with the lowest oscillator mode, $\omega_{\pm 1} = 2\pi v/L$, which fixes $\zeta = 1$. Thus, the compactification radius is $R = N$. The velocity can be read off from the slopes in Fig. 6.8 as $v = \Delta/2\pi$. Within our accuracy, $v = 2$. The rest of our spectrum is consistent with these parameters. For instance, we find a unique, zero-momentum state with $a = b = 0$, which consists of one right- and one left-moving oscillator mode with $n = 2\pi/L$ at energy $E = 2E_1$. Note that ζ is fixed only by counting degeneracies, not by fitting any parameters.

6.3.c Higher Order Corrections

The preceding discussion is valid to first order in t/V . The next terms are of order t^2/V and involve virtual transitions to adatom configurations that are not in the degenerate subspace S . The generic form is

$$-\frac{t^2}{V} \mathcal{P}_S \left[\sum_{\langle ij \rangle \langle kl \rangle} b_i^\dagger b_j b_k^\dagger b_l \right] \mathcal{P}_S, \quad (6.19)$$

where \mathcal{P}_S is a projection operator into S . Another way of writing the second order perturbation is the familiar form,

$$\langle \sigma' | \mathcal{H} | \sigma \rangle \rightarrow \langle \sigma' | \mathcal{H} | \sigma \rangle - \sum_{\lambda} \frac{\langle \sigma' | \mathcal{H} | \lambda \rangle \langle \lambda | \mathcal{H} | \sigma \rangle}{E_{\lambda} - E_{\sigma}}, \quad (6.20)$$

where $|\sigma\rangle, |\sigma'\rangle \in S$ while $|\lambda\rangle \notin S$. E_{λ} is the energy of the virtual state. $E_{\sigma} = E_{\sigma'}$ are, of course, constant, and all energy differences are due to the nearest neighbor repulsion $V n_i n_j$.

There are three types of virtual processes: (i) single particle hopping from σ to $\sigma \neq \sigma'$, (ii) two particle correlated hopping from σ to $\sigma \neq \sigma'$ and (iii) single particle diagonal hopping from σ back into σ . For concreteness, consider process (iii) in the $(5,0)$ state in fig. 6.6. Whenever there is a kink in σ , such as in the third layer from the top, the contribution to eqn. (6.20) from all virtual hops is $-(35/6)4t^2/V$. For example, the adatom on site 3 can hop into any one of its six neighbors with the energy denominators $1/2 + 1/2 + 1/2 + 1/2 + 1/2 + 1/3$ (in units of t^2/V). Similarly, the adatom on site 5 contributes $1 + 1 + 1$, for a total of

35/6 (it is forbidden to hop one site over to the right because the resulting state is in S). On the other hand, if there is no kink, the contribution is $-8 \cdot 4t^2/V$. The criterion for a kink in layer i is $2[1/4 - (\tilde{n}_i - 1/2)(\tilde{n}_{i+1} - 1/2)] = 1$, where $\tilde{n}_i = c_i^\dagger c_i$; otherwise this quantity vanishes. Similarly, the absence of a kink is synonymous with the nonvanishing of $2[1/4 + (\tilde{n}_i - 1/2)(\tilde{n}_{i+1} - 1/2)]$. Thus, the total diagonal contribution to \mathcal{H} can be written

$$\begin{aligned} \mathcal{H} &\rightarrow \mathcal{H} - \frac{8t^2}{V} \sum_{\sigma} \sum_i \frac{35}{6} \left[\frac{1}{4} - \left(\tilde{n}_i - \frac{1}{2} \right) \left(\tilde{n}_{i+1} - \frac{1}{2} \right) \right] + 8 \left[\left(\tilde{n}_i - \frac{1}{2} \right) \left(\tilde{n}_{i+1} - \frac{1}{2} \right) + \frac{1}{4} \right] |\sigma\rangle\langle\sigma| \\ &= \mathcal{H} - \frac{4t^2}{V} \sum_{\sigma} \left[\frac{13}{3} \sum_i \tilde{n}_i \tilde{n}_{i+1} - \frac{13}{3} \sum_i \tilde{n}_i + 8 \right] |\sigma\rangle\langle\sigma|. \end{aligned} \quad (6.21)$$

For general N , the correction scales like N . The essential term in the last line of eqn. (6.21) is the first one. This four-fermion interaction renormalizes the radius R by corrections of order t/V .

Let us return to processes (i) and (ii). An example of (i) is the adatom in the third layer from the top, site 5, hopping to the second layer, site 1, and then back into the third layer, site 1. The intermediate state is not in S . This process serves only to renormalize t because its amplitude is the same for all kinks. An example of (ii) is the particle in the fourth layer, site 5, hopping to site 4, *followed by* the particle in the third layer, site 5, hopping to site 1 in the same layer. This correlated hopping occurs in a configuration containing the sequence particle-hole-hole or hole-particle-particle, which corresponds to a next-nearest neighbor interaction $c_{i+2}^\dagger c_{i+1}^\dagger c_{i+1} c_i + h.c.$. We have not analyzed all such terms in detail, and it is possible that there is a delicate cancellation of the terms (ii) and (iii) when the fields are linearized around $|k_F|$, but we consider it more likely that they do not cancel so that R is renormalized at order t/V .

One can also consider the extreme limit in which $t \gg V$. In this case, the XXZ Hamiltonian in eqn. (6.2) is simply the XY model on a cylinder. Let us denote the spin angle relative to the cylindrical surface by $\varphi(x, \theta)$, where x is the coordinate along the tube and θ is the coordinate around the perimeter. Uniqueness of the wavefunction requires that φ has the periodicity $\varphi(x, \theta + 2\pi) = \varphi(x, \theta) + 2\pi m$, where m is an integer. The low energy excitations are purely along the length of the tube; excitations around the perimeter will cost an energy on the order of $1/N$, which is large compared to $1/L$. Thus we can freeze

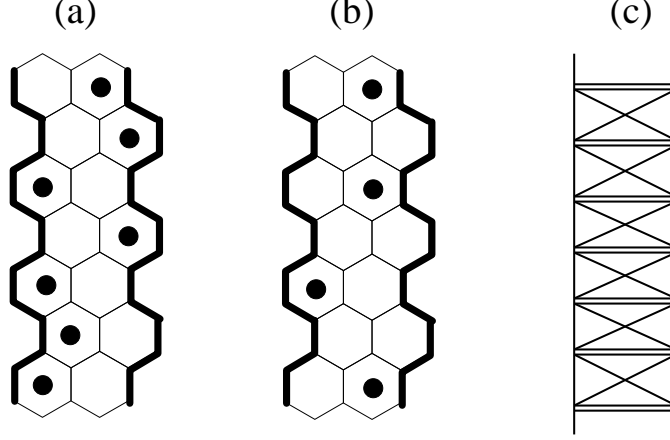


Figure 6.9: The fillings for $N = 2$. $n_+ = 1/2$ (a) and $n_- = 1/4$ (b). Each adatom can live at either site in its layer because each site is connected to every site in the neighboring layers. (c) shows the triangular lattice in the plane; the horizontal double bond is due to the periodicity around a cylinder. (c) is exactly the geometry of the spin ladder studied by other authors (albeit with different coupling).

the θ coordinate, and the energy density is proportional to $|\partial_x \varphi|^2$. Since the periodicity is still $\varphi \equiv \varphi + 2\pi m$, we end up with a free boson compactified on radius $R_{XY} = 1$. The question is how the adsorption regime $t \ll V$, which is also a compactified boson but on radius $R = N$, is reached.

6.4 Special Case: $N = 2$

Before concluding with the effective theory, we should point out that the geometry of the $(2, 0)$ tube is special; all sites in adjacent layers are interconnected. As a result, all of its plateaus have an extensive entropy, and we find that hopping opens a gap in both plateaus. Fig. 6.9 illustrates this exception. At either filling, the adatom in each layer is free to hop to either site—both configurations are iso-energetic because each site is contiguous to all sites in the neighboring layers. Hence both plateaus are macroscopically degenerate. In the presence of hopping, each adatom lives in a double well potential, which has a gap of order t . In fact, this tube can be written as a spin chain that has been studied at isotropic coupling[87], $-2t = V$. Two plateaus were found in this case, and it is tempting to speculate

whether the two regimes are connected adiabatically.

6.5 Discussion and Conclusion

One observable consequence of conformal symmetry is that the low temperature heat capacity is fixed by c [84]:

$$C = c \frac{\pi v k_B^2}{3} T = \frac{\pi v k_B^2}{3} T \quad (6.22)$$

It is noteworthy that, even though the dispersion of the oscillator modes is independent of N , the spectrum remembers, via the zero-modes, the finite radius of the nanotube. Furthermore, R is quantized by N ; in the language of Luttinger liquids, this means that the Luttinger parameter is fixed by topology, similarly to the case of edge states in a fractional quantum Hall fluid[85], and in contrast to quantum wires (where the Luttinger parameter can vary continuously). Because there is no inter-layer hopping, ϕ is tied to transverse, rather than to longitudinal, density fluctuations along the tube.

Finally, let us briefly view the spin tube as a quantum spin ladder to see if it yields a gapless state in the degenerate plateaus. A standard approach is to use a Lieb-Schultz-Mattis (LSM) argument, in which the spins are deformed slowly along the length[86]. Applying it to our tube, we find that a plateau is gapless if $S - M$ is *not* an integer, where S and M are the total spin and magnetization, respectively, per layer (a layer being the N sites around the perimeter). Using $S = N/2$ and the magnetizations from Eqn. (6.3), we find that $S - M$ is an integer in the macroscopically degenerate plateaus, so that the LSM argument is insufficient in this case. A conclusive argument must take the geometric frustration into account, which is further evidence that our state is strongly correlated.

In conclusion, we have studied the problem of monolayer adsorption on carbon nanotubes and identified several interesting filling fraction plateaus. Since the difference between the plateaus decreases slowly, as the inverse of the tube diameter, experimental measurement should be feasible for large enough tubes. We have identified the zig-zag tubes as exceptional, in which the geometric frustration together with quantum fluctuations lead to conformal symmetry. The effective theory is free compactified boson, which has a quantized radius to first order in the hopping. The only other such theory in nature that we are aware

of are the chiral edge states in a quantum Hall fluid, where the radius is quantized by the bulk filling fraction. There are interesting questions related to the large hopping limit.

Chapter 7

Summary

It is widely believed by both theorists and experimentalists that the composite particle construct is required for a full understanding of the fractional quantum Hall effect (FQHE). In this thesis we take the point of view that a great deal of the FQHE physics can be understood by projecting to the lowest Landau level (LLL) at the outset, which allows us to develop a composite particle formalism at various filling fractions, ν . Initially the composites are abstract operators building up the many-particle Fock space, but later analysis of physical operators, many-particle wavefunctions, and response functions reveals an interpretation in terms of vortices bound to an underlying particle. Our theory departs from most other theoretical work in this area, which uses singular flux attachment to map the problem into a Chern-Simons action. We treat both fermionic and bosonic statistics of the underlying particles.

When the underlying particles (or particles, for short) are bosons, the appropriate formulation is in terms of composite fermions. The original Hamiltonian for the bosons is mapped exactly into a Hamiltonian for composite fermions with an infinite number of constraints. To preserve the constraints, we use a conserving approximation to derive an effective theory microscopically. In addition to a self-consistent theory of incompressible quantum liquids in the LLL, our approach provides a method to calculate the effective mass (gap) and the single particle spectrum of the composite fermions, which arise solely from the interactions between the particles. This calculation extends previous work in the special case $\nu = 1$ to arbitrary ν . A recent proposal raises the intriguing prospect of observing a FQHE of bosons

in rotating atomic Bose-Einstein condensates.

The complementary case is composite bosons. The ground state for a perturbation expansion is macroscopically degenerate, which precludes a microscopic derivation of an effective theory. We follow an alternate approach by constructing a phenomenological Landau-Ginzburg action based on a symmetry analysis. A crucial ingredient in the action is the internal structure of the composite particle, which, at $\nu = 1/p$, consists of p vortices bound to the particle. For $p = \text{even}$ the particles are bosons while for $p = \text{odd}$ they are fermions. Our model incorporates this structure through gauge potentials that couple to the internal degrees of freedom. The spectrum of the effective theory contains the so-called magnetoroton excitation, which seems to be the first analytic observation of this phenomenon.

The next portion of the thesis is an examination of paired states of bosons or fermions in two dimensions. The class of pairings that we investigate includes non-zero relative angular momentum, which is a state that breaks both parity and time reversal invariance. Part of our method is based on Bardeen-Cooper-Schrieffer (BCS) theory and is largely independent of the FQHE. However, in the context of the FQHE, we use a mean field approximation that maps particles in a net magnetic field into composite particles in zero field. The BCS approach then applies to the composite particles.

For bosonic particles, we consider p-wave pairing of spin-1/2 bosons and d-wave pairing of spinless bosons. In the FQHE, the former case is a singlet known as the “permanent” state and the latter is the “Haffnian”. Each state can be written as a trial wavefunction that is the unique ground state of its corresponding Hamiltonian. By analyzing the spectrum of the Hamiltonian directly or by applying the mean field BCS theory, we find that the permanent sits on the transition between the polarized Laughlin state (a Bose condensate of composite particles) and a Bose condensate with helical order. The spin order of the permanent is that of an anti-Skyrmion. Similarly, the Haffnian is on the transition between a Laughlin state and a strong coupling paired state. Of course, these conclusions can stand alone without reference to the FQHE because they can be derived solely within the BCS framework.

For fermionic particles, we carry through a conserving approximation for the spin con-

ductivity. We show that the induced action for an external gauge field that couples to spin is a Chern-Simons (CS) term. In the d-wave case we obtain the non-abelian $SU(2)$ CS term because the system is spin-rotationally invariant, whereas the p-wave case gives an abelian $U(1)$ term since it has only $U(1)$ symmetry. In both cases, the Hall spin conductivity is a topological invariant, which characterizes the winding of the order parameter in momentum space. This is a microscopic proof of quantization that was proposed in earlier works by other authors.

The last part of the thesis deals with adsorption on carbon nanotubes, which is a one-dimensional problem. The hexagon centers serve as adsorption sites for hard core atoms, allowing the system to be treated as a lattice gas on a triangular lattice wrapped on a cylinder. This model is equivalent to a type of quantum spin tube. The wrapping introduces geometric frustration on top of the frustration of the triangular lattice, leading to interesting physics. In the spin language, we find magnetization plateaus in all tubes in the Ising limit, which is confirmed both analytically and numerically. However, the zig-zag tubes are exceptional and contain plateaus that are macroscopically degenerate. When quantum hopping is allowed, the special plateaus become gapless phases that are described by a $c = 1$ conformal theory of a compactified boson. The theory is derived analytically and confirmed numerically. Perhaps the most remarkable feature is that the radius of compactification is quantized by the tube diameter. This brings us back to the FQHE, where the theory of edge states is also characterized by a (chiral) conformal boson compactified on a quantized radius.

Appendix: Non-Commutative Fourier Transform

Our ultimate aim in this subsection is to introduce constructs that will allow us to take the thermodynamic limit, $N \rightarrow \infty$, and to introduce the momentum \mathbf{k} so as to take advantage of translational invariance. As discussed by several authors [12, 15, 18], \mathbf{k} is a good quantum number and $\hat{\mathbf{z}} \times \mathbf{k}$ will turn out to be the dipole moment. The formalism in this appendix has been discussed in more detail by [18], and we include it here for completeness.

Consider the special case of one attached vortex with $B_1 = -B_2$, as introduced in Sections 2.1.b and 2.1.c. We first introduce real space wavefunctions by analogy to the usual matter field:

$$\begin{aligned} c(z, \bar{\eta}) &= \sum_{mn} u_m(z) \overline{u_n(\eta)} c_{mn} \\ c^\dagger(\eta, \bar{z}) &= \sum_{mn} u_n(\eta) \overline{u_m(z)} c_{nm}^\dagger . \end{aligned} \tag{7.1}$$

Our convention is to use z for the left coordinate and $\bar{\eta}$ for the right. Complex conjugation reflects the two opposite charges. There is only one magnetic length ℓ_B in this problem because the magnitude of the charges is equal. This is a rather singular limit of our two-particle construction in Section 2.1.b; in this limit the effective magnetic field is $B = B_1 + B_2 = 0$, and the pseudomomentum and translation operators, π and K , are identical (eqn. (2.21)).

In the z, η basis, the densities become

$$\begin{aligned} \rho^R(\eta, \bar{\eta}') &= \int d^2 z c^\dagger(\eta, \bar{z}) c(z, \bar{\eta}') \\ \rho^L(z, \bar{z}') &= \int d^2 \eta c^\dagger(\eta, \bar{z}') c(z, \bar{\eta}) \end{aligned} \tag{7.2}$$

Thus integration has replaced summation over indices. It is convenient to introduce a binary operation $*$ to represent integration over one set of coordinates,

$$(\hat{a} * \hat{b})(z, \bar{z}') = \int d^2 z_1 a(z, \bar{z}_1) b(z_1, \bar{z}') , \quad (7.3)$$

of two operators, \hat{a} and \hat{b} , which is just matrix multiplication. It is also convenient to define the $*$ -commutator by

$$[\hat{a} *, \hat{b}] = \hat{a} * \hat{b} - \hat{b} * \hat{a} . \quad (7.4)$$

This allows us to write

$$\begin{aligned} \hat{\rho}^R &= \hat{c}^\dagger * \hat{c} \\ \hat{\rho}^L &= : \hat{c} * \hat{c}^\dagger : \end{aligned} \quad (7.5)$$

Note the normal ordering in $\hat{\rho}^L$ necessary to avoid sign ambiguities.

Consider the plane wave, $e^{i\mathbf{k}\cdot\mathbf{r}}$, projected to the LLL. Following the previous discussion of two particles in Section 2.1.b, eqn. (2.22), $\mathbf{r} = (\mathbf{R}_1 + \mathbf{R}_2)/2$ in zero effective field. The plane wave operator now becomes

$$e^{i\mathbf{k}\cdot\mathbf{r}} = e^{i\mathbf{k}\cdot(\mathbf{R}_1+\mathbf{R}_2)/2} . \quad (7.6)$$

Its representation in the z, η coordinates is obtained by acting on the lowest weight eigenfunction $\psi_{0,0}$. Recall that, for $B_1 = -B_2$, $\psi_{0,0}(z, \bar{\eta}) = \frac{1}{2\pi} e^{-\frac{1}{4}|z|^2 - \frac{1}{4}|\eta|^2 + \frac{1}{2}z\bar{\eta}}$, where the magnetic length has been set to unity. It is not difficult to show that $\psi_{0,0}(z, \bar{\eta})$ is identical to the delta function in the LLL.

$$\delta(z, \bar{\eta}) = \sum_m u_m(z) \overline{u_m(\eta)} . \quad (7.7)$$

In the LLL, δ acts as expected: $\hat{\delta} * \hat{a} = \hat{a} * \hat{\delta} = \hat{a}$. The constraint is thus $\hat{\rho}^R = \hat{\delta}$, or

$$\rho^R(\eta, \bar{\eta}') = \delta(\eta, \bar{\eta}') .$$

The differential representation of $\mathbf{R}_{1,2}$ in the z, η coordinates was constructed in Section (2.1.b). According to the prescription, the plane wave acting on $\hat{\delta}$ yields the LLL representation

$$\tau_{\mathbf{k}}(z, \bar{\eta}) = \delta(z, \bar{\eta}) e^{\frac{1}{2}i(\bar{k}z + k\bar{\eta}) - \frac{1}{4}|k|^2} . \quad (7.8)$$

By either straightforward integration or by using the commutator of $\mathbf{R}_{1,2}$, eqn. (2.19), we find that the $\hat{\tau}_{\mathbf{k}}$ obey

$$\hat{\tau}_{\mathbf{k}} * \hat{\tau}_{\mathbf{k}'} = \hat{\tau}_{\mathbf{k}+\mathbf{k}'} e^{\frac{1}{2}i\mathbf{k}\wedge\mathbf{k}'} , \quad (7.9)$$

where we have introduced the shorthand notation, $\wedge\mathbf{k} = -\hat{z} \times \mathbf{k}$ and $\mathbf{k} \wedge \mathbf{k}' \equiv \mathbf{k} \cdot \wedge\mathbf{k}'$. The phase factor is the area of a triangle formed by \mathbf{k} and \mathbf{k}' so that the phase counts the flux enclosed by the triangle. Hence we interpret $\hat{\tau}_{\mathbf{k}}$ as a magnetic translation in the plane by $\wedge\mathbf{k}$ [18]. The connection to plane waves extends to completeness and orthonormality properties, which defines a “noncommutative Fourier transform”. In particular,

$$\text{Tr } \hat{\tau}_{\mathbf{k}} * \hat{\tau}_{\mathbf{k}'} = 2\pi\delta(\mathbf{k} + \mathbf{k}') , \quad (7.10)$$

$$\int \frac{d^2\mathbf{k}}{2\pi} \tau_{\mathbf{k}}(z, \bar{z}') \tau_{-\mathbf{k}}(\eta, \bar{\eta}') = \delta(z, \bar{\eta}') \delta(\eta, \bar{z}') . \quad (7.11)$$

The Tr stands for a trace defined by $\text{Tr } \hat{a} = \int d^2z a(z, \bar{z})$. We can now define the Fourier transform and its inverse:

$$c(z, \bar{\eta}) = \int \frac{d^2\mathbf{k}}{(2\pi)^{3/2}} c_{\mathbf{k}} \tau_{\mathbf{k}}(z, \bar{\eta}) , \quad (7.12)$$

$$c_{\mathbf{k}} = (2\pi)^{1/2} \text{Tr } \hat{c} * \hat{\tau}_{-\mathbf{k}} . \quad (7.13)$$

The extra $\sqrt{2\pi}$ factors are not used in general; they are specific to the Fourier transform of the \hat{c} 's in order for the commutators to retain their conventional form

$$[c_{\mathbf{k}}, c_{\mathbf{k}'}^{\dagger}]_{\pm} = (2\pi)^2 \delta(\mathbf{k} - \mathbf{k}') . \quad (7.14)$$

Therefore, we have constructed composite particles with momentum \mathbf{k} and dipole moment $\wedge\mathbf{k}$, which emerged from magnetic translations perpendicular to \mathbf{k} . When the underlying particles are bosons, anticommutators are required in eqn. (7.14). This defines the composite fermion. The Fock space of fermions at $\nu = 1$ is trivial, consisting of exactly one function, so composite bosons are not useful in this case.

Next we would like to apply the Fourier transform to the left and right densities in eqn. (7.2), which become

$$\hat{\rho}_{\mathbf{q}}^R = \int \frac{d^2\mathbf{k}}{(2\pi)^2} e^{-\frac{1}{2}i\mathbf{k}\wedge\mathbf{q}} c_{\mathbf{k}-\frac{1}{2}\mathbf{q}}^{\dagger} c_{\mathbf{k}+\frac{1}{2}\mathbf{q}} \quad (7.15)$$

$$\hat{\rho}_{\mathbf{q}}^L = \int \frac{d^2\mathbf{k}}{(2\pi)^2} e^{\frac{1}{2}i\mathbf{k}\wedge\mathbf{q}} c_{\mathbf{k}-\frac{1}{2}\mathbf{q}}^{\dagger} c_{\mathbf{k}+\frac{1}{2}\mathbf{q}} , \quad (7.16)$$

The commutators of $\hat{\rho}_{\mathbf{q}}$ are familiar in the quantum Hall effect [55, 90, 91], defining an infinite Lie algebra known as W_{∞} . The constraints appear particularly simple in momentum space:

$$\hat{\rho}_{\mathbf{q}}^R - 2\pi\bar{\rho} \delta(\mathbf{q}) = 0 , \quad (7.17)$$

which enforces a uniform vortex density, $\bar{\rho}$.

Bibliography

- [1] *The Quantum Hall Effect*, 2nd ed., edited by R.E.Prange and S.M.Girvin (Springer-Verlag, NY, 1990).
- [2] B.I. Halperin, P.A. Lee, and N. Read, Physical Review B **47**, 7312 (1993).
- [3] N. Read, cond-mat/0011338.
- [4] R.B. Laughlin, Physical Review Letters **50**, 1395 (1983).
- [5] B.I. Halperin, Physical Review Letters **52**, 1583 (1984).
- [6] D. Arovas, J.R. Schrieffer, and F. Wilczek, Physical Review Letters **53**, 145 (1984).
- [7] W. Pan, et. al., Physica E **9**, 9 (2001);
I.V. Kukushkin, J.H. Smet, K. von Klitzing, and K. Eberl, Physical Review Letters **85**, 3688 (2000);
R.L. Willett, K.W. West, and L.N. Pfeiffer, Physical Review Letters **83**, 2624 (1999);
A.E. Dementyev et. al., Physical Review Letters, **83**, 5074 (1999). H.L. Stormer, Solid-State-Communications, **107**, 617-22 (1998);
H.L. Stormer, Solid State Communications, **107**, 617 (1998);
L.P. Rokhinson, Physical Review B **56**, R1672 (1997);
R.L. Willett, Semiconductor Science and Technology, **12**, 495 (1997);
R.L. Willett, Advances in Physics, **46**, 447 (1997);
- [8] E. Shimshoni, S.L. Sondhi, and D. Shahar, Physical Review B **55**, 13730 (1997).
- [9] V.J. Goldman, Physica B **280**, 372 (2000).

- [10] S.-C. Zhang, H. Hansson, S.A. Kivelson, Physical Review Letters **62**, 82 (1989);
N. Read, Physical Review Letters **62**, 86 (1989);
D.-H. Lee and M.P.A. Fisher, Physical Review Letters **63**, 903 (1989);
D.-H. Lee and S.-C. Zhang, Physical Review Letters **66**, 1220 (1991);
S.-C. Zhang, Int. J. Mod. Phys. B. **6**, 25 (1992).
- [11] S. Deser, R. Jackiw, S. Templeton, Physical Review Letters **48**, 975 (1982); *ibid*, Annals
of Physics **140**, 372 (1982).
- [12] N. Read, Semicond. Sci. Technol. **9**, 1859 (1994).
- [13] J. K. Jain, Physical Review Letters **63**, 199 (1989); Physical Review B **40**, 8079 (1989);
ibid. **41**, 7653 (1990).
- [14] F.D.M. Haldane, Physical Review Letters **51**, 605 (1983).
- [15] R. Shankar and G. Murthy, Physical Review Letters **79**, 4437 (1997);
R. Shankar, Physical Review Letters **84**, 3946 (2000);
G. Murthy, cond-mat/0008259.
- [16] R. Shankar, Physical Review Letters **83**, 2382.(1999).
- [17] R. Shankar, Physical Review B **63**, 85322 (2001).
- [18] N. Read, Physical Review B **58**, 16262 (1998).
- [19] V. Pasquier and F. D. M. Haldane, Nucl. Phys. B **516** 719 (1998).
- [20] D.-H. Lee, Physical Review Letters **80**, 4745 (1998).
- [21] J.R. Schrieffer, *Theory of Superconductivity* (Addison-Wesley, Reading, MA, 1984).
- [22] D. Vollhardt and P. Wölfle, *The Superfluid Phases of Helium 3*, (Taylor and Francis,
London, 1990).
- [23] D. Nozières and D. Saint-James, J. Physique **43**, 1133 (1982);
M.J. Rice and Y.R. Wang, Physical Review B **37**, 5893 (1988).

- [24] G.M. Luke et al., Nature **394**, 558 (1998);
T.M. Riseman et al., Nature **396**, 242 (1998);
K. Ishida et al., Nature **396**, 658 (1998);
A.P. Mackenzie et al., Physical Review Letters **80**, 161 (1998);
K. Yoshida et al., Physical Review B **58**, 15062 (1998).
- [25] M. Sigrist et al., Physica C **134**, 317 (1999).
- [26] W. Hardy et al., Physical Review Letters **70**, 399 (1993);
D. Wollman et al., Physical Review Letters **71**, 2134 (1993);
D.J. Van Harlingen, Rev. Mod. Phys. **67**, 515 (1995);
J. Kirtley et al., Nature **373**, 225 (1995);
J. Kirtley et al., Physical Review Letters **76**, 1336 (1996).
- [27] B.I. Halperin, Helv. Phys. Acta **56**, 75 (1983).
- [28] G. Moore and N. Read, Nucl. Phys. B **360**, 362 (1991);
N. Read and G. Moore, Prog. Theor. Phys. (Kyoto) Suppl. **107**, 157 (1992).
- [29] F.D.M. Haldane and E.H. Rezayi Physical Review Letters **60** 956, 1886 (E) (1988).
- [30] N. Read and E. Rezayi, Physical Review B **54**, 16864 (1996).
- [31] M. Greiter, X.G. Wen, and F. Wilczek, Physical Review Letters **66**, 3205 (1991); *ibid*,
Nucl. Phys. **B374**, 567 (1992).
- [32] X.-G. Wen and Y.-S. Wu, Nucl. Phys. B **419**, 455 (1994).
- [33] R.H. Morf Physical Review Letters **80**, 1505 (1998).
- [34] K. Park, V. Melik-Alaverdian, N.E. Bonesteel, and J.K. Jain, Physical Review B **58**,
R10167 (1998).
- [35] N. Read and D. Green, Physical Review B **61**, 10267 (2000).
- [36] W. Pan, H.L. Stormer, D.C. Tsui, L.N. Pfeiffer, K.W. Baldwin, K.W. West, cond-
mat/0103144;

- [37] T. Senthil, J.B. Marston, and M.P.A. Fisher, Physical Review B **60** 4245 (1999).
- [38] G.E. Volovik, Zh. Eksp. Teor. Fiz. **94**, 123 (1988) [Sov. Phys. JETP **67**, 1804 (1988)];
 G.E. Volovik and V.M. Yakovenko, J. Phys. Cond. Matter **1**, 5263 (1989);
 G.E. Volovik, Physica B **162**, 222 (1990);
 G.E. Volovik, Sov. Phys. JETP Lett. **51**, 125 (1990);
 G.E. Volovik, Sov. Phys. JETP Lett. **55**, 368 (1992).
- [39] P.W. Anderson, Phys. Rev. **110**, 827 (1958); *ibid.*, **112**, 1900 (1958).
- [40] M. Bretz, J. Phys. Col. **39**, C6/1348-51 (1978).
- [41] M. Schick, J. S. Walker and M. Wortis, Physical Review B **16**, 2205 (1977).
- [42] G. Murthy, D. Arovas, A. Auerbach, Physical Review B **55**, 3104 (1997).
- [43] R. Moessner, S. L. Sondhi and P. Chandra, cond-mat/9910499.
- [44] *Science of Fullerenes and Carbon Nanotubes*, M. S. Dresselhaus, G. Dresselhaus and P. C. Eklund (Academic Press, 1996).
- [45] G. Stan and M. W. Cole, Surf. Sci. **395**, 280 (1998).
- [46] G. Stan, M. J. Bojan, S. Curtarolo, S. M. Gatica, M. W. Cole, cond-mat/0001334.
- [47] S. M. Garcia, G. Stan, M. M. Calbi, J. K. Johnson and M. W. Cole, cond-mat/0004229.
- [48] E. Orignac, R. Citro and N. Andrei, cond-mat/9912200;
 D. C. Cabra, A. Honecker, P. Pujol, Phys. Rev. B **58** 6241 (1998).
- [49] X.G. Wen, Mod. Phys. Lett. **B5**, 39-46 (1991);
 X.G. Wen, Physical Review B **41**, 12838 (1990);
- [50] *Field theories of condensed matter systems*, E. Fradkin (Addison-Wesley, 1991).
- [51] N. K. Wilkin and J. M.F. Gunn, Physical Review Letters **84**, 6 (2000).
- [52] N. Read, unpublished.

- [53] A.L. Fetter and J.D. Walecka, *Quantum Theory of Many Particle Systems*, (McGraw-Hill, New York, 1971).
- [54] *The Theory of Quantum Liquids*, Vol. I, D. Pines and P. Nozières (W.A. Benjamin, Inc., NY, 1966).
- [55] S.M. Girvin, A.H. MacDonald and P. Platzman, Physical Review B **33**, 2481 (1986).
- [56] *Many-Particle Systems*, G.P. Mahan (Plenum Press, NY, 1990).
- [57] A. Lopez and E. Fradkin, Physical Review B **47**, 7080 (1993);
ibid **47**, 7080 (1993); *ibid*, Physical Review Letters **69**, 2126 (1992).
- [58] K. Park and J.K. Jain, Solid State Communications, **115**, 353 (2000).
- [59] U. Fano, D. Green, T.A. Heim, and J. Bohn, J. Physics B **32**, R1-R37 (1999).
T.A. Heim and D. Green, J. Math. Phys. **40**, 2162 (1999).
- [60] *Quantum Field Theory*, C. Itzykson and J.B. Zuber (McGraw-Hill, NY, 1980).
- [61] N. Read and S. Sachdev Physical Review Letters **75**, 3509 (1995).
- [62] D. Yoshioka, A.H. MacDonald and S.M.Girvin, Physical Review B **38**, 3636 (1989).
- [63] T.T. Wu and C.N. Yang, Nucl. Phys. B **107**, 365 (1976).
- [64] M. Milovanović and N. Read, Physical Review B **53**, 13559 (1996).
- [65] S.M. Girvin and T. Jach, Physical Review B **29**, 5617 (1984).
- [66] *Interacting Electrons and Quantum Magnetism*, Assa Auerbach (Springer-Verlag, 1994).
- [67] C. Kallin and B.I. Halperin, Physical Review B **31**, 3635 (1985).
- [68] S. Sondhi et. al. Physical Review B **47**, 16419 (1993).
- [69] K. Moon et al., Physical Review B **51**, 5138 (1995).

- [70] F.D.M. Haldane and E.H. Rezayi, Physical Review Letters **60**, 956 (1988);
60, 1886(E) (1988).
- [71] D. Green, N. Read and E. Rezayi, in preparation.
- [72] N.E. Bonesteel, Physical Review Letters **82**, 984 (1999).
- [73] S.M. Girvin and A.H. MacDonald, Physical Review Letters **58**, 1252 (1987).
- [74] *Angular Momentum in Quantum Mechanics*, A.R. Edmonds (Princeton University Press, 1960).
- [75] M.P.A. Fisher, P.B. Weichmann, G. Grinstein, D.S. Fisher, Physical Review B **40**, 46 (1989).
- [76] E. Rezayi, unpublished.
- [77] A.W.W. Ludwig, M.P.A. Fisher, R. Shankar, and G. Grinstein, Physical Review B **50**, 7526 (1994).
- [78] A.N. Redlich, Physical Review Letters **52**, 18 (1984);
I. Affleck, J. Harvey, and E. Witten, Nucl. Phys. B **206**, 413 (1982).
- [79] J. Goryo, J. Phys. Soc. Japan **69**, 3501 (2000).
- [80] D. Green and C. Chamon, Physical Review Letters **85**, 4128 (2000).
- [81] *Statistical Mechanics*, K. Huang (Wiley, NY, 1987).
- [82] H.W.J. Blöte and M.P. Nightingale, Physical Review B **47**, 15046 (1993);
J.D. Noh and D. Kim, Intl. J. Mod. Phys. **B6**, 2913 (1991).
- [83] C.L. Henley and N.-G. Zhang, cond-mat/0001411.
- [84] P. Ginsparg in *Fields, Strings and Critical Phenomena*, E. Brezin and J. Zinn-Justin, eds., Elsevier (1988);
J. L. Cardy, *ibid.*
- [85] X. G. Wen, Physical Review B **41**, 12838 (1990).

- [86] M. Oshikawa, M. Yamanaka and I. Affleck, Physical Review Letters **78**, 1984 (1997).
- [87] T. Sakai and N. Okazaki, cond-mat/0002113.
- [88] F.D.M. Haldane, J. Phys. C **14**, 2585 (1981).
- [89] V. Pasquier, Nucl. Phys. **B285**, 162 (1987);
V. Pasquier, J. Phys. **A20**, L1229 (1987).
- [90] M. Flohr and R. Varnhagen, J. Phys. A, **27**, 3999 (1994).
- [91] G. Dunne, R. Jackiw, and C. Trugenberger, Physical Review D **41**, 661 (1990);
G. Dunne, R. Jackiw, Nuclear Physics Proceedings Supplement **33C**, 114 (1993).